ORP4L IS A PHOSPHO-REGULATED LIPID BINDING PROTEIN REQUIRED FOR CELL GROWTH AND MAINTENANCE OF TGN MORPHOLOGY

by

Antonietta C. Pietrangelo

Submitted in partial fulfilment of the requirements
for the degree of Doctor of Philosophy

at

Dalhousie University
Halifax, Nova Scotia
March 2018

To my family.

TABLE OF CONTENTS

LIST OF TABLES

LIST OF FIGURES

ABSTRACT

Oxysterol-binding protein (OSBP) and OSBP-related proteins (ORPs) constitute a 12-member family of mammalian lipid binding and transport proteins with variable tissue expression patterns and ligand affinities. The common feature of the ORP family is an OSBP-homology domain that binds sterol and/or phospholipid ligands, and additional domains involved in membrane-specific interactions that confer a complex suite of organelle-specific ORP functions. The focus of this dissertation is the OSBP paralog ORP4, which is a sterol and phosphatidylinositol-4-phosphate (PI(4)P) binding protein enriched in the brain, testes and retina. In addition to the ligand binding domain, full-length ORP4 (ORP4L) contains an FFAT motif and PH domain that recognize the resident ER protein VAP and PI(4)P, respectively. The PH domain is truncated and absent in medium (ORP4M) and short (ORP4S) isoforms, respectively. While ORP4 levels are elevated in metastatic cancers and known antineoplastic drugs target ORP4 by competitive inhibition, the primary cellular function of ORP4 remains elusive. This research provides evidence that ORP4 is a phospho-regulated lipid binding protein required for cell growth, likely through regulation of *trans*-Golgi network (TGN) morphology. ORP4 localized to the TGN in an OSBP- and PI(4)P-dependent manner independently of sterol-binding, and ORP4 depletion caused dispersion of the TGN and reduced *cis*/medial-Golgi PI(4)P levels. ORP4 membrane associations are controlled by ligand-binding and protein-protein interactions, both of which are in turn regulated by phosphorylation of ORP4 at a previously uninvestigated tract of serine residues in the ligand-binding domain.

LIST OF ABBREVIATIONS USED

22OH – 22-hydroxycholesterol

25OH – 25-hydroxycholesterol

2D-DIGE – two-dimensional difference gel electrophoresis

6xHis – hexahistidine tag

ABCA1 – ATP binding cassette subfamily A member 1

ADP – adenosine diphosphate

ALS – amyotrophic lateral sclerosis

ANK – ankyrin

apoA, apoB – apolipoprotein A or B

ARHGAP12 – Rho GTPase activating protein 12

ATP – adenosine triphosphate

BSA – bovine serum albumin

C-terminal – referring to the carboxy terminus of a protein

CARTS – carriers of the *trans*-Golgi network to the cell surface

CDK – cyclin-dependent kinase

cDNA – complimentary DNA

CERT – ceramide transport protein

CID – collision induced dissociation

CLM – chronic myeloid leukemia

CMT – camptothecin

CNS – central nervous system

COP – coatomer protein complex

CTxB – cholera toxin β subunit

DDA – data-dependent acquisition

dH_2O – deionized water

DIAPH1 – diaphanous-related protein 1

DMEM – Dulbecco's modified Eagle medium

DPM – disintegrations per minute

DTT - dithiothreitol

EDTA – ethylenediaminetetraacetic acid

EMT – epithelial-to-mesenchymal transition

ER – endoplasmic reticulum

ERK – extracellular signal-regulated kinase

ESI – electrospray ionization

EtOH - ethanol

EV – empty vector

FBS – fetal bovine serum

FFAT – two phenylalanines in an acidic tract

GALNT – polypeptide N-acetylgalactosaminyl transferase

GATE-16 – Golgi-associated ATPase enhancer of 16 kDa

GF-HPLC – gel filtration-high-performance liquid chromatography

GFP – green fluorescent protein

GM1 – monosialotetrahexosyl ganglioside

GM130 – Golgi matrix protein

GOLD – Golgi dynamics domain

GS28, GS15 – Golgi SNARE, with associated molecular weight

GSK – glycogen synthase kinase

GST – glutathione-*S*-transferase

GWAS – genome-wide association study

HCC – hepatocellular carcinoma

HCD – higher-energy collisional dissociation

HCV – hepatitis C virus

HDAC – histone deacetylase

HDL – high-density lipoprotein

HEK293 – human embryonic kidney cell line

HeLa – human cervical carcinoma cell line

HEPES – 4-(2-hydroxyethyl)-1-piperazineethanesulfonic acid

HFD – high-fat diet

HUH7 – human hepatocellular carcinoma cell line

IB - immunoblot

IEC – rat intestinal epithelial cell

IP - immunoprecioitation

IPTG – isopropyl β-D-1 thiogalactopyranoside

IUP – ideal upper phase

IVF – *in vitro* fertilization

JNK – cJun N-terminal kinase

KO – knockout

LC-MS/MS – liquid chromatography-tandem mass spectrometry

LD – lipid droplet

LDL – low-density lipoprotein

LEL – late-endosome/lysosome

LRH-1 – liver receptor homolog-1

LTP – lipid transport protein

LXR – liver X receptor

MCS – membrane contact site

miRNA – micro-RNA

MOI – multiplicity of infection

MTOC – microtubule organizing centre

mTOR – mammalian target of rapamycin

MβCD – methyl-β-cyclodextrin

N-terminal – referring to the amino terminus of a protein

NA – no addition

Nir2 – Pyk2 N-terminal domain-interacting receptor 2

NPC – Niemann-Pick type C

NS (in figures) – not significant

NS (in text) – non-structural

Nup62 – nucleoporin 62

Obr – OSBP-related protein (in *Caenorhabditis elegans*)

OHD – OSBP homology domain

ORP – OSBP-related protein

OSBP – Oxysterol binding protein

OSBPL – OSBP-like

Osh – oxysterol-binding homology

P150^{GLUED} – dynactin subunit 1

PA – phosphatidic acid

PAGE – polyacrylamide gel electrophoresis

PARP – poly(ADP) ribose polymerase

PBS – phosphate-buffered saline

PC – phosphatidylcholine

PC-1, PC1.0 – hamster pancreatic ductal carcinoma cell lines

PCR-RFLP – polymerase chain reaction-restriction fragment length polymorphism

PE – phosphatidylethanolamine

PEI – polyethylenimine

PH – pleckstrin homology

PI – phosphatidylinositol

PI(X)P – phosphatidylinositol-(x)-phosphate, where x indicates the position of phosphorylation on the inositol headgroup

PI4K – phosphatidylinositol-4-kinase (mammalian)

Pik1p – phosphatidylinositol-4-kinase (*S.cerevisiae*)

PIP – phosphatidylinositol phosphate

PLC – phospholipase C

PM – plasma membrane

PRALINE – PRofile ALIgNEment

PS - phosphatidylserine

qRT-PCR – quantitative reverse-transcriptase polymerase chain reaction

RAS – rat sarcoma viral proto-oncogene

RhoA – Ras homolog family member A

RILP – Ras-interacting lysosomal protein

RNA – ribonucleic acid

S100A11 – S100 calcium-binding protein A11

S6K – ribosomal protein S6 kinase

Sac1 – suppressor of actin mutations (phosphatidylinositol phosphatase)

SDS – sodium dodecyl sulfate

SE – standard error of the mean

Sec14 – secretory 14 (*S.cerevesiae* phosphatidylinositol/phosphatidylcholine transfer protein)

SF21 – Insect cell line derived from the ovaries of *S.frugiperda*

shRNA – short-hairpin ribonucleic acid

SidM – refers to the P4M domain of secreted *L.pneumophila* protein SidM

SM – sphingomyelin

SNARE – soluble N-ethylmaleimide sensor attachment protein receptor

SNP – single nucleotide polymorphism

SRE – sterol regulatory element

SREBP – sterol regulatory element binding protein

START – steroidogenic acute regulatory protein-related lipid-transfer

T-ALL – T-cell acute lymphoblastic leukemia

TAG - triacylglycerol

TBS – Tris-buffered saline

TBST – Tris-buffered saline with Tween-20 detergent

TGN – *trans*-Golgi network

TIRF – total internal reflection fluorescence

TLC – thin-layer chromatography

TM – transmembrane domain

Tris – tris(hydroxymethyl)aminomethane

TWB – Talon wash buffer

V5 –GKPIPNPLLGLDST epitope tag

VAP – vesicle-associated membrane protein-associated protein

v/v – volume per volume

WT – wild-type

w/v – weight per volume

ACKNOWLEDGEMENTS

First and foremost, I have to thank Neale, who has been a fantastic mentor and has always provided constructive feedback. Thanks for letting me chase ideas, and for reminding me to focus when there were too many of them. I'm also grateful to my committee members Dr. Barbara Karten, Dr. Aarnoud van der Spoel and Dr. Graham Dellaire for always being approachable and providing excellent guidance, and to Dr. Christopher Beh and Dr. Petra Kienesberger who read this thesis and provided valuable feedback. Thanks as well to the government of Nova Scotia for financial support.

I'm lucky to have had the pleasure of working with the past and present members of the ARC. In particular, this work would have been very difficult without the assistance, advice, and atrocious wordplay of Mark Charman. Rob Douglas, Stephen Whitefield and Dr. Alejandro Cohen provided excellent technical guidance, and in leaving Dalhousie I'll dearly miss the support of Debbie Hayes and Roisin McDevitt (and the chats).

My brother Agostino inspired me to love science and pursue a research career, and I strive to follow in his footsteps; the following 150 pages of esoteric scientific discussion largely unrecognized by Microsoft Word's English dictionary suggest that I'm nailing it so far. Thanks to my parents Anna and Tony Pietrangelo for *everything* (including almost six years of consistent "good morning" texts and nightly phone calls), and to Dawn and Jeff McCluskey for support and encouragement. Valbona made my unlimited Canada-wide phone plan worthwhile, and Halifax has only become a home because people like Crissy, Jill and Fraser have become a family. Finally, I came to Dalhousie University for a degree, and I'm leaving with a husband (and also the degree). Thanks, Greg, for everything. I'd write more, but this thesis is already long enough.

CHAPTER 1 INTRODUCTION

This chapter is adapted from the following publication:
Pietrangelo, A., Ridgway, N. D. Bridging the molecular and biological functions of the oxysterol-binding protein family. *Cell. Mol. Life Sci.* (2018). https://doi.org/10.1007/s00018-018-2795-y (2014). *See Appendix A for permissions.*

Intracellular lipid transport creates and maintains the unique lipid composition of membranes that define organelle function and regulate communication with the external environment. While vesicular transport and membrane fusion are responsible for the bulk transfer of lipids and sterols, the specific and localized movement of individual lipid species between membranes is mediated by lipid transport proteins (LTPs) [1]. While LTP gene families are numerous and diverse in structure, they share the ability to bind lipids within a hydrophobic fold for lipid transfer, substrate presentation or signaling [2]. Oxysterol-binding protein (OSBP) and OSBP-related proteins (ORPs) constitute a large family of eukaryotic LTPs that bind cholesterol, oxysterols and anionic phospholipids within a conserved hydrophobic binding domain. Additional membrane-targeting motifs allow OSBP/ORPs to simultaneously associate with a diverse set of protein and lipid partners in organelle membranes, thus positioning the lipid binding domain in close apposition to donor and acceptor membranes to facilitate transfer or signaling functions. The potential for redundancy in this large gene family adds complexity to any analysis of individual OSBP/ORP function in normal and disease states.

ORP4 is currently the only ORP known to be necessary for proliferation and survival in cultured immortalized and transformed cells, but its primary function remains elusive. The focus of this doctoral research project was to further characterize ORP4 in an attempt to better understand its role in the cell. This dissertation is introduced by a general review

of the structure and function of OSBP and the ORPs, which informed this study, followed by a more in-depth review of the relatively limited ORP4 literature.

1.1 THE ORP FAMILY

OSBP was identified in 1985 by Taylor and Kandutsch as a soluble receptor for oxysterols [3], which are oxidized cholesterol derivatives that promote cholesterol esterification and efflux, and inhibit *de novo* cholesterol synthesis and uptake [4]. Cloned in 1989, OSBP was initially thought to be an oxysterol-regulated transcription factor due to a central leucine repeat reminiscent of some DNA binding proteins [5]. However, OSBP was later shown to undergo sterol-dependent localization to the Golgi apparatus [6]. In 1999, Ikonen and colleagues cloned the cDNAs for 6 human OSBP-related proteins (termed ORPs) [7], and the remaining members of the 12-gene family were cloned in 2001 [8]. Mammalian OSBP/ORPs contain a conserved C-terminal lipid binding domain designated the OSBP homology domain (OHD) that harbours a highly-conserved motif (EQVSHHPP) that is found in homologues across species (Figure 1.1). All but one of the *OSBP* genes encode full-length or long (L) forms that contain additional membrane-targeting domains (Figure 1.1 A). For example, all full-length OSBP/ORPs have an N-terminal pleckstrin homology (PH) domain that recognizes phosphatidylinositol phosphates (PIPs) with varying degrees of specificity and affinity. OSBP and ORPs 1, 2, 3, 4, 6, 7 and 9 also contain a two-phenylalanines-in-an-acidic-tract (FFAT) motif that interacts with the resident ER protein vesicle-associated membrane protein-associated protein (VAP) [9]. As a result, OSBP/ORPs that contain PH and FFAT motifs are peripherally anchored to the ER and to organelles enriched in PIPs, such as the Golgi apparatus, PM or endosomes [10-15].

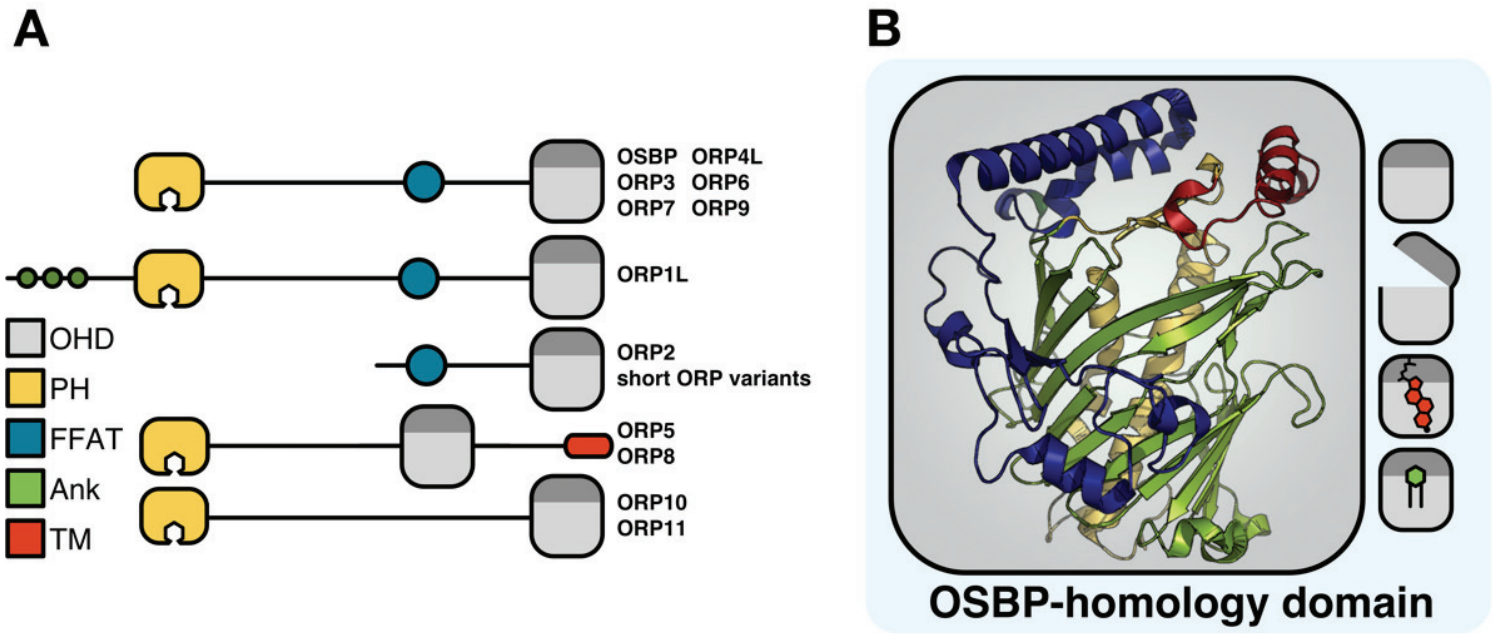

Figure 1.1 *Structural organization of the OSBP/ORP family.* **A)** Domain organization of the OSBP/ORP family. OHD, OSBP homology domain; PH, pleckstrin homology; FFAT, two phenylalanines in an acidic tract; Ank, ankyrin; TM, transmembrane. **B)** Shown is the structure of the *S. cerevisiae Osh3p* OHD composed of an incomplete β-barrel (green) flanked by two central helices (yellow), N-terminal region (blue) and α-helical lid (red). The OHD binds sterols and phospholipids competitively and in opposite orientations; the acyl chains of phospholipids are buried in the pocket, while the iso-octyl side chain of sterols interacts with the lid.

ORP5 and ORP8 provide a variation on this theme: both have C-terminal membrane-spanning domains that anchor them to the ER, as well as PH domains that facilitate interaction with other organelles (Figure 1.1 A) [16-18]. Collectively, these dual membrane-binding properties could facilitate transient association-dissociation with individual membranes or simultaneous association at a membrane contact site (MCS) between organelles [2] (Figure 1.2). How this is involved in lipid transfer and regulation is discussed further in Section 1.3.

Much of the structural and functional information we have for the OSBP/ORP family is derived from study of the *S. cerevesiae* oxysterol-binding homology (Osh) proteins. Osh1p-Osh3p are long forms that contain N-terminal PH, FFAT and ankyrin or GOLD domains, and Osh4p-Osh7p contain only the OHD. While the seven Osh proteins associate with different membranes and cellular processes [19], they are functionally redundant such that any one Osh protein can rescue the lethality caused by deletion of all seven Osh proteins [20].

Studies of the cholesterol auxotrophs *C.elegans* and *D.melanogaster*, which each express four ORPs, revealed similar functional redundancy. Deletion of Obr-1 – Obr-4 in *C. elegans* caused embryonic lethality not observed with individual gene deletions [21], and individual deletion of *Osbp* genes in *D.melanogaster* yields viable mutants [22]. However, *Osbp* deletion or overexpression in *D.melanogaster* caused aberrant Golgi cholesterol accumulation with deleterious effects on spermatogenesis and wing expansion, suggesting a vital role in regulating the lipid composition of organelles in the absence of *de novo* sterol biosynthesis [22,23].

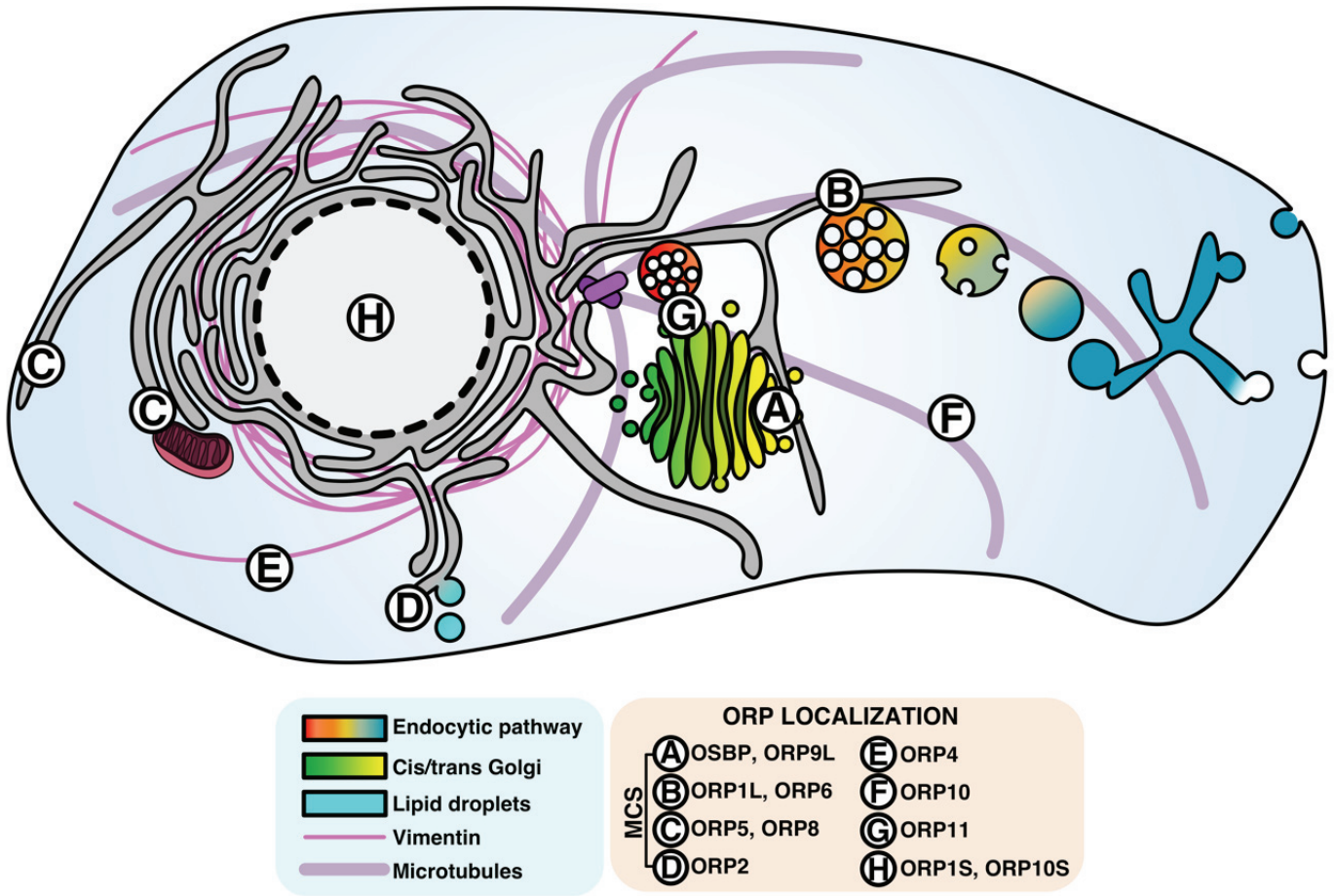

Figure 1.2 *Subcellular localization of the OSBP/ORP family.* Aside from ORP5 and ORP8, all ORPs display partial cytosolic localization, but most also have discrete localization patterns, including membrane contact sites between organelles, on cytoskeletal elements and in the nucleus (see figure for details). For simplicity, only well-characterized localization patterns relevant to known or predicted protein functions have been included. ORP3 and ORP7 do not have well-defined localization patterns and have been omitted.

1.2 Structure and Specificity of the OSBP Homology Domain

Osh4p was the first member of this family to have its structure solved by X-ray crystallography, revealing an OHD comprised of an incomplete 19-strand beta-barrel (Figure 1.1 B, green) with an alpha-helical lid (Figure 1.1 B, red), which together form a hydrophobic binding cavity that accommodates cholesterol and oxysterols [24]. Cholesterol co-crystalized in the Osh4p OHD pocket is oriented 'head-first' (Figure 1.1 B, cartoon); the 3-hydroxyl is coordinated at the bottom of the pocket while the iso-octyl side chain interacts with the lid in a closed position, making the pocket inaccessible to other ligands. Interestingly, protein-sterol interactions are mediated by water molecules that line the binding pocket, bridging basic residues at the base of the pocket with the 3-hydroxyl of the bound sterol. Indirect, water-mediated binding may explain the broad range of sterols that are bound by OSBP/ORP and Osh proteins.

Despite similarities in the sequence and structure of OHDs amongst the Osh and OSBP/ORP family, it is apparent that sterol binding is not a core activity [25]. Crystallization of the OHDs of Osh4p [26] and Osh3p [27] revealed that PI(4)P also occupies the OHD, but in a 'tail-first' orientation (Figure 1.1 B, cartoon); the acyl chains extend into the binding pocket while the inositol 4-phosphate headgroup interacts with two histidine residues close to the entrance of the binding fold. Notably, the two histidine residues are part of the OSBP/ORP signature motif and not required for sterol binding [27], suggesting a primary function may involve the binding and transfer of anionic phospholipids. The "tail first" orientation of PI(4)P in the OHD suggests that the alpha-helical lid of the OHD is capable of inserting into membranes to excise embedded lipids for binding in the proper orientation [28]. This configuration for PI(4)P was confirmed for Osh1p, which also binds ergosterol [28].

While the structure of mammalian OHDs have not been solved, i*n vitro* assays of lipid binding and extraction from liposomes have shown that mammalian OSBP/ORPs bind both sterols and phospholipids, including phosphatidylserine (PS) and PIPs (summarized in Table 1 and reviewed in [29]).

Competition for phospholipid and sterol binding allows an Osh/OSBP/ORP to potentially exist in binary states; each ligand induces conformational changes in the OHD that direct protein and membrane association to potentially drive lipid-exchange between organelles. This concept was first demonstrated for Osh4p, a prototypical OHD-only protein that does not physically bridge donor and acceptor membranes during a lipid transfer cycle. Liposome-based Osh4p lipid transfer assays showed that the rate of delivery of ergosterol from a donor membrane to an acceptor membrane increased when the acceptor membrane was enriched with anionic lipids [26]. However, Osh4p only dissociated from the acceptor membrane once bound to another ergosterol molecule, therefore resulting in no net change in the ergosterol content of the acceptor membrane. When the acceptor membrane was enriched with PI(4)P, which is an anionic lipid and Osh4p ligand, ergosterol delivery to acceptor membranes was increased while the back-transfer of ergosterol was inhibited by competitive binding of PI(4)P, thereby driving directional transport of ergosterol to the acceptor membrane.

Complementation studies in yeast suggest that Osh4p functions similarly *in vivo* (Figure 1.3), transferring ER-derived cholesterol to the Golgi in exchange for Golgi-derived PI(4)P, which is then hydrolyzed in the ER by the PI(4)P phosphatase Sac1p [30]. In yeast, the phosphatidylinositol (PI) transfer protein Sec14p drives PI(4)P synthesis by providing substrate for the PI-4 kinase Pik1p. In the absence of Sec14p, unchecked Osh4p-

Table 1 ORP localization and function.

Name	Isoforms	Domains	Tissue Expression	Localization	Ligands (k_d)	Intracellular functions
OSBP (*OSBP*)		OHD, FFAT, PH	Ubiquitous [31]	Golgi, cytosol [6], ER [32]	25OH (8 nM) [3,5,33], cholesterol (173 nM)[33], PI(4)P [34]	Catalyzes sterol/PI(4)P counter-current transport at ER/Golgi. Recruits CERT [14,34,35] and regulates SM synthesis [36].
ORP1 (*OSBPL1*)	ORP1L	OHD, ANK, PH	brain, lung [37]	LEL, ER [37,38]	25OH (83-97 nM) [39,40], cholesterol (1.4 μM), PI(4)P [39]	Endosome positioning [38] and cholesterol efflux [39] via Rab7/RILP/ $p150^{GLUED}$ assembly [15].
	ORP1S	OHD	heart, skeletal muscle, macrophages [37]	Cytosol [37], nucleus [33]	25OH (8.4 nM) [37], PI(4)P [39]	LXR regulation [40] and sterol transport from PM to LD [41].
ORP2 (*OSBPL2*)		OHD, VAP	Ubiquitous, enriched in CNS [42]	LD, ER, Golgi [42]	22(R)OH (14 nM), 7-ketocholesterol (160 nM), cholesterol [43], 25OH (3.9 μM) [40]	Cholesterol efflux [42], endocytosis [44] and PM-to-ER sterol transport [41]. Regulates TAG hydrolysis [11] and actin dynamics [45]. Binds LXR and regulates cortisol biosynthesis [46].
ORP3 (*OSBPL3*)		OHD, VAP, PH	Kidney, lymph nodes, thymus [47], macrophages [37]	Cytosol, ER, PM [47], nuclear envelope [48]	Photo-25OH (weak), photo-cholesterol [40]	Regulates actin dynamics via interaction with R-Ras [49], and PI levels [50].
	ORP4L	OHD, FFAT, PH	Brain, heart, testis, skeletal muscle [51]	Cytosol, ER, vimentin [51]	25OH (17-27 nM) [52,53], cholesterol (68 nM) [52]	
ORP4 (*OSBP2*)	ORP4M	OHD, FFAT	N/A	Vimentin aggregates [52]	N/A	Regulates Ca^{2+} homeostasis [54-56]. Murine KO has oligo-astheno-teratozoospermia and sterility [57]. Silencing in cell culture causes apoptosis [52].
	ORP4S	OHD	Brain, heart [51]	Vimentin aggregates [51]	25OH (23 nM), cholesterol (60 nM) PI(4)P [52]	

Name	Isoforms	Domains	Tissue Expression	Localization	Ligands (k_d)	Intracellular functions
ORP5 (*OSBPL5*)		OHD, PH, TM	Heart, brain, lung, liver, kidney [58]	ER [59], PM [17], mitochondria [16]	Photo-25OH [40], All PIPs (0.8-26.8 μM) [18], PS [60]	Cholesterol efflux from endosomes. PS/PI(4)P counter-current transport [59] at ER/PM [17]. PS transport to mitochondria [16].
ORP6 (*OSBPL6*)		OHD, FFAT, PH	Brain, skeletal muscle [47]	Nuclear envelope, cytosol, ER, PM [47], LEL [61]	Photo-25OH and photo-cholesterol (weak) [40]	Regulated by LXR. Involved in cholesterol efflux from early endosomal compartment [61].
ORP7 (*OSBPL7*)		OHD, FFAT, PH	Gastrointestinal tract [47]	Cytosol, ER, PM [47]	Photo-25OH and photo-cholesterol (weak) [40]	Promotes proteosomal degradation of Golgi snare GS28 via 25OH-dependent interaction with GS28 partner protein GATE-16 [62].
ORP8 (*OSBPL8*)		OHD, PH, TM	Macrophages, spleen, kidney, liver, brain [63]	ER, PM [17], mitochondria [16]	25OH [63], All PIPs (1.7-6.0 μM) [18], PS [60]	Counter-current transport of PS/PI(4)P at ER/PM [17]. PS transport to mitochondria [16]. Involved in macrophage motility and hepatic lipid efflux [63,64].
ORP9 (*OSBPL9*)	ORP9L	OHD, FFAT, PH	Brain, heart, kidney, liver [10]	ER, Golgi [10]	Cholesterol [65], PI(4)P, cholestatrienol, dehydroergosterol [66]	Recruits ORP11 to the Golgi [49]. Regulates Golgi organization via cholesterol [65] or PI(4)P trafficking [66].
	ORP9S	OHD, FFAT	Liver [10]	ER [10]	PI(4)P, cholestatrienol, dehydroergosterol [66]	Involved in Golgi organization, growth inhibition [65] and PI(4)P regulation [66].
ORP10 (*OSBPL10*)	ORP10L	OHD, PH	N/A	Microtubules [67,68], Golgi [68]	Photo-25OH [43], cholesterol [68], PS [60]	Dimerizes with ORP9L [68]. Negative regulator of hepatic lipid biosynthesis and apoB-100 secretion [67,68].
	ORP10S	OHD	N/A	Cytosol, nucleus [68]	N/A	N/A
ORP11 (*OSBPL11*)		OHD, PH	Ovary, testis, brain, liver, kidney, stomach, adipose tissue [69]	Golgi, LEL [69]	N/A	Dimerizes with ORP9L [69]. involved in cellular TAG storage and induced during adipocyte differentiation [70].

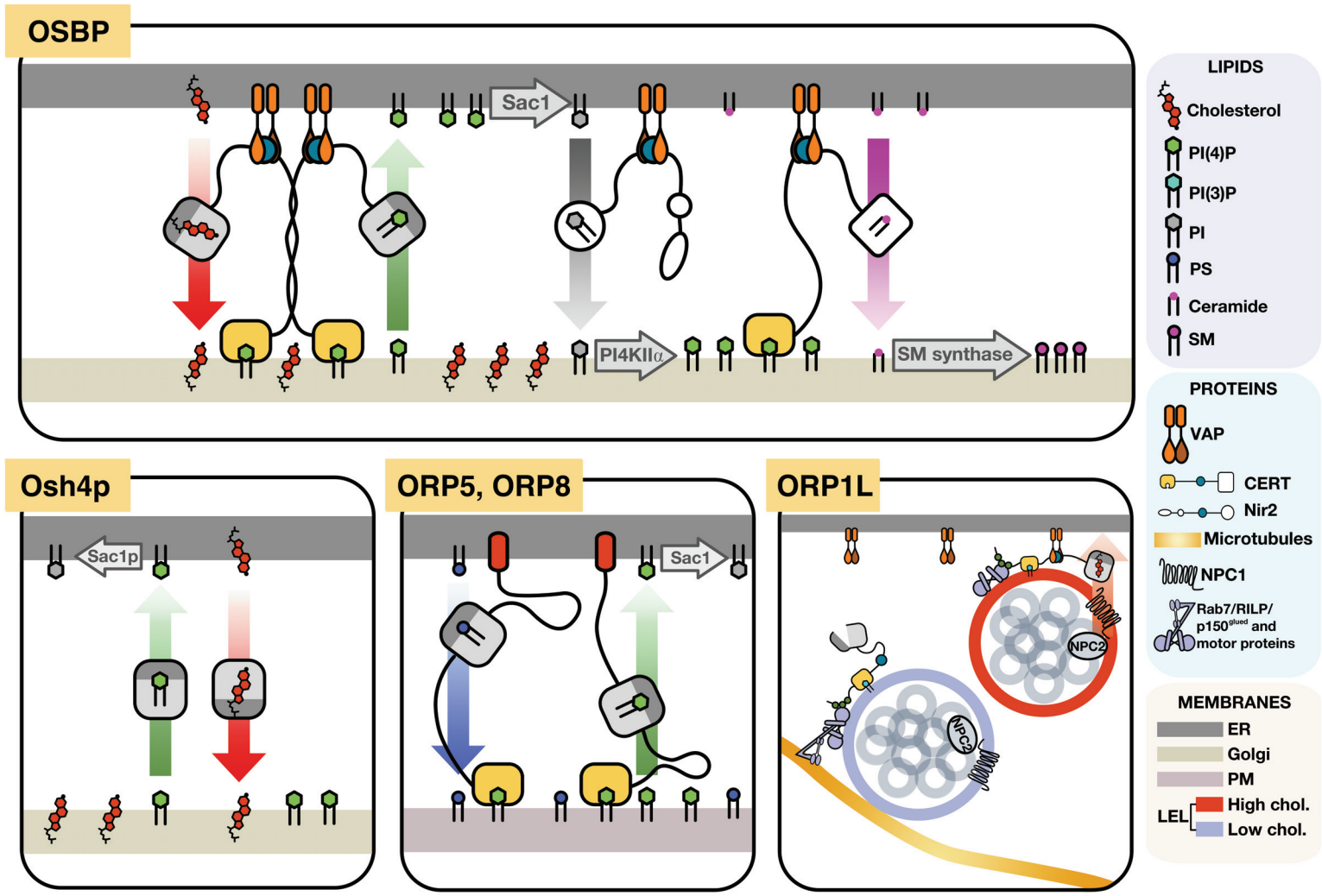
OSBP
Sac1
PI4KIIα
SM synthase
Osh4p
Sac1p
ORP5, ORP8
Sac1
ORP1L
NPC2
NPC2
LIPIDS
Cholesterol
PI(4)P
PI(3)P
PI
PS
Ceramide
SM
PROTEINS
VAP
CERT
Nir2
Microtubules
NPC1
Rab7/RILP/
p150glued and
motor proteins
MEMBRANES
ER
Golgi
PM
LEL
High chol.
Low chol.

Figure 1.3 *Models of ORP function at membrane contact sites.* **OSBP** localizes to closely opposed ER/Golgi membranes, where it exchanges PI(4)P and cholesterol. The resulting cholesterol enrichment on the Golgi activates PI4KIIα, which phosphorylates PI delivered by Nir2, into a PI(4)P pool that recruits CERT, resulting in ceramide delivery to SM synthase and consequent SM synthesis. Consumption of ER PI(4)P by Sac1 phosphatase maintains a concentration gradient that drives the PI(4)P/cholesterol counter-current transport. Yeast **Osh4p** functions similarly to OSBP but without tethering to the ER or Golgi apparatus. **ORP5 and ORP8** are ER-tethered proteins that extend to the PM via PH domain interaction with PIPs, using the transport of PI(4)P to the ER to drive PS transport to the PM. **ORP1L** is localized to the LEL via interaction between N-terminal ankyrin repeats and Rab7. When cholesterol is low in the limiting membrane of LEL, ORP1L promotes the assembly of a microtubule-tethering complex (Rab7/RILP/$p150^{glued}$) that facilitates minus-end movement of the LEL. When cholesterol on the LEL limiting membrane is elevated, the complex dissembles and ORP1L tethers the LEL to the ER via VAP and facilitates cholesterol efflux to the ER.

mediated PI(4)P depletion causes cytotoxic failure of the secretory system [71], a phenotype that can be rescued by deletion of Osh4p but not any other Osh [20,71].

Interestingly, Osh3 [27], Osh6 and Osh7 [72] do not bind sterols despite binding PI(4)P [27] and PS [60], respectively, but each has sufficient functional redundancy with the sterol-binding Osh proteins to circumvent cell death caused by depletion of Osh1-7 [20]. It is therefore unlikely that the core function of the Osh/ORP family is limited to sterol transport and metabolism; indeed, sterol enrichment of the PM is retarded by deletion of Osh3 and Osh6, which do not bind sterols and therefore cannot have a direct contribution to this phenotype via nonvesicular sterol transport [73]. Studies by Georgiev and colleagues show that traffic of intracellular dehydroergosterol or radiolabeled ergosterol to the PM occurs normally in a temperature-sensitive yeast strain lacking all Osh family activity when grown at 37°C, suggesting that Osh protein activity does not contribute significantly to PM sterol content [74]. That ORPs are not limited to sterol binding, and that sterol binding is not a ubiquitous feature of Osh proteins, suggests that Osh/ORP function is likely a complex network of lipid-dependent protein interactions and membrane remodelling. For example, in addition to catalyzing nonvesicular lipid transport, Osh4p is also a sterol-regulated signaling protein necessary for polarized cell growth [75]. Osh4p regulates exocyst formation by increasing Sac1p activity, leading to a local reduction in PI(4)P on exocytic vesicles that causes dissociation of proteins that inhibit the secretory protein Sec4. Active Sec4 forms a complex required for docking and fusion of the exocyst with the PM, which is disrupted by temperature-sensitive Osh1-7 inactivation or expression of a sterol-binding deficient, hyperactive Osh4p. Together, these data provides further evidence that despite

lipid binding and transfer functions, the core function of the Osh/ORP family likely involves the regulation of cellular processes by lipid-dependent signaling.

1.3 ORP-Mediated Lipid Transfer at Membrane Contact Sites

The membrane-targeting domains N-terminal to the OHD equip most OSBP/ORPs with dual-membrane targeting properties, making them excellent candidates for lipid transport between cellular compartments at MCS. In fact, OSBP, ORP9L, ORP1L, ORP6, ORP5, ORP8 and ORP2 have all been observed at organelle interfaces (Figure 1.2). In the case of OSBP, ORP1L, ORP5 and ORP8, localization to closely apposed membranes is a critical determinant of their function [76]. Like OSBP, ORP4 is equipped for dual-membrane targeting with a PH domain and FFAT motif, but has not been observed at MCS. Here we provide a brief review of the cellular processes mediated by ORPs at MCS, which informed and directed this study.

1.3.1 Metabolic Regulation by OSBP at the Golgi/ER Interface

OSBP is a prototypical dual membrane-interacting protein that transfers lipids and regulates lipid metabolism at MCS. Over a decade of research has described OSBP as a sterol-sensitive regulator of sphingomyelin (SM) and PI(4)P synthesis at the Golgi/ER interface (Figure 1.3). OSBP is a cytosolic protein that associates transiently with the *trans*-Golgi and trans-Golgi network (TGN) via the PH domain [77], and the ER via interaction between its FFAT motif and the ER-resident protein VAP-A [32]. When cells are treated with exogenous oxysterols (a signal of excess cholesterol) or depleted of cholesterol to stimulate *de novo* synthesis, OSBP associates with ER/Golgi MCS [6,14]. There, OSBP transports ER-

derived cholesterol to the Golgi and Golgi-derived PI(4)P to the ER, where it is degraded by Sac1 [34]. OSBP-mediated cholesterol enrichment in the Golgi apparatus leads to recruitment of phosphatidylinositol-4-kinase (PI4K) IIα [78] and consequently a local increase in PI(4)P, which in turn leads to recruitment of ceramide transport protein (CERT) via PH and FFAT domain-dependent targeting to the MCS [35]. The transport of ceramide to the Golgi apparatus provides substrate for the synthesis of SM, thereby matching the increased transport of cholesterol to maintain the relative proportions of SM and cholesterol-rich microdomains, which are important for protein and lipid sorting in the secretory pathway [79]. For example, the biogenesis of carriers of the *trans*-Golgi network to the cell surface (CARTS) requires VAP localization to ER/Golgi MCS and lipid-transfer mediated by OSBP [80]. Reduction in the levels of VAP, OSBP or CERT prevented the secretion of CARTS cargo, as did expression of OSBP or CERT with mutations in the FFAT motifs. This suggests a requirement for OSBP in the maintenance of cholesterol and sphingolipid-enriched membranes at TGN/ER contacts, and in the resulting directional transport of CARTS cargoes.

Less than 1% of cellular cholesterol is present in the endoplasmic reticulum (ER) [81], where the sterol regulatory element binding protein (SREBP) pathway is subject to negative feedback-inhibition by cholesterol and oxysterols [82]. Thus, subtle changes in sterol levels in the ER can initiate rapid changes in cholesterol biosynthetic capacity. While the ER is relatively cholesterol poor, there is a cholesterol gradient from the *cis*/medial to *trans*-Golgi to PM [83], which constitutes approximately 60-80% of cellular cholesterol [84]. A model for the maintenance of heterogeneous cholesterol distribution between the ER and TGN posits that OSBP couples the transport of PI(4)P down its concentration gradient from

the TGN to ER to power the counter-transport of cholesterol against its concentration gradient from the ER to TGN [85]. The hydrolysis of the 4-phosphate of PI(4)P by Sac1 in the ER maintains the PI(4)P gradient, effectively harnessing the energy of PI(4)P synthesis and hydrolysis to drive cholesterol transport by OSBP [86]. The OSBP-inhibitor OSW-1 doubled total cellular PIP content [86], of which PI(4)P is the predominant species [87]. This finding suggests that an OSBP-mediated 'lipid pump' mechanism could consume up to 50% of cellular PI(4)P mass to power this cholesterol transport process. Preventing the replenishment of PI(4)P by pharmacological inhibition of PI4KIIIβ caused oscillation of PI(4)P levels at the TGN. In this scenario, OSBP consumes PI(4)P and consequently dissociates from the TGN until PI4KIIα activity eventually replenishes the TGN PI(4)P pool, at which point OSBP is recruited to MCS and restarts the cycle [86]. It should be noted that ORP4 is also inhibited by OSW-1 [88], and while it is likely that OSBP inhibition is largely responsible for the observations made by Mesmin and colleagues, potential involvement of ORP4 in the modulation of Golgi PI(4)P levels cannot be discounted until ORP4 function is better understood.

The phenotypes of OSBP silencing in cultured cells have indicated a role in ER-to-Golgi cholesterol transport. These include reduction in TGN cholesterol content [78] leading to the mislocalization of *cis*/medial-Golgi tether proteins [89], and accumulation of PI(4)P in Golgi and endosomal membranes leading to disruption of retromer-mediated transport and increased actin nucleation [90]. Silencing of OSBP expression had no effect on the morphology of the *cis*/medial-Golgi or TGN; however, the perinuclear intra-Golgi v-SNARES GS28 and GS15 become dispersed in the cytosol. GS28 and GS15 traverse the Golgi in COP-I transport vesicles, the fusion of which requires cholesterol-dependent

conformational changes in SNARE proteins. Treatment of cells with lovastatin, an inhibitor of cholesterol biosynthesis, replicated the effects of OSBP silencing on GS28 and GS15 localization, suggesting that mislocalization is the result of aberrant cholesterol distribution due to the absence of OSBP [90].

Early reports that OSBP overexpression increased cholesterol biosynthesis and inhibited cholesterol esterification suggested a role in cholesterol transport or regulation in the ER [77]. Recently, inhibition of OSBP by OSW-1 was shown to increase lipid droplet formation indicative of ER cholesterol accumulation and enhanced esterification. However, OSBP silencing in Chinese hamster ovary (CHO) cells had no effect on cholesterol synthesis or esterification in the ER [35]. These data suggest OSBP-mediated cholesterol export to the Golgi apparatus may involve a relatively small fraction of the ER cholesterol pool that has minimal impact on esterification by ACAT or the SREBP regulatory machinery.

1.3.2 PS Transfer by ORP5 and ORP8 at Membrane Contact Sites

ORP5 and ORP8 associate with the ER via tail-anchored C-terminal transmembrane domains while the N-terminal PH domains interact with di- and tri-phosphorylated PIPs in the PM [18]. ORP5 and ORP8 are involved in maintaining the pool of PS on the cytoplasmic leaflet of the PM by exchanging PM-associated PI(4)P [17] and $PI(4,5)P_2$ [18] for PS [60] in the ER (Figure 1.3). The OHD and PS binding activity are required for ORP5 and ORP8 to also localize to ER/mitochondria contact sites, but this activity is PH domain-independent. Silencing of ORP5 and ORP8 caused defects in mitochondrial function and morphology without affecting the number of ER/PM or ER/mitochondrial MCS, indicating that ORP5 and ORP8 localize to pre-existing MCS and are not required

for their formation [16]. Together, these results suggest that ORP5 and ORP8 may transfer PS from the ER to the mitochondria where it is decarboxylated to phosphatidylethanolamine required for mitochondrial structure and function [91].

1.3.3 Sterol Transfer by ORP1L and ORP6 at Endosome/ER Contact Sites

In addition to *de novo* cholesterol biosynthesis in the ER, cells also acquire exogenous cholesterol by the uptake and processing of lipoproteins, primarily low-density lipoprotein (LDL), in the endo-lysosomal pathway. After receptor-mediated endocytosis, the cholesterol esters in LDL are hydrolyzed in late endosomes/lysosomes (LEL) [92]. The bulk of LDL-derived cholesterol is exported from the late endosomes before lysosomal maturation, as evidenced by the discrepancy in cholesterol content between the two compartments [93]. Cholesterol export from the LEL is facilitated by the concerted action of NPC2, a soluble protein that binds cholesterol in the LEL lumen, and NPC1, a multi-pass transmembrane protein that receives cholesterol from NPC2 and transfers it to the limiting membrane of the LEL [94]. Once on the external leaflet of the limiting membrane, cholesterol is transferred to other organelles by poorly understood mechanisms; however, a portion of LDL-derived cholesterol that flows to the ER [92] likely does so at contact sites with LELs [95]. The dual membrane-targeting ORP1L and ORP6 have been implicated in this pathway.

Initial studies showed that ORP6 mRNA increased in response to cholesterol loading in cultured cells [96]. Later studies confirmed that expression of ORP6 is regulated by the liver X receptor (LXR) and miRNA 33 and 27b, and increased under conditions of cholesterol loading in macrophages and animal models [61]. In ORP6-silenced and cholesterol-loaded macrophages, cholesterol accumulated in abnormally clustered early endosomes and cholesterol esterification by ACAT was inhibited, indicative of reduced

cholesterol transport to the ER. Conversely, overexpression of ORP6 stimulated cholesterol esterification and cholesterol efflux from cells. Collectively this indicated that that coordinated activation of ORP6 and cholesterol efflux proteins by LXR is a mechanism to promote the transport of sterols from early endosomes to suppress cholesterol biosynthesis in the ER and promote efflux by ABC transporters.

OSBPL1 encodes two variants due to alternate promoter start sites; full-length ORP1L, which has N-terminal ankyrin repeats and a PH domain, and the truncated variant ORP1S that contains only the OHD [37]. Both proteins are induced during the differentiation of macrophages [37]. ORP1L interacts with endosomal Rab7 via the ankyrin motif and with VAP via its FFAT motif [38]. Rocha and colleagues initially reported that when lysosomes are cholesterol-loaded, ORP1L dissociates from VAP and promotes assembly of the Rab7/RILP/p150^{glued} complex that tethers the LEL to the microtubule network for transport toward the microtubule organizing centre (MTOC) [15,97,98]. However, lysosomal cholesterol loading in this study was performed by inhibition or silencing of NPC1, which causes internal cholesterol accumulation in LEL but prevents cholesterol egress to the limiting membrane [99]. As a result, this model counter-intuitively mimics a cholesterol-starved lysosome, which effectively reverses the conclusion of the study. It was later confirmed that the Rab7/RILP/p150^{glued} complex is actually assembled when the limiting membrane of the LEL is depleted, and elevated cholesterol on the limiting membrane of the LEL causes ORP1L to interact with VAP on the ER to establish a peripheral distribution of LEL and mediate cholesterol shuttling to the ER (Figure 1.3) [39]. ORP1L knockout cells display sequestration of endosomes at the MTOC, defective cholesterol delivery to the ER and increased *de novo* cholesterol biosynthesis [39]. Interestingly, the OHD of ORP1 also binds

PI(4)P[39]; however, evidence does not currently exist for a countercurrent transport model such as that described for OSBP and Osh4p [85]. ORP1L is also implicated in the transfer of cholesterol from the ER to a subpopulation of multivesicular endosomes tethered by a calcium-regulated annexin A1/S100A11 complex, and is required for epidermal growth factor receptor sorting into intraluminal vesicles [95].

ORP1S is a soluble sterol receptor that partially localizes to the nucleus in response to ligand binding and enhances the activity of LXR [33]. Whether ORP1S also participates in a cholesterol transport pathway involving ORP1L is unknown.

1.3.4 ORP2 at ER/lipid Droplet Contact Sites

The ER contains ACAT and DGAT that synthesize cholesterol esters and triacylglycerol (TAG) that coalesces within the bilayer of ER membranes, eventually budding to form specialized storage organelles called lipid droplets (LD) [100]. The lipids stored in LDs are a source of fatty acids for oxidation or can be packaged into lipoproteins for secretion and transport to other cells. ORP2 is composed of an OHD, which binds cholesterol and oxysterols, and a FFAT motif [43]. ORP2 is present at ER/LD contact sites [11] and dissociates from LDs upon ligand binding [46]. The function of ORP2 at ER/LD contacts is not well understood, but silencing of ORP2 lead to increased cellular cholesterol levels [46] and aberrant metabolism of TAGs [11,43] and fatty acids [101]. Overexpression of ORP2 increased cellular cholesterol efflux [42,44] and LD dispersion [46]. Together, these studies suggest ORP2 regulates LD positioning by establishing ER contacts in a sterol-dependent manner, which facilitates lipid exchange between the organelles.

1.4 THE INVOLVEMENT OF OSBP/ORPS IN HUMAN DISEASE

OSBP/ORPs display both ubiquitous and tissue-specific expression patterns (Table 1). Despite the size of the family and the potential for redundant function within specific tissues, high-throughput genetic and targeted functional studies have implicated OSBP/ORPs in a range of rare and common human disorders (summarized in Table 2) and viral infections. Genetic screens of cancerous tissues and cell lines have detected elevated protein and/or mRNA expression of ORP1 [102], ORP2 [102], ORP4 [103,104], ORP5 [105], ORP7 [102] and ORP10 [106,107], and shown that ORP3 is frequently mutated in metastatic versus non-metastatic breast cancers [108]. In some cases, targeted research on individual ORPs has led to a limited mechanistic understanding of their contribution to the disease phenotype. This section outlines our current understanding of how OSBP/ORPs contribute to a range of human disorders and infections, followed by a section dedicated to an overview of ORP involvement in cancer.

1.4.1 OSBP/ORPs in Viral Infection, Replication and Release

Single-stranded RNA viruses replicate in the cytosol of host cells and employ the Golgi apparatus, ER and/or endosomal membranes as replication platforms, altering the morphology of the organelles using a combination of viral and host factors. The morphology of the hijacked host membranes, termed replication organelles, depends on the infecting virus. For example, dengue virus forms double-membrane vesicles of ER origin, while the single-membrane vesicles formed by poliovirus are ER-, Golgi- and lysosome-derived and arranged in rosettes [109]. As outlined below, OSBP, ORP1, ORP4 and ORP10 contribute to viral egress or replication processes.

Table 2 ORPs in human diseases.

Protein	Pathology	Notes	Study type	Ref
OSBP	Cholangiocarcinoma	Increased expression	qRT-PCR and immunohistochemistry	102
	ALS	Overexpression rescues mutant VAP-B phenotype	Drosophila study	110
ORP1	Dyslipidemia	Nonfunctional mutant is associated with HDL cholesterol <1st percentile	Small cohort study (n=80), genome sequencing and blood analysis	111
ORP2	Autosomal dominant nonsyndromic hearing loss	Truncation/deletion due to frameshift mutation causes hereditary hearing loss	Whole-exon sequencing of affected Chinese and German families	112,113
	Dyslipidemia	Expression inversely correlated with levels of hepatic steatosis marker Hsa-miR-855-5p and HDL cholesterol	microRNA profiling	114
ORP3	ALS	Overexpression rescues mutant VAP-B ER-stress phenotype	Cell culture study	110,115
	Glioblastoma	Expression associated with positive treatment response	RNA-seq	116
	Breast cancer	More frequently mutated in metastatic breast cancer than early breast cancer	Next-gen seq	108
	Dyslipidemia	Gain-of-function mutation in LRH-1 induces NAFLD in mice via ORP3 expression	Mouse study	117
ORP4	Pancreatic ductal carcinoma	High expression associated with poor prognosis	Microarray database analysis, immunohistochemistry	118
	Metastasis	Highly expressed in disseminated tumor cells	Differential display PCR	104,119
	T-cell acute lymphoblastic leukemia	High ORP4 expression provides energetic advantage via calcium signaling	Cell culture study, including patient samples	55
	Chronic myeloid leukemia	ORP4 elevated in 80% of CLM patients studied	RT-PCR of patient samples	103,120

Protein	Pathology	Notes	Study type	Ref
ORP4	Spermatogenesis	ORP4 KO causes male infertility by oligo-astheno-teratozoospermia	Mouse KO study	57
	Cholangiocarcinoma	Increased expression	qRT-PCR and immunohistochemistry	102
ORP5	Pancreatic cancer	Expression positively correlated with cancer cell invasiveness and poor prognosis	Cell culture studies based on patient gene expression profiles, includes patient samples	105,121
	Triploidy	Rare *OSBPL5* mutation may contribute to recurrent IVF failure by triploidy	Genotyping, whole-exome seq, methylation analysis	118
	Metastatic lung cancer	Increased expression in metastatic lung vs nonmetastatic lung tumor	2D-DIGE/antibody screen, tissue microarrays, cell culture studies	122
	Alcohol dependence	SNPs in *OSBPL5* are associated with alcoholism	GWAS	123
	Dyslipidemia	Expression level in leukocytes is positively correlated with plasma lipid levels	Microarray expression profiling	124
ORP6	Dyslipidemia	Expression level is positively correlated with HDL cholesterol levels	Cell culture studies and patient screen	61
	Alzheimer's	SNPs in *OSBPL6* are associated with familial Alzheimer's	GWAS	125
ORP7	Cholangiocarcinoma	Increased expression	qRT-PCR and immunohistochemistry	102
	Dyslipidemia	SNPs in *OSBPL7* are associated with total cholesterol and LDL levels	GWAS and genotyping	126,127
ORP8	Gastric cancer	Reduced expression	Cell culture study based on patient screen	128
	Cholangiocarcinoma	Increased expression	qRT-PCR and immunohistochemistry	102
	Dyslipidemia	SNPs in *OSBPL8* associated with HDL cholesterol levels	GWAS	129
		Obesity-related miRNA-143 reduced insulin-induced AKT activation in liver cells via reduction of ORP8 levels	Mouse study	130

Protein	Pathology	Notes	Study type	Ref
ORP8		Activin A from epicardial adipose tissue reduced ORP8 levels via miRNA-143	Cell culture study with primary rat cells	131,132
		ORP8 KD reduced arterial lesion size by 20% in HFD-fed LDLR-KO mice	Mouse study	133
		Lenz-Majewski disease mutations in PS synthesis alter counter-current transport by ORP8	Cell culture study	134
		Expression level in leukocytes is negatively correlated with plasma lipid levels	GWAS	
	Hepatocellular carcinoma	ORP8 expression is low in gastric and hepatic cancers; overexpression decreases tumor growth and increases apoptosis by mitochondrial and ER stress	Cell culture and mouse studies based on patient expression profiles	128,135
ORP9	Colorectal cancer	Elevated expression is positively correlated with survival	Whole genome expression profiling	136
	Dyslipidemia	SNPs in *OSBPL9* may be associated with increased risk of cerebral infarction	PCR-RFLP screen of Chinese cohort	137
ORP10	Dyslipidemia	SNPs in *OSBPL10* associated with extreme high TAG levels (>95th percentile), silencing increases lipogenesis and apoB-100 secretion in hepatic cell line	Cell culture experiments based on genotyping in Finnish dyslipidemic families	67,68
		SNPs in *OSBPL10* associated with hypercholesterolemia	Japanese cohort study	138
		RNA expression in leukocytes is positively correlated with plasma lipid levels	GWAS	124
		SNP in *OSBPL10* intron strongly associated with peripheral arterial disease	GWAS	139
	Prostate cancer	Potential cancer marker	Microarray analysis	106,107
	Hypertension	SNPs in *OSBPL10* may contribute to hypertension	Next-generation linkage association	140
ORP11	Dyslipidemia	SNPs in *OSBPL11* associated with metabolic syndrome	Genotyping of obese individuals	141
		Granular cholesterol staining in dermal tissue of individuals with homozygous *OSBPL11* missense mutation	Case study of family with rare neurodegenerative disease	142

Currently, the best-studied example of viral dependence on ORP function is the requirement for OSBP and ORP4 in development of the hepatitis C virus (HCV) replication organelle. HCV replication involves the translation of polyproteins, cleavage into active peptides and the establishment of a replication organelle, called the membranous web, from host membranes. A screen for host proteins associated with non-structural (NS) HCV proteins revealed that the ER-anchored viral protein NS5A interacts with both OSBP and VAP-A, and established that OSBP is required for the replication and egress of HCV particles [143]. Tai and colleagues determined that OSBP supplies the membranous web with cholesterol in a PI(4)P-dependent manner, similar to the exchange between the Golgi apparatus and ER (Section 1.3.1) [144]. The requirement for OSBP to supply cholesterol extends to the development of replication organelles by poliovirus and dengue [144], with concurrent studies showing similar results in picornavirus [145] and encephalomyocarditis virus infections [146]. These mechanistic findings conceptualized OSBP as a target for known and novel antiviral compounds; OSBP was identified to be a target of the anti-enteroviral compounds itraconazole and TTP-8307 [147,148] and overexpression of ORP4 or OSBP circumvent the antiviral properties of the ORPphilin OSW-1, suggesting these antiviral properties are a result of ORP4 and OSBP inhibition [41]. Interestingly, despite the dependence of OSW-1 antiviral activity on ORP4, ectopic expression of ORP4L or ORP4S inhibited the replication of HCV and produced infection-related lipid droplets on the membranous web [149], suggesting that ORP4 may contribute to cellular lipid metabolism by a different mechanism than OSBP.

In addition to viral replication and egress, OSBP has also been implicated in viral entry. Treatment of cells with interferon-inducible transmembrane protein 3 inhibited the

interaction between OSBP and VAP-A and cholesterol egress from the ER, leading to aberrant accumulation of cholesterol in the endocytic system that prevented cytosolic release of endocytosed vesicular stomatitis virus [150].

A study of dengue susceptibility in African, Asian and European populations revealed that SNPs which affect the expression of *OSBPL10* are protective in African populations. Functional studies using THP-1 leukemia cells demonstrated that ORP10 silencing significantly reduced viral replication and secretion [151]. Expression of an OHD deletion mutant of ORP1L reduced the infectivity of vesicular stomatitis virus presenting the Ebola glycoprotein by 50%, suggesting a requirement for ORP1L related to cholesterol transport or endosome motility/maturation in Ebola infection [97].

1.4.2 ORP2 and Hearing Loss

Whole exome sequencing identified frameshift mutations in *OSBPL2* that have been linked to familial autosomal dominant non-syndromic hearing loss [112,113]. ORP2 is ubiquitously expressed and enriched in cells of the central nervous system, and expression has been detected in cochlear inner and outer hair cells [112]. The effect of truncation and deletion mutations in ORP2 was predicted to be deleterious to expression and activity, but this was not experimentally confirmed and a functional link to the auditory system has not been established [113]. However, ORP2 was recently identified as a regulator of cell morphology, attachment, motility and proliferation via actin remodelling through the RhoA signaling pathway [45]. CRISPR-Cas9-mediated ORP2 knockout in HUH7 hepatocarcinoma

cells affected the expression of a number of RhoA effectors, including ARHGAP12 and DIAPH1, with which ORP2 interacts [45,152]. Interestingly, ARHGAP12 is expressed in inner ear hair cells at cell-cell junctions [153], while mutations in DIAPH1 are causative in autosomal dominant, non-syndromic hearing loss in an extended Costa Rican family [154]. These studies suggest that interaction between ORP2 and DIAPH1 could be essential to the function and morphology of cochlear hair cells.

1.4.3 ORP3 and OSBP in Heritable Amyotrophic Lateral Sclerosis

Amyotrophic lateral sclerosis (ALS) is a poorly-understood sporadic neurodegenerative disorder of motor neurons in which 10% of cases are attributed to heritable genetic components [155]. One of these is ALS8, a subtype caused by a loss-of-function point mutation in the major sperm protein domain of VAP-B [156,157], which interacts with the FFAT motif of partner proteins such as OSBP/ORPs. Mutant VAP-B forms aggregates with itself and wild-type VAP-A and VAP-B in detergent-insoluble vacuoles that sequester ER proteins, leading to mis-localization of Sac1 [115]. The resulting accumulation of PI(4)P on intracellular membranes impairs retrograde transport, a process crucial for trafficking neurotrophic cargo along axonal processes to the cell body in motor neurons, and which is often perturbed in ALS [158]. Interestingly, overexpression of ORP3 in HeLa cells prevented mutant VAP-B aggregation and rescued both PI(4)P accumulation and secretory phenotypes [115].

It is unclear whether lipid transport by ORP3 contributed to rescue of the mutant VAP-B phenotype, or if its overexpression titrated the mutant VAP-B, freeing wild-type VAP-A and B to interact with partner proteins. However, observations of the same VAP-B mutant in *D.melanogaster* support a model by which restoration of lipid transport rescues

the ALS8 defect [110]. Moustaqim-Barrette and colleagues noted that VAP depletion or expression of the ALS8 VAP-B mutant caused mislocalization of OSBP to the Golgi apparatus. This indicates that interaction between the FFAT domain of OSBP and mutant VAP is impaired by the ALS8 VAP-B mutation, making it unlikely that ORP3 over-expression titrated mutant VAP-B. To recapitulate *Osbp* function, but circumvent the need for an FFAT motif, human ORP8 was expressed in the *D.melanogaster* ALS8 model and rescued the ALS8 phenotype, suggesting that dissociation of the VAP-B mutant from FFAT-containing ORPs may induce catastrophic PI(4)P accumulation by preventing lipid egress from the Golgi apparatus.

1.4.4 ORPs and dyslipidemia

Dyslipidemia is defined as elevated levels of one or more lipoprotein species in the blood, which predisposes individuals to cardiovascular events, hepatic disease and metabolic syndrome. Dyslipidemias have genetic and lifestyle-related contributions, and can result from increased lipid production, decreased lipid clearance or increased lipid absorption from the diet. In cases of hypercholesterolemia, elevated LDL imposes cardiovascular risk while elevated high density lipoprotein (HDL) is considered beneficial [159]. Systemic HDL and LDL levels are dependent on cellular cholesterol synthesis, uptake, processing and secretion. Genetic screens of dyslipidemic patients and functional studies on mouse and cell culture models have confirmed a role for the OSBP/ORP family in all steps of this process.

Studies have implicated OSBP/ORPs in lipid dysregulation without identifying specific mechanisms. ORP3 was recently identified as a liver receptor homolog-1 (LRH-1) target gene responsible for the increased *de novo* cholesterol synthesis and hepatic

steatosis observed in mice expressing a gain-of-function LRH-1 mutant [117]. In a genetic screen of 871 Finnish adults, increased levels of the hepatic steatosis marker hsa-miR-885-5p were found to be inversely correlated with ORP2 expression and HDL cholesterol levels [114]. Studies of hyperlipidemic Finnish [67] and Japanese [139] families identified SNPs in the *OSBPL10* gene that were linked to elevated plasma TAG and HDL levels. These findings prompted cell culture studies in which ORP10 was found to associate with microtubules and the Golgi apparatus to promote lipoprotein secretion [67,68]. However, the connection between the *OSBPL10* SNPs and plasma lipid levels remains obscure.

A heterozygous loss-of-function mutation in ORP1L, which delivers lipoprotein-derived cholesterol from the LEL to the ER for storage and efflux (Section 2.3), was identified in patients with extremely low levels of HDL cholesterol [111]. Individuals with the loss-of-function ORP1L mutation exhibited decreased plasma levels of apolipoprotein A-1 (apoA-1) as well as decreased cholesterol efflux to available apoA-1. Therefore it remains unclear whether the mutation is associated with impaired cholesterol efflux by ATP binding cassette subfamily A member 1 (ABCA1) to apoA-1 or impaired secretion of apoA-1 from the liver or other tissues. The former mechanism is supported by ORP1L silencing experiments in cultured macrophages that showed significantly reduced efflux of [^{3}H]cholesterol to apoA-1in the media [13]. Overall, these findings are consistent with a model in which ORP1L-mediated export of cholesterol from the LEL is coupled to efflux from cells by a ABCA1-dependent pathway. ORP6 may have a related function since its expression was positively correlated with HDL cholesterol levels in healthy human subjects, and decreased in the atherosclerotic plaques of LDL receptor knockout (LDLR-KO) mice [61].

Homozygous knockout of ORP4 in mice was also shown to reduce atherosclerotic lesion size by a mechanism independent of cholesterol efflux. Rather, ORP4 promotes macrophage survival in atherosclerotic plaques, attenuating oxysterol-induced cytotoxicity by a pro-survival calcium signaling pathway (Section 1.5.3) [54]. ORP8 expression is increased in human atherosclerotic plaques [63], and the macrophage-specific knockout of ORP8 in LDL receptor-null mice attenuated arterial lesion size and inflammation [133]. A potential link between ORP8 and lesion formation was strengthened by the finding that ORP8 negatively regulated cholesterol efflux by cultured macrophages via transcriptional suppression of ABCA1 [63] and *OSBPL8* knockout mice have significantly elevated HDL levels [13]. Consistently, overexpression of ORP8 in cultured hepatocytes reduced lipid secretion by interaction with nucleoporin Nup62 [64]. Reduction of ORP8 by obesity-associated miR-142 in both liver and vascular smooth muscle cells attenuated stimulation of hepatic AKT by insulin, but the mechanism by which ORP8 expression affects AKT activation is currently unknown [130-132].

Like ORP8, SNPs in *OSBPL11* were associated with altered metabolism of lipids and glucose in obese populations [141], and siblings homozygous for a loss-of-function ORP11 missense mutation display abnormal dermal cholesterol deposits [142]. Interestingly, ORP8 and ORP11 normally follow opposing expression patterns during adipocyte differentiation (reduced and increased, respectively), and in cell culture studies the overexpression of ORP8 or silencing of ORP11 impedes TAG storage [70]. In general, these studies show that select ORPs are involved, either directly or indirectly, in pathways that remove or prevent accumulation of cholesterol in cells of the cardiovascular system, leading to reduced risk of atherosclerosis.

1.5 ORPs IN CANCERS

While genetic screens have associated the expression and/or mutation of individual ORPs with various cancers (Table 2), only ORP5, ORP8, ORP4 and OSBP were investigated to confirm a functional role in malignancy. Here, we review the current understanding of how these ORPs contribute to cancer cell invasion, evasion of apoptosis and proliferation.

1.5.1 ORP5 and Invasiveness in Pancreatic Ductal Carcinoma

Chemical-induction of pancreatic ductal carcinoma in hamsters yielded two cell lines, PC1 and the more invasive PC1.0, that are used as models of the human disease [160,161]. Analysis of mRNA profiles of the two cell lines revealed *OSBPL5* and 4 genes that were differentially expressed in PC1.0 cells. Silencing of ORP5 in PC1.0 cells significantly decreased invasiveness while the converse result was obtained by ORP5 overexpression in PC1 cells [105]. Similar results were obtained in human pancreatic cancer cell lines [121]. In pancreatic cancer patients, increased *OSBPL5* expression was correlated with a 50% reduction in 1-year survival, and a nearly 70% reduction in median survival time in patients with stage I, II and III cancers [105].

The mechanism by which ORP5 increases cancer cell invasiveness could involve upregulation of oncogene expression through effects on the cholesterol biosynthetic pathway. Under cholesterol-replete conditions, SREBP2 is sequestered in ER membranes, whereas lowering ER cholesterol promotes SREBP translocation to the Golgi apparatus for proteolytic processing to release the soluble transcription factor, which translocates to the nucleus and binds sterol response elements (SREs) in gene promoters [162]. The promoter

region of the histone deacetylase 5 gene *HDAC5* has an SRE, placing oncogenic HDAC5 expression under sterol control [163]. Treatment with the HDAC inhibitor trichostatin-A significantly reduced cell growth in ORP5-positive pancreatic cancer cell lines [121]. However, the mechanistic link between ORP5 and SREBP2 is uncertain; ORP5 binds and transfers cholesterol *in vivo* and is required for the delivery of LDL-derived cholesterol to the ER [40,59], which would in theory restrict SREBP2 activation and subsequent *HDAC5* expression. Also, this study observed synergistic antiproliferative effects of trichostatin-A and the cholesterol synthesis inhibitor simvastatin, which would have opposing functions if HDAC expression were being induced by the SREBP2 [163]. Future studies to evaluate how ORP5 affects SREBP2 processing in the ER, and the link to expression of oncogenic genes, are warranted.

Recently, a possible connection between ORP5 and SREBP2 activation has been identified. ORP5 over-expression increases cell proliferation and invasiveness in HeLa cells via activation of mammalian target of rapamycin complex 1 (mTORC1) that requires interaction between mTOR and the ORP5 OHD, as well as functional ORP5 ligand binding [164]. ORP5 depletion was found to modestly decrease cell growth by preventing the lysosomal localization and subsequent activation of mTORC1. mTORC1 is a nutrient-sensitive signaling complex that, when active, activates downstream proliferative signaling cascades such as the Akt and S6K pathways, and in turn activates lipid biosynthetic proteins [165] including SREBP2 [166,167]. Whether ORP5 promotes lysosomal localization and activation of mTORC1 via direct interaction with mTOR or remodeling of the PM and lysosomal membranes is currently unknown and provides a promising avenue for new ORP5 research.

1.5.2 ORP8 Promotes Apoptosis by the Fas-Receptor Pathway

Fas receptor binding of autocrine or paracrine-secreted Fas ligand leads to the initial activation of caspase 8 and a resulting cascade of caspase autoproteolysis that ultimately leads to cell death [168]. Immunohistochemical analysis of liver tissue from patients with hepatocellular carcinoma (HCC) revealed that malignant cells contained less cell-surface and more internal Fas receptor than non-malignant counterparts, implying that HCC cells may avoid apoptosis due to insufficient Fas receptor presentation [169]. ORP8 was identified as a necessary factor for the PM presentation of Fas in HCC cell lines and patient tissue samples in which ORP8 expression is reduced by miR-143 [135]. Expression of ORP8 in HCC cells induced Fas-mediated apoptosis by shifting cytosolic Fas to the PM, while expression of ORP8 reduced the size of mouse tumor xenographs. However, the apoptotic effect of ORP8 may be specific to HCC; ORP8 expression was increased in a hamster model of cholangiocarcinoma [102], and ORP8 expression in HepG2 cells mediated cell-cycle inhibition by 25-hydroxycholesterol but did not induce apoptosis [62].

1.5.3 ORP4 in Leukemia and Metastasis

ORP4 is a closely related paralogue of OSBP [8], sharing domain organization and approximately 75% sequence identity, but differing in tissue expression, localization and function. Alternate promoter start sites in *OSBPL2* produce three ORP4 variants; full-length ORP4L [31], and ORP4M [52] and ORP4S [170] that have truncated and deleted N-terminal PH domains, respectively. Like OSBP, ORP4 binds cholesterol, oxysterols and PI(4)P at the OHD [40,51,53] and has a central FFAT motif. ORP4L also has a PH domain that recognizes PI(4)P in the Golgi apparatus and negatively regulates interactions between the OHD of ORP4 and vimentin intermediate filaments, and absence or truncation of the PH

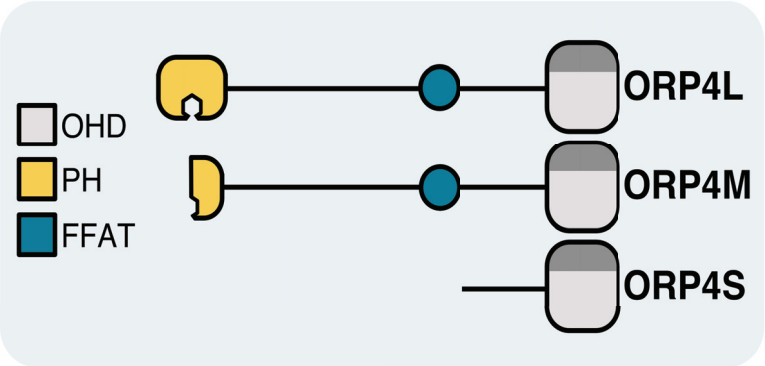

Figure 1.4 *ORP4 is expressed as three isoforms*. Differential splicing of ORP4 leads to variable transcriptional start sites, yielding three ORP4 isoforms: a 101 kDa full-length protein (ORP4L), an 85 kDa medium isoform with a truncated PH domain (ORP4M) and 60 kDa short variant lacking both the FFAT motif and PH domain (ORP4S).

domain collapses the vimentin network [51-53].

ORP4 is the only member of the ORP family required for the proliferation of cultured cells [52]. Silencing of ORP4L induced growth arrest and cell death in immortalized and cancerous cell lines, which was exacerbated by knockdown of all three variants. Despite the apparent involvement of ORP4 in signaling pathways that are essential for cell survival and proliferation, ORP4 knockout mice develop normally except for male sterility due to defective sperm elongation [57]. Thus, the cytotoxic effects of ORP4 depletion seem to be specific to cultured malignant cells, which display increased expression of ORP4 variants relative to normal controls [52,55]. Moreover, ORP4 is inhibited by naturally-occurring antineoplastic saponins termed ORPphilins for their ability to inhibit OSBP with low-nanomolar affinity [88]. The ORPphilins, which include OSW-1 (from *Ornithogalum saundersiae*), cephalostatin 1 (from *Cephalodiscus gilchristi*), ritterazine B (from *Ritterella tokioka*) and schweinfurthin A (from *Macaranga schweinfurthii*) (Figure 1.5), compete for sterol ligands in the OHD of both ORP4 and OSBP and ultimately induce cell death and growth arrest. ORPphilin cytotoxicity was abolished by over-expression of OSBP and ORP4, or by addition of exogenous sterols that competed for binding to the ORP4 and OSBP OHD [88].

Due to the absence of a reliable antibody for endogenous ORP4, the majority of the study characterizing the ORPphilins was performed with a focus on OSBP; however, some interesting insights into ORP4 function can be extrapolated from this study. Firstly, the antineoplastic effects of the ORPphilins may be primarily due to inhibition of ORP4 rather than OSBP, considering that growth arrest is observed in cells expressing shORP4 [52,55,56,171] but not shOSBP [172]. Secondly, while Schweinfurthin A, which had 40x lower affinity for

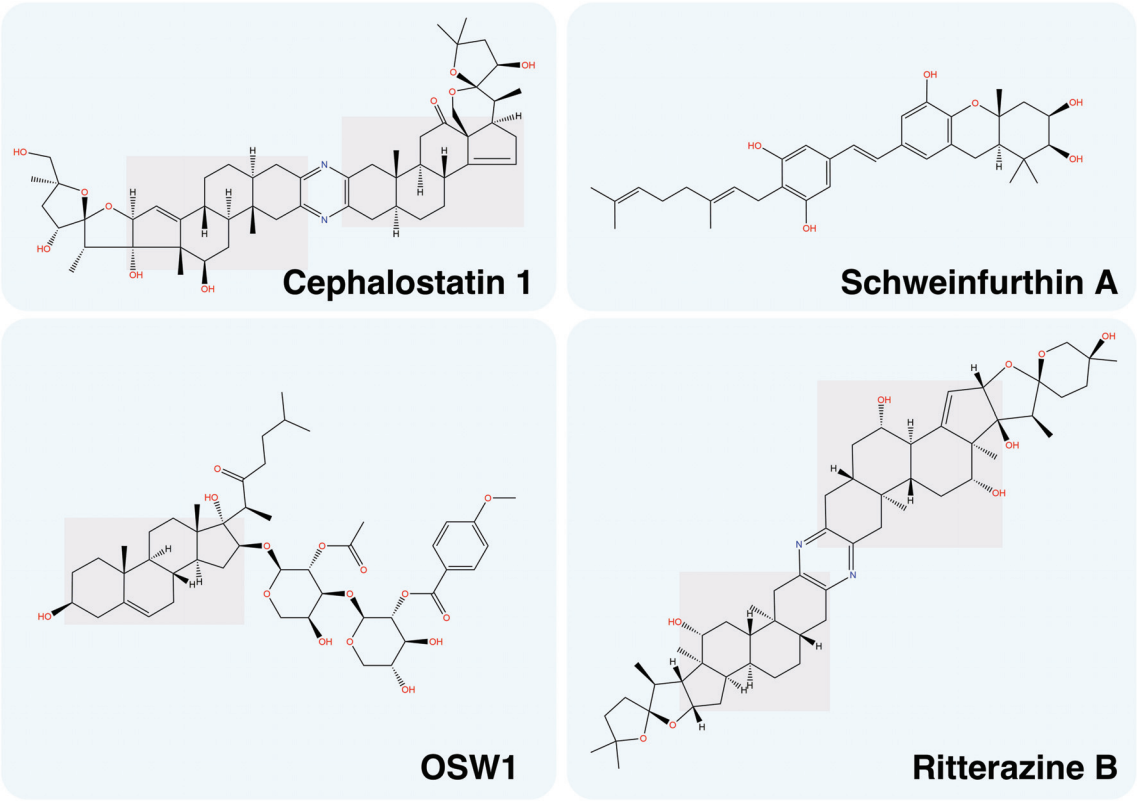

Figure 1.5 *The ORPphilins*. A family of naturally-occurring antineoplastic ORP4 and OSBP inhibitors. The tetracyclic sterol ring structures are highlighted.

ORP4 than OSBP, induced Golgi localization of OSBP similarly to 25OH treatment, OSW-1 and cephalostatin 1 induced perinuclear and PM OSBP staining, respectively, while dispersing a TGN marker p230. Interestingly, OSW-1 and cephalostatin 1 induce proteolysis of OSBP, but TGN dilation has not previously been observed in OSBP-depleted cells [173]. Also, schweinfurthin A, which lacks the tetracyclic sterol moieties highlighted in the rest of the class in Figure 1.5, bound ORP4 with approximately 40x lower affinity than OSBP (K_D = 2.6 μM) and did not disperse the TGN. Together, these results suggest that ORP4 may regulate the function and morphology of the TGN, though ORP4 has not previously been observed in that compartment.

Elevated ORP4 transcripts in disseminated tumor cells and the leukocytes of patients with chronic myeloid leukemia distinguished this ORP as a potential bio-marker or regulator of metastasis [103,104,119,120]. The limited expression profile of ORP4 in normal tissues (brain and testis, see Table 1) but markedly increased expression in transformed cells suggests that aberrant expression of ORP4 provides a proliferative advantage. Yan and colleagues reported a proliferative mechanism whereby ORP4 expression in T-cell acute lymphoblastic leukemia (T-ALL) caused increased oxidative phosphorylation not observed in normal T-cells, which did not express ORP4 [55]. In T-ALL cells, ORP4L bridges cell surface receptor CD3ε with PLC3β and its PM-associated G protein activator, $G_{\alpha q/11}$, forming an activation complex that is otherwise absent in normal T-cells. ORP4L-mediated activation of PLC3β produces inositol triphosphate which induces ER calcium release and ATP production, thereby providing cells aberrantly expressing ORP4 with an energetic advantage compared to their non-transformed counterparts [55,56]. In the absence

of ORP4L, inositol triphosphate signaling is attenuated, leading to mitochondrial dysfunction and T-ALL cell death.

Direct interactions between ORP4 and the vimentin intermediate filament network suggest that the correlation between ORP4 expression and tumor dissemination may involve the epithelial-to-mesenchymal transition (EMT). EMT is a complex intracellular signaling process by which epithelial cells differentiate into mesenchymal cells, often contributing to metastasis outside the context of development [174]. During EMT, extracellular stimuli such as growth factors or cytokines cause deactivation of glycogen synthase kinase (GSK) by Ras or mitogen-activated protein kinase. GSKa and GSKb normally prime Snail family transcriptional repressors and transcription factor β-catenin for proteosomal degradation. Therefore, GSK inactivation consequently activates these transcription factors and begins the EMT transcriptional program. This ultimately results in the loss of epithelial cell characteristics, such as cell polarity and cell-cell contacts, and the adoption of mesenchymal cell characteristics, such as increased motility and fewer intercellular junctions. Vimentin expression is increased as a result of the EMT transcriptional program, and contributes to the increased motility and invasiveness of cells undergoing this process [175]. The increased motility conferred by vimentin expression is due to increased turnover of cell adhesion molecules such as integrins. While vimentin has no associated motor proteins, integrin-containing transport vesicles are sequestered on vimentin and released in a recycling pathway, the rate of which determines the direction and rate of cell movement.

All three ORP4 variants interact with the vimentin intermediate filament network but ORP4M and ORP4S collapse the network, suggesting negative regulation of this

interaction by the ORP4L PH domain [51-53]. However, the ORP4/vimentin interaction is independent of sterol binding [51], and it is therefore unknown how this regulation is itself controlled. Large-scale phosphoproteome studies [176-178] suggest that ORP4 is phosphorylated at a number of serine residues, but the functional significance of these phosphorylation events is unknown. Considering the elevated expression of ORP4 in metastases [103,104,119,120] and the regulatory role of vimentin in cell adhesion and motility [175], a better understanding of what regulates the ORP4/vimentin interaction is needed.

To summarize, most studies implicating ORPs in cancers are large-scale genomic analyses which have associated ORP genes SNPs with either cancer progression or survival (Table 2). However, the consequences of these SNPs on gene transcription or protein function are unknown. The limited analysis available suggest that those ORPs implicated in cancer initiation or progress do so downstream of their primary lipid binding/transfer functions. However, the role for ORP4L in survival of lymphoblastic T-cells indicates that other scaffold/signaling mechanisms may apply.

1.6 Significance and Rationale for this Study

Changes in ORP4 expression are implicated in metastatic cancers and infections by common pathogenic viruses, but the fundamental role of ORP4 in the cell remains obscure. An emerging recognition that OSBP/ORPs mediate lipid transport and regulate metabolism at MCS suggest that growth arrest associated with loss of ORP4 expression is due to deleterious changes in the intracellular distribution of its ligands, cholesterol and PI(4)P. Alternatively, considering that ORP4 exhibits nanomolar affinity for oxysterols, it may act as a high-affinity receptor that regulates signaling pathways via protein-protein or protein-

membrane interactions. While both are attractive possibilities as primary functions of the ORP4, the multivalent roles of other ORPs suggest these could be dichotomous functions. For example, sterol-binding by ORP1L [97] and OSBP [179] alter interactions with their respective protein partners, making them candidate sterol-regulated scaffolding proteins for functional complexes at membranes. However, both have also been shown to bind and transport lipids *in vitro* [34,39]. ORP4 may contribute to cell proliferation in a similar way, both transporting lipids between intracellular compartments and scaffolding protein complexes in a ligand-dependent manner.

I have applied both cell culture techniques and *in vitro* analysis to characterize the ligand binding properties of ORP4, and how post-translational modification affects the ability of ORP4 to interact with organelle membranes and protein partners vimentin and OSBP. Rather than mediating the bulk transfer of lipids that would largely affect lipid metabolism or membrane composition on a large-scale, I hypothesize that ORP4 may mediate cell proliferation via subtle effects on the phospholipid composition of small, discrete membrane regions significant in cell signaling events at the Golgi, ER and PM. Chapter 3 summarizes my contributions to the finding that ORP4 is a sterol- and PI(4)P-binding protein required for the proliferation of cultured cells [52]. In an attempt to elucidate how ORP4 depletion causes growth arrest and apoptosis, we discovered morphological TGN defects induced by ORP4 silencing and characterized the Golgi localization of ORP4 and how it is regulated by ligand binding, which is summarized in Chapter 4. Finally, Chapter 5 describes the discovery that ORP4 ligand extraction and the ORP4/vimentin interaction are phospho-regulated, and describe for the first time evidence of ORP4 homodimerization. Chapter 6 concludes this dissertation with a comprehensive review of

our findings and how they can be interpreted with the current body of knowledge to inform future studies of ORP4 function.

CHAPTER 2 METHODS

2.1 MATERIALS

Thin-layer chromatography (TLC) plates were purchased from Analtech (Newark, DE). Gel filtration-high performance liquid chromatography (GF-HPLC) was performed using a YARRA SEC-3000 column purchased from Phenomenex (Torrance, CA). Hybond-C nitrocellulose and protein A-Sepharose were obtained from GE Healthcare (Little Chalfont, UK). EDTA-free protease inhibitor was obtained from Roche (Basel, Switzerland). mCherry-SidM was a gift from Tamas Balla (Addgene plasmid # 51471) and mCherry-PLCδ-PH was a gift from Narasjmhan Gautam (Addgene plasmid # 36075). Lipofectamine 2000 transfection reagent and the BaculoDirect Baculovirus Expression System were purchased from Life Technologies (Carlsbad, CA). SF-900 insect cell medium, Dulbecco's modified Eagle medium (DMEM), minimal essential medium α (αMEM) and FluoroBrite medium were purchased from Gibco (Waltham, MA). Talon cobalt affinity resin was purchased from Clontech (Mountain View, CA), and GelCode Blue stain reagent was purchased from ThermoFisher Scientific (Waltham, MA).

2.1.1 Antibodies

Antibodies against TGN46 (Cat.# A304-435A, Bethyl Laboratories, Montgomery TX), PI(4)P (Cat.# Z-P004, Echelon, Salt Lake City, UT), vinculin (Cat.# Ab130007, Abcam, Cambridge UK) and V5 (Cat.# SV5-Pk1, BioRad, Raleigh NC) were used for immunostaining and western blotting. Antibodies for immunostaining of giantin and GALNT were purchased from BioLegend (Cat.# 924302 and 682302, respectively, San Diego, CA). Antibodies for immunoblotting of PARP and caspase-3 antibodies were

purchased from Cell Signaling (Cat.# 9542 and 9662, respectively, Danvers, MA). An affinity-purified rabbit polyclonal was raised against a GST-fusion protein encompassing amino acids 380-473 of ORP4L [51]. Vimentin antibody and a polyclonal antibody targeting amino acids 342-465 of ORP4L were purchased from Sigma-Aldrich (Cat.# V6630 and HPA041127, respectively, St. Louis, MO). OSBP 11H9 monoclonal [6] and polyclonal antibodies [180] were used to detect over-expressed and endogenous OSBP, respectively, by immunoblotting or immunostaining. Secondary IRDye 800CW- and IRDye 680LT-conjugated antibodies (LI-COR Biosciences, Lincoln, NE) and Alexa Fluor 488- and Alexa Fluor 594-conjugated antibodies (Molecular Probes, Eugene OR) were used for immunoblotting and immunostaining, respectively.

2.1.2 Lipids

Cholesterol and 25-hydroxycholesterol were purchased from Steraloids (Newport, RI). L-[^{3}H(G)]-serine, [1, 2-^{3}H]-cholesterol and 25-[26, 27-^{3}H]-hydroxycholesterol were purchased from PerkinElmer Life Sciences (Boston, MA). [^{14}C]-dipalmitoyl-phosphatidylcholine was purchased from American Radiolabeled Chemicals (St. Louis, MO). Phosphatidylcholine (PC), phosphatidylethanolamine (PE), lactosyl-PE and PS were purchased from Avanti Polar Lipids (Alabaster, AL). Glucosylceramide was purchased from Matreya LLC (State College, PA).

2.2 SITE-DIRECTED MUTAGENESIS AND PLASMID CONSTRUCTION

2.2.1 Production of V5-tagged ORP4 Ligand Binding Mutants

An shRNA-resistant pcDNA-ORP4L-V5-His (ORP4L-V5) was used to mutagenize H589 and H590 to alanine (ORP4L-HH/AA-V5), Y415 and F416 to alanine (ORP4L-YF/AA-V5) and to create an amino acid 501-505 deletion (ORP4L-Δ501-505-V5). The mutagenic primers are listed in Table 3. Mutations were confirmed by sequencing. pEGFP-ORP4L was prepared by restriction digestion of ORP4L-V5-His with SacII and HindIII and ligation into pEGFP-N1 digested with the same enzymes.

2.2.2 Construction of ORP4 Phosphorylation Site Mutants

pcDNA-ORP4L-V5 was subjected to site-directed mutagenesis at S_{762}, S_{763}, S_{766} and S_{768} to prepare phospho-mimetic (serine-to-aspartate) and phospho-resistant (serine-to-alanine) mutations referred to hereafter as "S/D" and "S/A", respectively. The His-tag was not used for detection or purification of ORP4L expressed in mammalian cells in this study, and has therefore been omitted from labeling for simplicity. ORP4S-S/D-V5 and ORP4S-S/A-V5 constructs were made by endonuclease digestion of pcDNA-ORP4L-V5 S/D and S/A constructs with AfeI and EcoRV and ligation into pcDNA3.1-V5-HIS digested with EcoRV. To create the baculoviral constructs, S/A and S/D mutations were made by site-directed mutagenesis of a previously described pENTR/D-TOPO-ORP4L vector (Invitrogen, Carlsbad CA) [52]. Mutations were verified by sequencing and ORP4L-S/D and ORP4L-S/A were cloned into linear baculovirus DNA by recombination using the Gateway cloning system to introduce a C-terminal 6xHis-tag (Invitrogen). Mutagenic primers are listed in Table 3.

Table 3 Mutagenic primers.

Primer	Sequence (5'-3')
HH/AA For	CTC TGT GAG CAG GTG AGC GCC GCA CCA CCC TCA GCT GCG
HH/AA Rev	CGC AGC TGA GGG TGG TGC GGC GCT CAC CTG CTC ACA GAG
501-505 F2	GGC CGG GAG CTC TCC AGG ATC TTC AAT GAG CCG CTG TCC ATG CTC CAG
501-505 R2	CTG GAG CAT GGA CAG CGG CTC ATT GAA GAT CCT GGA GAG CTC CCG GCC
YF/AA For	GAT GAA GAT ACC GAG GCC GCT GAT GCC ATG GAA GAC
YF/AA Rev	GTC TTC CAT GGC ATC AGC GGC CTC GGT ATC TTC ATC
ForORP4-S/A	G GTC ATG CAT GCC GCT CCC AGC GCA CCC GCC TCT GAC GGG AAG C
RevORP4-S/A	G CTT CCC GTC AGA GGC GGG TGC GCT GGG AGC GGC ATG CAT GAC C
ForORP4-S/D	G GTC ATG CAT GAC GAT CCC AGC GAT CCC GAC TCT GAC GGG AAG C
RevORP4-S/D	G CTT CCC GTC AGA GTC GGG ATC GCT GGG ATC GTC ATG CAT GAC C

2.3 CELL CULTURE

2.3.1 Culture Conditions and Transient Transfection

HeLa and HEK 293T cells were cultured in DMEM supplemented with 10% (v/v) FBS (Medium A). HeLa cells stably expressing a lentiviral shOSBP were cultured in Medium A with blasticidin (2 mg/ml). CHO cells expressing lentiviral non-targeting shRNA (CHO-shNT) and shOSBP (CHO-shOSBP) were previously described [181], and cultured in DMEM supplemented with 35 μg/mL proline, 5% (v/v) FCS and blasticidin (2 mg/ml). IEC-18 and the H-ras-transformed IEC clone RAS3 were cultured in α-minimal essential media supplemented with FBS (5% v/v), insulin (12.74 μg/mL), glutamine (2.92 mg/mL), streptomycin (100 μg/ml), penicillin (600 μg/ml) and D-glucose (3.6 g/mL). Transient transfection of cells with plasmids was performed with Lipofectamine 2000 for 24 or 48 h, as appropriate for the experiment.

SF21 cells were cultured in monolayers or in suspension at 27°C with constant shaking at 150 rpm, in SF900-II medium supplemented with 5% (v/v) FBS, 10 μg/mL G418, 0.25 μg/mL fungizone and 100 U/mL penicillin-streptomycin-glutamine (Gibco) (SF21 media). Transfection of SF21 cells with baculovirus DNA was performed using Cellfectin transfection reagent according to the manufacturer's protocol to produce a preliminary low-titre viral stock used to infect a larger culture. Viral stocks were collected from subsequent infections until an optimal titre of 2-3x10^8 plaque-forming units/mL was achieved.

2.3.2 Lentiviral Production and Transduction

HEK 293T cells [182] were transfected with lentiviral packaging (psPAX2, 2 μg) and envelope (pMD2.G, 1 μg) vectors and pLKO.1 constructs encoding non-targeting shRNA (shNT; CAA CAA GAT GAA GAG CAC AAC) or an shRNA targeting all three ORP4 isoforms (shORP4; CAT CAC ATC CAA TGC TAT GAT) using polyethyleneimine (PEI). DNA was incubated with PEI in DMEM (final volume 1 mL) for 15 min at room temperature, then added to 7 mL of DMEM and applied to cells at 37°C and 5% CO_2 for 4-6 h, after which time the media was supplemented with FBS to a final concentration of 10%. After 72 h, media was collected and filtered (0.45 μm pore size), supplemented with 5 mg/mL polybrene, flash-frozen in liquid nitrogen and stored at -80 °C. For transduction, lentivirus was applied to cell monolayers in medium A containing 5 mg/mL polybrene and incubated for 48 h prior to selection with 2 μg/mL puromycin for an additional 48 h. IEC were more susceptible to shORP4-induced apoptosis and as such were not subjected to 48 h puromycin selection.

2.4 RECOMBINANT PROTEIN PRODUCTION

2.4.1 Bacterial Expression of GST Fusion Proteins

pGEX-3X constructs encoding wild-type, sterol-binding deficient (Δ501-505) or PI(4)P-binding deficient ($H_{589}H_{590}$/AA) glutathione *S*-transferase (GST)-tagged ORP4-OHD (amino acids 380-878) were described by Wyles and colleagues [53]. Overnight cultures of BL21 cells harbouring the pGEX-ORP4-OHD constructs were used to inoculate 600 mL of Luria-Bertani broth (10 g/L peptone, 5 g/L each NaCl and yeast extract) and cultures were grown to an OD_{600} of approximately 0.5 at 24°C with constant shaking.

Protein induction was initiated by addition of 1 mM isopropyl-1-thio-β-D-galactopyranoside (IPTG) for 3 h at 37°C with constant shaking. Cells were harvested by centrifugation at 4°C, washed in Buffer A (10 mM Tris, 30 mM EDTA, 25% sucrose (w/v), pH 7.5) and incubated with 2 mg/mL lysozyme for 1 h on ice. Cells were lysed in Buffer B (10 mM Tris, 1 mM EDTA, 1 mM DTT and 1x protease inhibitor cocktail, pH 7.4) by repeated passage through an 18-gauge needle, mixed with Buffer C (20 mM HEPES, 100 mM KCl, 0.2 mM EDTA, 20% glycerol, 1 mM DTT and 1x protease inhibitor cocktail, pH 7.6) containing 1% Triton X-100 and passed through the needle again. Cell debris was removed by centrifugation at 35,000 rpm for 30 min at 4°C, and protein was purified by gravity-flow chromatography on glutathione-Sepharose at room temperature in Buffer C. Protein was eluted in Buffer C supplemented with 25 mM glutathione and stored at -80°C. Protein quantified by the μLowry method (described in Section 2.5) was adjusted for degradation according to the ratio of tagged protein to cleaved GST observed by SDS-PAGE.

2.4.2 Baculoviral Expression of 6xHis-Tagged Proteins

Baculovirus encoding 6xHis-tagged ORP4L, ORP4L-S/A and ORP4L-S/D were made by recombination of pENTR-ORP4L constructs with baculovirus DNA arms using Baculodirect™ Expression System (Invitrogen) according to manufacturer's protocol. SF21 suspension cultures (0.1 and 0.2 L) were transduced with baculovirus at approximately 0.1 MOI for 72 h, collected by centrifugation and stored at -80°C. Cell pellets were resuspended in Talon wash buffer (TWB; 10 mM Tris, 150 mM NaCl, 30 mM imidazole, pH 7.0) supplemented with EDTA-free protease inhibitor cocktail and disrupted

by 3 passages through an 18 G needle and 1 pass through a 25 G needle. Cells were lysed on ice by sonication and insoluble cell debris was removed by centrifugation at 17,000 *g* for 1 h (4°C). Lysates were incubated with Talon cobalt affinity resin on a rotating mixer for 2 h (4°C). Bound protein was batch-washed 3 times in 10-20-volumes of TWB, and eluted in TWB containing 150 mM imidazole. Protein was concentrated by centrifugation in Millipore Amicon columns (30 K cut-off), diluted in storage buffer (10 mM Tris, 150 mM NaCl) and concentrated again. Aliquots were flash-frozen in N_2 and stored at -80°C.

2.5 PROTEIN QUANTIFICATION

Purified recombinant proteins were quantified using the μLowry method [183]. In brief, samples diluted to 400 μL dH_2O were mixed with 400 μL of a solution of equal parts dH_2O, 0.8 N NaOH, 1% (v/v) SDS and copper tartrate/carbonate (10% sodium carbonate, 0.1% copper sulfate, 0.2% potassium tartrate, all w/v). After 10 min at RT, 200 μL of 5x diluted Folin & Ciocalteau's phenol reagent (Sigma-Aldrich, St. Louis MO) was added to each sample and incubated for 30 min at RT. Absorbance was measured at 660 nm and compared to a BSA standard curve.

To measure whole-cell protein content (such as for assays of sphingomyelin synthesis described below in section 2.11), a commercial microplate-based bicinchonic acid assay was used (Pierce, Rockford IL). Cell extracts were allowed to dry at room temperature and resuspended in 200 μL 1N NaOH. Assays were performed according to manufacturer protocol and quantified by measuring absorbance at 562 nm.

2.6 PROTEIN-LIPID OVERLAY BLOT

Lipid overlay blots were performed as described by Munnik and Wierzchowiecka [184]. Phosphatidylinositol mono- and polyphosphates were spotted on Hybond-C nitrocellulose alongside PC and solvent negative controls. Membranes were dried for 1 h and then blocked with TBST (20 mM Tris-HCl, 150 nM NaCl, 0.1% (v/v) Tween 20, pH 7.4) supplemented with 3% (w/v) fatty acid-free BSA overnight at 4°C. Membranes were incubated with recombinant ORP4S (50 nM), OSBP (100 nM) or ORP4L (100 nM) for 1 h in blocking buffer. Membranes were then probed with the appropriate primary and IRDye-conjugated antibodies and visualized using an Odyssey infrared imager (LI-COR Biosciences, Lincoln NE).

2.7 LIPID EXTRACTION ASSAYS

2.7.1 PI(4)P Radiolabeling and Purification

For PI(4)P extraction assays, [^{32}P]PI(4)P was purified from HeLa cells radiolabeled with 0.5 mCi/dish $^{32}PO_4$ for 16-20 h in phosphate-free DMEM supplemented with 2% FBS. Cells were harvested and lipids were extracted with 3.8 mL chloroform:methanol:12 N HCl (2:4:0.1, v/v), 1.2 mL chloroform and 1.2 mL dH_2O. Phases were separated by centrifugation and the organic phase was dried under N_2 and lipids were resolved by TLC with a mobile phase of chloroform:methanol:4 M ammonium hydroxide (90:70:20, v/v). PI(4)P was identified by autoradiography and iodine staining in comparison to unlabeled PI(4)P (Avanti Polar Lipids), scraped from the plate and extracted again as described above. The resulting radiolabeled PI(4)P was resuspended in chloroform, quantified by liquid scintillation counting and stored under N_2.

2.7.2 Liposome Preparation

Liposomes for cholesterol extraction assays contained 120 DPM/pmol [^{14}C]PC and 60,000 DPM/pmol [^{3}H]cholesterol, and were composed of PC/PE/PS/lactosyl-PE/[^{3}H]cholesterol (59:20:10:10:1). PI(4)P extraction liposomes contained 40 DPM/pmol [^{32}P]PI(4)P in PC/PE/PS/lactosyl-PE/PI(4)P (60:20:10:10:0.5, mol/mol). Liposomes were prepared by drying lipid mixtures under N_2, then resuspending in extraction buffer (25 mM HEPES, 150 mM NaCl, 1 mM EDTA, pH 7.4) by frequent vigorous vortexing over the course of 1 h. Liposomes were then extruded through 400 nM diameter membranes using the AVESTIN LiposoFast system (Ottawa, ON) and aggregates were removed by centrifugation at 15,000 *g* for 5 min.

2.7.3 Quantification of Lipid Extraction from Liposomes

Extraction assays were performed by incubating 20 μL of liposomes with 100 pmol protein in extraction buffer (final assay volume of 80 μL) for 20 minutes at 25°C. Liposomes were precipitated by incubation on ice with 10 μg *R. communis* agglutinin for 15 min. Liposomes were sedimented by centrifugation and 50 μL of the supernatant, containing protein and extracted PI(4)P, was measured by liquid scintillation counting. Liposomes were solubilized in 100 μL 1% SDS in a bath sonicator and 50 μL of solubilized liposomes were measured by scintillation counting. Extraction is expressed as the percentage of radioactivity in the supernatant compared to the liposome pellet, and values are adjusted for background measured by conducting the experiment with no added protein.

2.8 STEROL BINDING ASSAYS

Recombinant ORP4L-WT, ORP4L-S/A or ORP4L-S/D (8 pmol) was incubated with [^{3}H]25OH, with or without 40-fold excess unlabelled sterol, in assay buffer (10 mM HEPES, 150 mM KCl, pH 7.4) containing 2% (w/v) polyvinyl alcohol (final assay volume 75 μL). Following 2 h at room temperature, 25 μL of a Talon resin slurry (1:1) was added to each tube and vortexed for 25 minutes. Resin was washed twice in assay buffer, transferred to new tubes and washed once more. Protein was eluted in 100 μL of assay buffer containing 150 mM imidazole and 75 μL of eluate was measured for protein-bound [^{3}H]25OH by scintillation counting. To calculate specific binding, [^{3}H]25OH bound in the presence of 40-fold excess unlabeled 25OH was measured and subtracted from total bound [^{3}H]25OH. Specific binding was plotted on a saturation binding curve using GraphPad Prism 7 software.

2.9 IMMUNOPRECIPITATION AND IMMUNOBLOTTING

Cells grown to 80% confluence on 60 mm dishes and transiently transfected for 24-48 h were rinsed and scraped in PBS and sedimented by low-speed centrifugation. The resulting pellets were lysed on ice for 15 min in 0.1 mL of HEPES lysis buffer (25 mM HEPES, 150 mM NaCl, 2 mM EDTA, 0.1% Triton X-100, pH 7.4) supplemented with EDTA-free protease inhibitor cocktail (Roche). Detergent-insoluble material was removed by centrifugation at 15,000 x *g* for 15 min at 4°C and supernatants were divided into a 10 μL input and two 45 μL samples for immunoprecipitation with either a relevant antibody or negative control antibody on ice for 2 h. Lysates were then mixed continuously at 4°C with 20 μl of a 1:1 slurry of protein A-Sepharose reconstituted in lysis buffer. Sepharose

beads were washed twice with lysis buffer, moved to new tubes and washed a third time. Protein was eluted in 2.5x SDS-PAGE reducing buffer (10% w/v SDS, 10 mM β-mercaptoethanol, 20% v/v glycerol, 200 mM Tris-HCl, 0.05% w/v bromophenol blue, pH 6.8) and heated at 95°C for 5 min. Samples were resolved by SDS-PAGE, transferred to nitrocellulose membranes and blocked in a 4:1 mixture of Tris-buffered saline (TBS; 50 mM Tris, 150 mM NaCl, pH 7.4) and Odyssey blocking buffer (LI-COR Biosciences). Subsequent antibody incubations were performed in TBS/0.1% Tween-20 (Bio-Rad):Odyssey blocking buffer (4:1, v/v), and washes were performed with TBS/0.1% Tween-20. Membranes were visualized using the LI-COR Odyssey infrared imaging system and associated secondary antibodies and software.

2.10 MICROSCOPY

2.10.1 Live-Cell and TIRF Microscopy

Cells were cultured on glass-bottomed dishes with #1.5 coverglass (170 μm). Following transfection of cDNAs encoding GFP- and mCherry-tagged proteins for 24 h, cell culture medium was replaced with FluoroBrite medium supplemented with 10% FBS (Gibco, Waltham MA) and cells were mounted on the environmentally-controlled stage of a Zeiss Cell Observer spinning disk confocal microscope with a Zeiss Axiocam MRm. TIRF images were captured at an incident angle of 67° with a 100x oil immersion objective (NA 1.45), and epifluorescence images were taken after resetting the incident angle to 0°.

2.10.2 Confocal Immunofluorescence Microscopy

For fixed-cell fluorescence microscopy, cells were cultured on glass coverslips and fixed with 4% (w/v) paraformaldehyde in PBS for 12 min at ambient temperature. Paraformaldehyde was quenched by rinsing with 50 mM ammonium chloride and cells were permeabilized for 12 min at 4°C with Triton X-100 (0.05%, w/v) in PBS. Permeabilized cells were blocked with PBS containing 1% (w/v) BSA and probed for 1 h with primary antibodies diluted in the same buffer, followed by probing with the appropriate Alexa Fluor 594 or -488 conjugated antibodies for 45 min. Cells were rinsed with distilled water prior to mounting in Mowiol 40-88. Confocal immunofluorescence microscopy was performed on a Zeiss LSM 510 laser scanning confocal microscope with a 63x objective (numerical aperture 1.4). Image acquisition and analysis was performed with Zen v2.3 image capture software by Zeiss (Oberkochen, Germany) and ImageJ image analysis software v1.49 [185,186].

2.10.3 Immunofluorescence Detection of PI(4)P

Cells were cultured on glass coverslips and Golgi-localized PI(4)P was immunstained according to Cheong and colleagues[187]. Cells were fixed in 2% formaldehyde in PBS for 10 min at RT, rinsed with PBS and permeabilized using 15 μg/mL digitonin in 100 mM glycine for 20 minutes. Cells were blocked for 1 h in PBS containing 1% BSA (w/v) and probed with a monoclonal IgM against PI(4)P in the same buffer, overnight at 4°C. Cells were probed with Alexa Fluor 594-conjugated anti-IgM secondary antibody for 45 min at room temperature, then with anti-giantin and Alexa Fluor-488

antibodies in sequence. Following washes, cells were rinsed in dH_2O and mounted in Mowiol 40-88.

2.11 QUANTIFICATION OF SPHINGOMYELIN SYNTHESIS

CHO-shNT and CHO-shOSBP cells were transfected with Lipofectamine 2000 for 48 h, and then treated for 4 h with 6 μM 25OH (Steraloids, Newport RI) or solvent control (ethanol). During the final 2 h of treatment, cells were pulse-labelled with [^{3}H]serine (10 μCi/ml) in serine-free medium A. Cells were harvested in methanol:water (5:4, v/v), lipids were extracted from cell lysates with chloroform:methanol (1:2) and 0.58% NaCl, and the organic phase was washed twice with ideal upper phase (IUP; methanol:58% NaCl:chloroform, 45:47:3, v/v). PE and PS in a portion of the lipid extract was resolved by TLC in chloroform:methanol:acetic acid:water (60:40:4:1, v/v). The remainder of the extracts were hydrolyzed in 0.1 N KOH for 1 h at 37°C (to remove labelled glycerolipids) and neutralized with 0.5 N HCl. This sphingolipid fraction was resolved by TLC in chloroform:methanol:water (65:25:4 v/v). Radioactivity in PE, PS and sphingolipids was quantified by scraping TLC plates and liquid scintillation counting, or by direct measurement of radioactivity on TLC plates using an Eckert & Ziegler TLC Scanner and WinScan software v3.14 (Hopkinton, MA). [^{3}H]Serine incorporation into lipids was expressed relative to total cell protein.

2.12 PHOSPHO-PEPTIDE MASS SPECTROMETRY

HeLa cells were transiently transfected with pcDNA3.1 containing ORP4L-V5 for 48 h and incubated with 0.5 μM okadaic acid for 2 h prior to lysis in modified RIPA buffer

(10 mM sodium phosphate buffer, 150 mM NaCl 2 mM EDTA, 2 mM EGTA, 10 mM NaF, 1 mM sodium pyrophosphate, 0.3% Triton X-100, pH 7.4) containing protease inhibitor cocktail and immunoprecipitates were resolved by SDS-8%PAGE and visualized with GelCode Blue, and the band corresponding to ORP4L-V5 at approximately 110-115 kDa was excised and digested using an automatic digestion robot (ProGest, Genomic Solutions) according to Shevchenko and colleagues [188], with minor modifications. Briefly, the gel bands were reduced with dithiothreitol, alkylated with iodoacetamide and then digested with trypsin. Peptides were extracted from the gel bands with 50% acetonitrile, 5% formic acid, dried by vacuum centrifugation and resuspended in 20 μL 3% acetonitrile, 0.5% formic acid in HPLC-grade water. Liquid chromatography-tandem mass spectrometry (LC-MS/MS) was performed using a nanoflow liquid chromatography system (Ultimate3000, ThermoScientific) interfaced to a hybrid ion trap-orbitrap high resolution tandem mass spectrometer (VelosPro, ThermoScientific) operated in data dependent acquisition (DDA) mode. Briefly, 1 μL of each sample was injected onto a capillary column (C18 Onyx Monolithic, 0.10 x 150 mm, Phenomenex) at a flow rate of 300 nL/min. Samples were electro-sprayed at 1.2 kV using a dynamic nanospray probe with fused silica non-coated emitters (20 μm ID with 10 μm ID tip, PicoTip Emitter from New Objective). Chromatographic separation was carried out using 60 min linear gradients (mobile phase A: 0.1% formic acid in MS-grade water, mobile phase B: 0.1% formic acid in MS-grade acetonitrile) from 3% B to 35% B over 40 minutes, then increasing to 95% B over 5 minutes. MS/MS spectra were acquired using both collision induced dissociation (CID) and higher-energy collisional dissociation (HCD) for the top 10 peaks in the survey 30000-resolution MS scan. The *.raw* files were acquired (Xcalibur, ThermoFisher) and

exported to Proteome Discoverer 2.0 (ThermoFisher) software for peptide and protein identification using the SequestHT DB search engine (full trypsin digestion with 2 maximum missed cleavages, 10 ppm precursor mass tolerance and 0.8 Da fragment mass tolerance). Database searching was done using the UniprotKB human database. Oxidized methionine residues and phosphorylation of serine, threonine and tyrosine were selected as dynamic (variable) modifications; carbamidomethyl cysteine was selected as fixed modification.

2.13 GEL FILTRATION-HPLC

Recombinant ORP4L-WT, ORP4L-S/A and ORP4L-S/D (0.5 mg/mL) were resolved by GF-HPLC using a YARRA SEC-3000 silica column (7.8 mm x 300 mm, 3 μm particle size, 290 Å pore size) under isocratic conditions (10 mM HEPES, 150 mM KCl, pH 7.4) according to the method used by McCluskey and colleagues [189]. Protein samples (20 μL) were injected by a Rheodyne 7725i sample injector and detected by intrinsic fluorescence (λ_{ex} 285 nm, λ_{em} 335 nm) using a Waters 474 scanning fluorescence detector. A Waters 510 pump and controller were used to deliver solvent at a flow rate of 0.5 mL/min. To estimate protein mass based on retention time, the column was calibrated using the protein standards carbonic anhydrase (29 kDa), BSA (66 kDa), β-amylase (200 kDa) and bovine thyroglobulin (669 kDa) (generously supplied by Dr. Stephen Bearne, Dalhousie University).

2.14 GLUTARALDEHYDE CROSSLINKING

Purified ORP4L-WT, ORP4L-S/A and ORP4L-S/D (2 μg/reaction) were incubated for 5 min at 37°C with a range of glutaraldehyde concentrations in a final volume of 10 μL HEPES buffer (20 mM, pH 7.5). The crosslinking reaction was stopped by addition of 1 μL Tris (1 M, pH 8.5) and boiling in 2.5x SDS-PAGE reducing buffer. Proteins were resolved by SDS-6%PAGE and stained with GelCode Blue (ThermoFisher Scientific, Waltham MA).

2.15 PROTEIN KINASE ASSAYS

Protein kinase assays were performed by Kinexus Bioinformatics (Vancouver, BC) using 20 μg purified wild-type and phospho-mutants of ORP4L (see Section 2.4.2) in a final volume of 25 μL. Samples were mixed with the appropriate kinases (10-50 nM each) in appropriate reaction buffers (not described in detail by Kinexus). The assay was initiated by the addition of 5 μL of [γ-^{33}P]ATP (0.8 μCi) and the reaction mixture was incubated at room temperature for 30 minutes. The assay was terminated by spotting 10 μl of the reaction mixture onto a multiscreen phosphocellulose P81 plate, which was washed 3 times for approximately 15 minutes each in a 1% phosphoric acid solution. The radioactivity on the P81 plate was counted in the presence of scintillation fluid in a Trilux scintillation counter.

2.16 STATISTICAL ANALYSIS

With the exception of the RGB line plots in Figure 4.2 which was produced using ImageJ software described in Section 2.10.2, all plots were generated by GraphPad Prism software (Versions 6 and 7). Bar graphs represent means, and box-and-whisker plots display the mean and 25^{th} and 75^{th} percentiles (box) and 5^{th} and 95^{th} percentiles (whiskers). Unless otherwise noted, error bars represent standard deviations and all pairwise analysis was performed assuming normal distribution using Student's t-tests. For the quantification of all immunofluorescence experiments except Figure 3.3 B, "cell number" indicates the total number of cells measured over the course of "n" experiments, both of which are indicated in associated figure legends. Figure 3.3 B is a display of raw data and is a representative of three separate experiments that yielded comparable results.

CHAPTER 3 ORP4 IS REQUIRED FOR CELL PROLIFERATION AND THE MAINTENANCE OF GOLGI MORPHOLOGY

Figures 3.1, 3.2 and 3.5 appear in the following publication:
Charman, M., Colbourne, T. R., Pietrangelo, A., Kreplak, L. & Ridgway, N. D. Oxysterol-binding protein (OSBP)-related protein 4 (ORP4) is essential for cell proliferation and survival. *J. Biol. Chem.* **289,** 15705–17 (2014). *See Appendix B for permissions.*

It should be noted that Figure 3.1 was produced by Mark Charman and has been included in this chapter with his permission.

3.1 ORP4 Depletion Causes Growth Arrest and Apoptosis

To elucidate the function of ORP4, its gene was silenced in HeLa and HEK293 cells by lentiviral transduction of shRNA targeting ORP4L (exon 1) or all three ORP4 variants (exon 3). The resulting ORP4 depletion significantly reduced the rate of cell growth in HEK293 (Figure 3.1) and HeLa cells, and had a more prominent effect on rat intestinal epithelial cells (IEC-18) ,which completely detached by 48 h post-transduction [52]. To determine whether the cells were undergoing apoptosis, we measured the cleavage of procaspase-3 to active caspase-3, which propagates and amplifies upstream apoptotic signals by activating other caspases [190] and deactivating substrates such as the DNA repair enzyme poly(ADP-ribose) polymerase (PARP) [191]. IEC-18 cells transduced with shORP4, but not shNT, displayed cleavage of both caspase-3 and its substrate PARP (Figure 3.2 A) as well as nucleosome release not evident in HeLa or HEK293 cells [52]. Interestingly, transformation of IEC-18 by human oncogenic H-Ras increased ORP4L and ORP4S expression in this cell type [52] and was protective against shORP4-induced apoptosis (Figure 3.2 B). The cell proliferation defect observed in ORP4 knockdown cells provides a possible explanation for the reported antineoplastic effects of the ORPphilins that are not associated with OSBP inhibition.

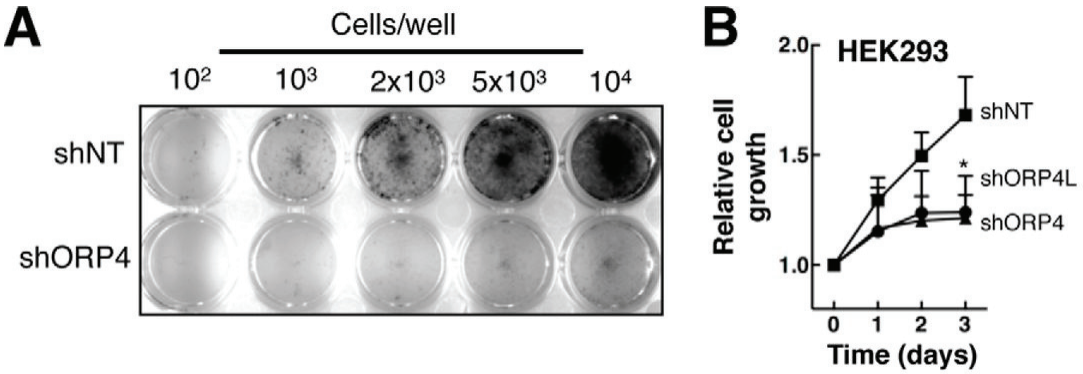

Figure 3.1 *ORP4 silencing inhibits proliferation of HEK293 cells.* **A)** HEK293 cells that were transduced with lentiviral shNT or shORP4 were seeded at the indicated densities on a 24-well plate, cultured for 3 days, and stained with crystal violet. **B)** HEK293 cells seeded on 35-mm dishes were transduced with lentivirus and selected with puromycin for 48 h. Medium was replaced and cells were cultured for up to 3 days. Cells were stained with crystal violet and quantified by densitometry. Bars are the mean and SE of 3 experments, *, $p<0.05$.

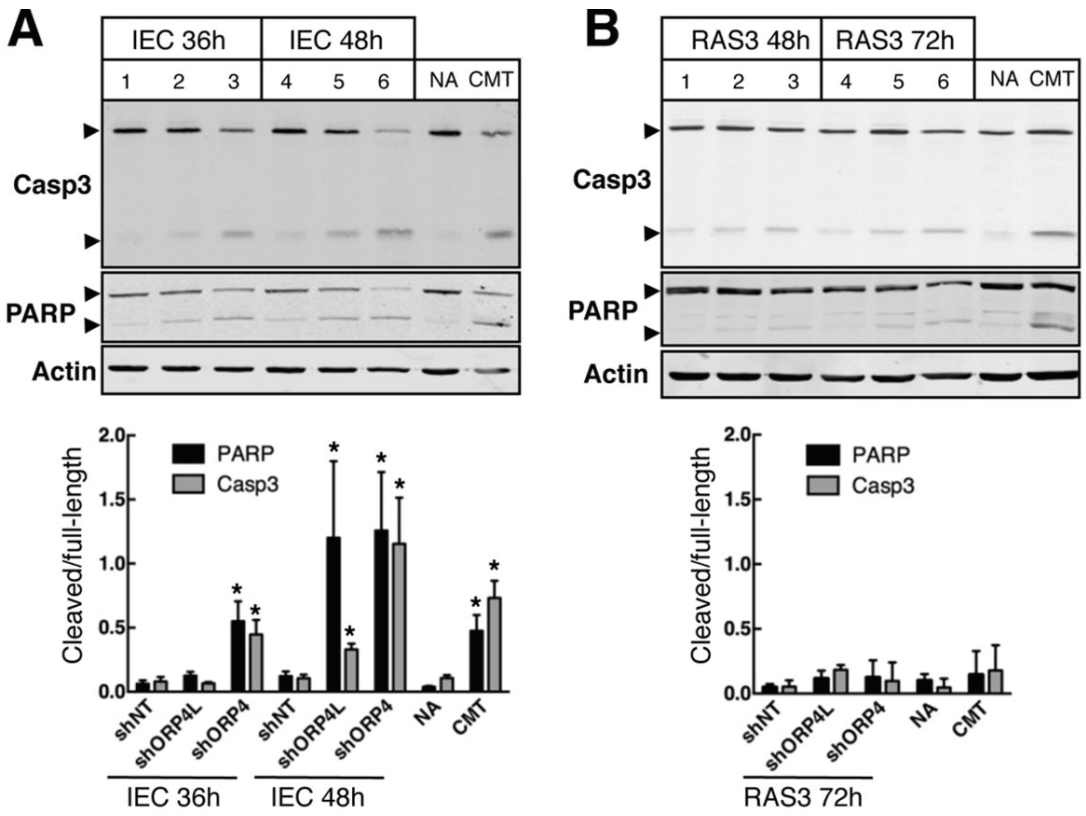

Figure 3.2 *ORP4 silencing induces apoptosis via activation of caspase-3 and inactivation of PARP.* **A)** and **B)**, IEC-18 and IEC-RAS3 cells were transduced with shNT (lanes 1 and 4), shORP4L (lanes 2 and 5), or shORP4 (lanes 3 and 6) for the indicated times or treated with camptothecin for 18 h. Total lysates were prepared and immunoblotted for caspase-3 and PARP, and the positions of full-length and proteolyzed caspase-3 and PARP are indicated by arrowheads. Quantification of cleavage (bar graphs) was performed using LI-COR software and is expressed as a ratio of the cleaved fragment/full-length protein. Camptothecin (CMT) was used as a positive control for both PARP and caspase-3 cleavage, with dimethyl sulfoxide as a vehicle control (NA). Bars are the mean and SE of 3-4 experments, *, $p<0.05$.

3.2 ORP4 Depletion Causes Fragmentation of the TGN

Another consequence of ORPphilin treatment not observed in OSBP-depleted cells is modest but notable vesiculation of the TGN, which is particularly evident in cells treated with OSW-1 or cephalostatin 1 [88]. To assess whether the morphological TGN defects induced by OSW-1 treatment are attributable to ORP4L inhibition, the morphology of the *cis*/medial-Golgi and TGN was visualized and quantified in HeLa cells transduced with shORP4. Compared to non-targeting controls (shNT), ORP4 silencing caused the TGN46 signal to become more dilated and reduced in the PM (Figure 3.3 A). Since the dispersed TGN phenotype made it difficult to quantify fluorescence intensity, maximum pixel intensity of whole-cell TGN46 staining was used as an indicator of dispersion (ie. cells with dispersed TGN had lower maximum pixel intensities). Based on this method, a significant decrease in maximum TGN46 intensity was evident in shORP4-transduced cells (Figure 3.3 B). The fluorescence intensity of giantin in the *cis*/medial-Golgi was unchanged but there was a modest reduction in the area occupied by this *cis*/medial-Golgi protein in shORP4 transduced cells (Figure 3.3 C).

3.3 ORP4 Regulates TGN Morphology

The dilation and reduction of the TGN46 signal in shORP4 transduced cells resembles the effects of altered PI(4)P metabolism in response to siRNA knockdown or transient overexpression of PI4KIIα [192]. This observation raised the possibility that ORP4 is involved in PI(4)P transport or metabolism at the TGN. To address this, giantin was used as a mask for the *cis*/medial-Golgi to quantify the fluorescence intensity of PI(4)P in that compartment. We observed that PI(4)P was modestly but significantly reduced in

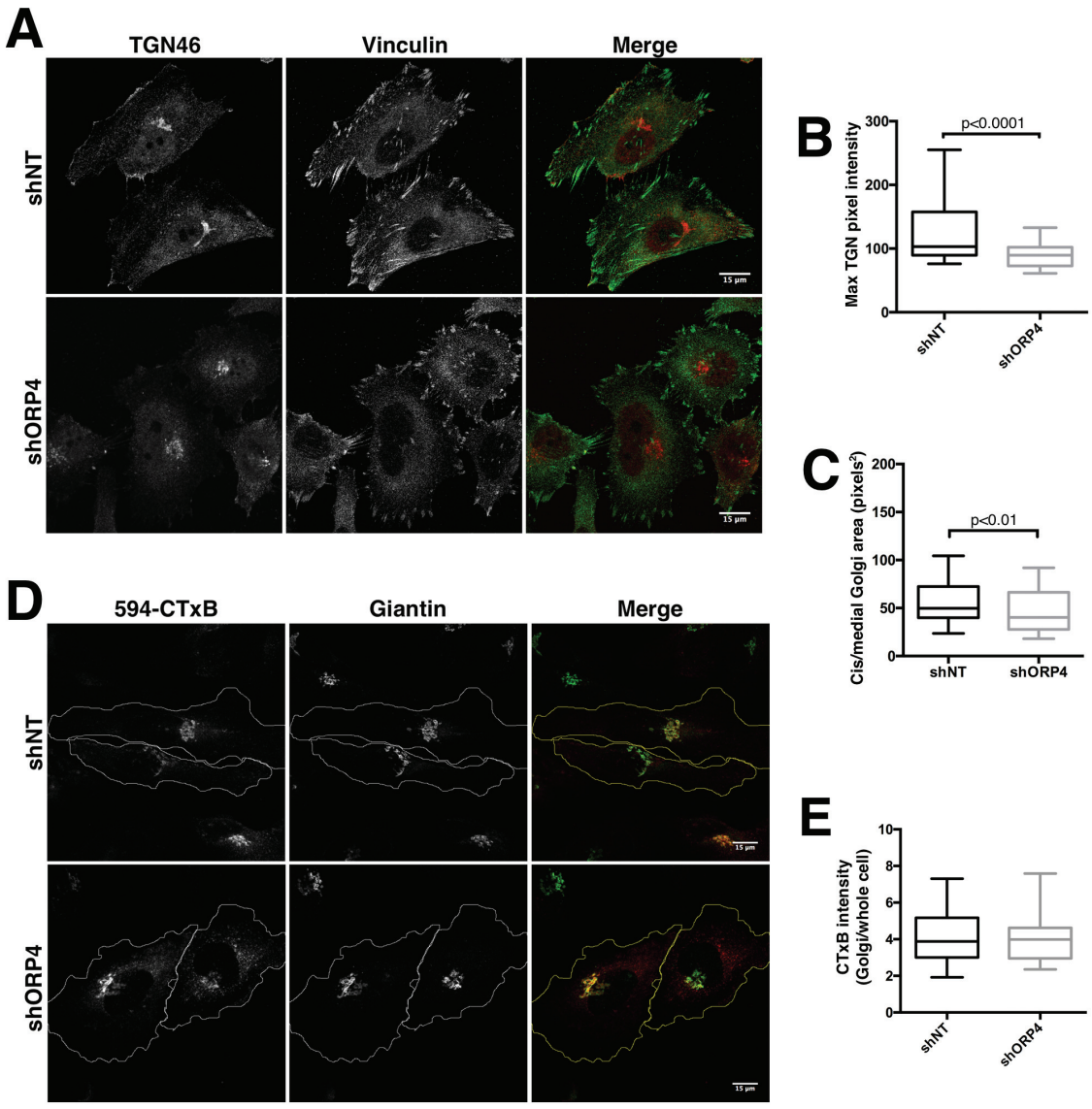

Figure 3.3 *ORP4 is required for maintenance of TGN morphology.* HeLa cells were transduced with lentivirus encoding non-targeting (shNT) or ORP4-targeted (shORP4) shRNA for 24 h and selected in 4 µg/mL puromycin for 48 h. **A)** Cells were fixed, permeabilized and probed for TGN46 and vinculin, followed by Alexa Fluor-594 and -488 secondary antibodies, respectively. **B)** TGN dispersion was measured by maximum pixel value of the TGN46 signal (shNT=33 cells, shORP4=50 cells, graph represents one of three experiments). **C)** The area of the *cis*/medial-Golgi was measured by quantifying the area of giantin immunofluorescence in fixed cells (shNT=108 cells, shORP4=124 cells, n=3). **D)** Cells were incubated with Alexa Fluor594-labeled cholera toxin β-subunit (ctxB) for 30 min followed by Medium A for 30 min. Cells were fixed and immunostained for giantin using a Alexa Fluor488 secondary antibody. Cell perimeter was drawn manually, using background fluorescence exacerbated by the ImageJ threshold tool as a guide. **E)** Golgi/whole cell CTxB intensity from cells from panel D (shNT=45, shORP4=44, n=3).

shORP4 transduced HeLa cells compared to shNT (Figure 3.4). To assess the functionality of dilated TGN in shORP4 cells, we observed the intracellular trafficking of a fluorescently-labeled cholera toxin β-subunit (CTxB). CTxB is endocytosed at the PM in a cholesterol- and SM-dependent manner via binding the ganglioside GM1, at which point it is thought to travel directly from early endosomal compartments to the TGN and *cis*/medial-Golgi and then to the ER, where it is proteolytically processed and released into the cytoplasm [193]. Despite changes in the morphology and PI(4)P level in *cis*/medial-Golgi and TGN compartments, the trafficking of CTxB to the Golgi apparatus was not affected (Figure 3.3 D and E). Thus ORP4L is involved in maintenance of Golgi structure and PI(4)P levels, but not the retrograde trafficking of cargo from the PM to the Golgi apparatus.

3.4 ORP4 HAS PI(4)P BINDING AND EXTRACTION ACTIVITY

OSBP has been shown to specifically interact with PI(4)P via the PH domain and to extract PI(4)P from membranes via the OHD [181], but the PI(4)P binding activity of ORP4 has not been similarly assessed. To determine the PIP specificity of the ORP4L PH domain, lipids immobilized on nitrocellulose were incubated with recombinant protein and protein-lipid interactions were visualized by immunodetection using an Odyssey infrared imaging system (LI-COR). Recombinant ORP4L displayed specificity for PI(4)P, and to a lesser degree PI(4,5)P_2 (Figure 3.5 A), consistent with the observed Golgi localization of a GFP-tagged ORP4 PH domain[52]. The multiple PIP interactions observed with recombinant ORP4S are consistent with electrostatic interactions that govern the localization of Osh4p to membranes despite the absence of a FFAT motif or PH domain [24,194,195].

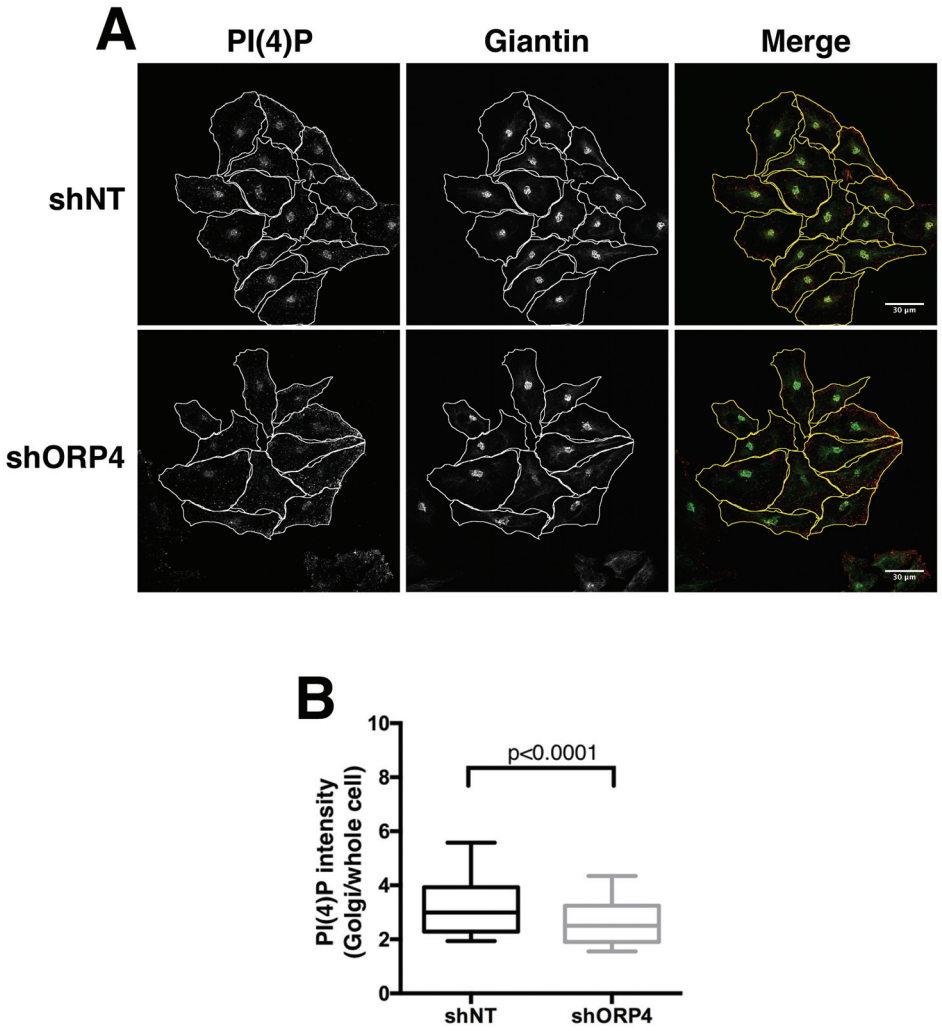

Figure 3.4 *ORP4 depletion reduces Golgi PI(4)P.* **A)** Cells transduced for 48 h were selected for 48 h and prepared for internal membrane staining of PI(4)P by paraformaldehyde fixation and digitonin permeabilization according to Section 2.10.3. Cells were probed for PI(4)P and giantin followed by Alexa Fluor-594 and -488, respectively, and observed by confocal microscopy. **B)** PI(4)P content of the Golgi in cells from panel A was measured by comparison of the PI(4)P signal within the giantin mask and in the whole cell (shNT=195 cells, shORP4=177 cells, n=3).

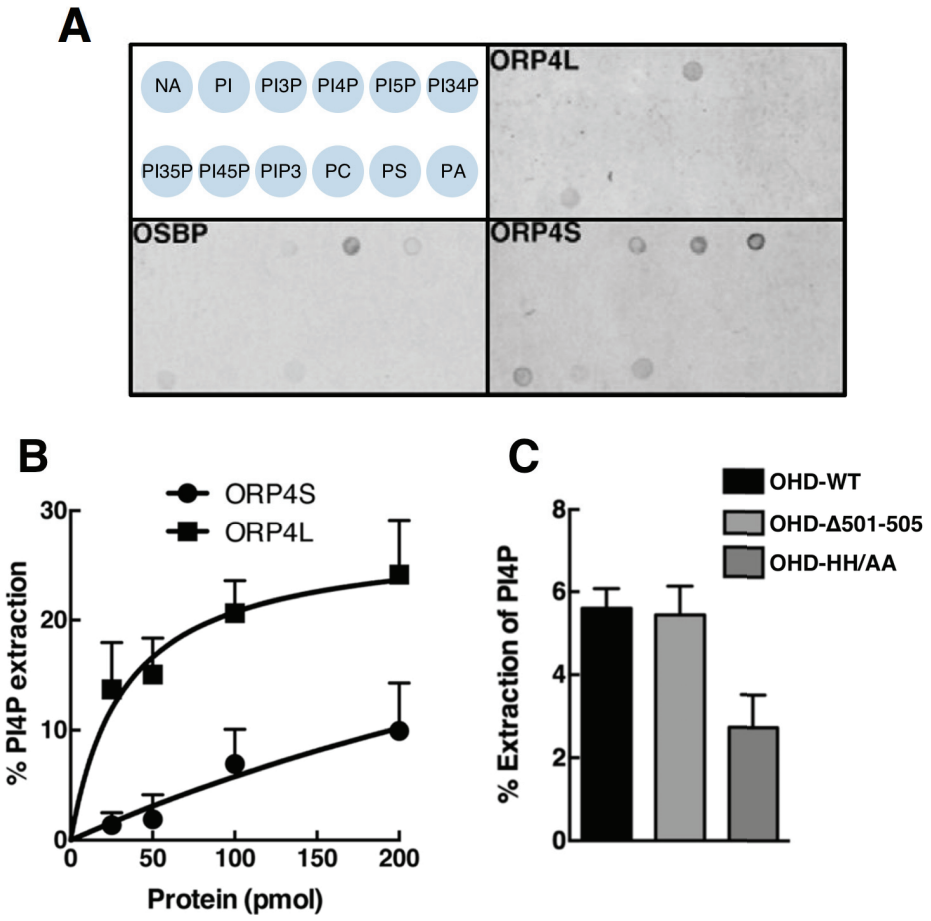

Figure 3.5 *ORP4 directly interacts with and extracts PI(4)P.* **A)** OSBP (100 nM), ORP4 (100 nM) or ORP4S (50 nM) was incubated with hybond-C nitrocellulose on which PC, PS, PA and various PIPs (100 nM) were immobilized. Proteins were detected using ORP4- or OSBP-specific antibodies and visualized using IRDye-conjugated secondary antibodies and the LI-COR Odyssey imaging system. **B)** Increasing amounts of ORP4L or ORP4S were incubated with liposomes containing 2000 DPM [^{32}P]PI(4)P for 20 min at 20°C. Radioactivity in the supernatant was measured after precipitation of liposomes with lectin as described in Figure 3.6. **C)** Extraction of PI(4)P from liposomes by the indicated ORP4-OHD GST fusion proteins (100 pmol) was conducted as described in Figure 3.6. Results are the mean and SE (error bars) of 3 experiments.

We then assessed the ability of the GST-ORP4-OHD, as well as ORP4L and ORP4S to extract PI(4)P from liposomes *in vitro* by a method described in Figure 3.6. In brief, liposomes containing [^{32}P]PI(4)P are incubated with recombinant protein and then sedimented by centrifugation, and the radioactivity is measured by scintillation counting and reflects lipid extraction by the protein. ORP4L and ORP4S (expressed and purified from Sf21 cells) extracted PI(4)P from liposomes, though ORP4S displayed reduced activity (Figure 3.5 B). To identify residues in the ORP4 OHD that bind PI(4)P, a previously constructed wild-type GST-ORP4-OHD fusion protein, a mutant with signature motif histidine residues 589 and 590 changed to alanine (GST-OHD-HH/AA) and a sterol-binding defective mutant (GST-OHD-Δ501-505) were assayed for PI(4)P extraction activity. OHD-HH/AA modestly reduced sterol binding [53] but reduced PI(4)P extraction activity by 60%, whereas OHD-Δ501-505, which bears a deletion in the lid that reduces sterol binding by 95% [53], displayed wild-type PI(4)P extraction activity (Figure 3.5 C). That extraction of liposomal PI(4)P by the ORP4 OHD is consistent with predictions based on the crystallization of the Osh3p OHD[27]. My data show that ORP4 is a PI(4)P binding protein and that histidine residues in the ORP signature motif, which are conserved throughout the family, are required for coordination of the phosphorylated inositol headgroup of PI(4)P but not for sterol binding.

3.5 DISCUSSION

The existence of 12 human ORPs with highly conserved lipid and protein binding domains suggests a lipid binding/transfer function with some degree of redundancy. It was therefore not anticipated that shRNA silencing of ORP4 would cause the proliferative

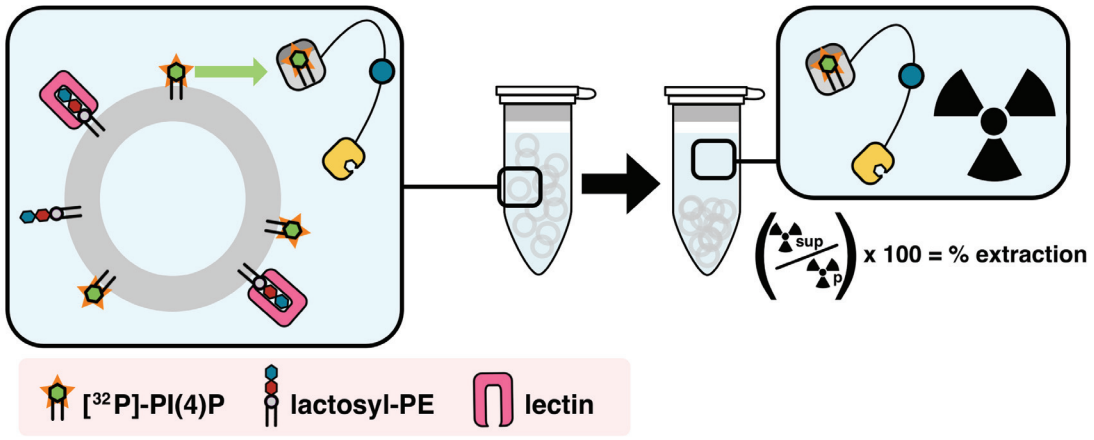

Figure 3.6 *Liposome-based PI(4)P extraction assay.* Liposomes produced as described in Chapter 2.7.2 are incubated with recombinant protein for 20 min at 25°C, during which time [^{32}P]PI(4)P is extracted from liposomes. Liposomes are then incubated with lectin (pink), which binds the sugar moieties on lactosyl-PE and allows for sedimentation of the liposomes by centrifugation. The radioactivity of the supernatant and pellet is measured by liquid scintillation counting, and extraction is measured as a percentage of [^{32}P]PI(4)P in the supernatant, with background (as measured by % extraction in a no-protein control) subtracted.

defects observed here in HeLa, HEK293 and IEC-18 cells [52], which was confirmed by other groups in human cervical cancer cell lines C33A and CaSki [56], murine macrophages [171] and both immortalized and primary leukemic T-cells [55]. These data suggest a unique proliferative function for ORP4 when aberrantly expressed, consistent with its limited expression in normal tissues [170] and elevated expression in malignancies [55,103,104,119,120]. That IEC-18 cells are more sensitive to ORP4 depletion and express less ORP4 than their Ras-transformed counterparts parallels recent observations that ORP4 is not expressed in normal T-cells but is highly expressed in leukemic T-cells. In leukemic T-cells, increased expression of ORP4 provides an abundant scaffold that links the T-cell receptor complex to PLCβ3, activating phospholipase activity to produce IP_3 that increases oxidative phosphorylation and promotes cell growth via calcium release from the ER [55]. These results suggest that increased ORP4 expression in malignant cells may provide a proliferative advantage not required for growth of the non-transformed tissue of origin.

While changes in morphology of the Golgi apparatus are typical of cells undergoing apoptosis [196,197], morphological Golgi defects in ORP4-depleted cells were limited to the TGN compartment. We have not ruled out the possibility that the dispersed TGN morphology is due to defective trafficking of the TGN46 protein, and it would be informative to observe another TGN-resident protein with a different trafficking route, such as members of the polypeptide N-acetylgalactosaminyl transferase (GALNT) family[198] or γ-adaptin [199], in shORP4 cells. However, the TGN dispersion observed in shORP4 cells is strikingly similar to the effects of aberrant PI(4)P metabolism [192,200] or ORPphilin treatment [88]. Considering the PI(4)P-binding and extraction activity of ORP4, it is possible that, in addition to the novel scaffolding properties described by Yan and

colleagues [55], ORP4 contributes to growth and proliferation by remodelling intracellular membranes. This model is supported by the significant decrease in Golgi PI(4)P observed in ORP4-depleted cells and by the PI(4)P binding and extraction activity of the ORP4 PH domain and OHD. It should be noted that although the decrease in Golgi PI(4)P is modest, dispersion of the TGN necessitated measuring PI(4)P content in the *cis*/medial-Golgi where PI(4)P is enriched and critical for organelle function [201]. Quantification of PIPs in whole-cell and Golgi fractions by HPLC or mass spectrometry methods should be conducted to determine the extent of Golgi-PI(4)P reduction in shORP4 cells.

The Golgi and TGN dispersion phenotype of ORP4L silencing could also be secondary to effects on other interacting factors, since VAP knockdown causes a similar TGN dispersion phenotype that did not extend to the *cis*/medial-Golgi [14] and OSBP knockdown caused the mislocalization of *cis*/medial-Golgi SNAREs [89]. Vimentin reorganization by ORP4 may also affect TGN morphology, as vimentin has been shown to position organelles throughout the cytoplasm through protein-mediated contacts that have been reported at the Golgi apparatus [202], lipid droplets [203], nucleus [204] and endo/lysosomal compartments [205]. While rescue experiments conducted in this study found that ORP4L and the vimentin-aggregating isoforms ORP4M and ORP4S all rescued cell viability in shORP4 HeLa to a similar extent [52], these rescue studies should be repeated to determine whether ORP4S or ORP4L re-expression in shORP4 cells can recover the contiguity of the TGN.

The normal trafficking of CTxB in shORP4 cells is unusual considering the morphological abnormalities of the TGN, but the existing literature regarding CTxB trafficking provides possible explanations. While the general trajectory of CTxB in cells is

known, the involvement of the *cis*/medial-Golgi and TGN are still not entirely understood. Pharmacological disruption of the *cis*/medial-Golgi, but not the TGN, has no effect on PM-to-ER trafficking of CTxB, suggesting that TGN is the primary Golgi compartment required for CTxB traffic [206]. However, CTxB is often shown to co-localize with resident *cis*/medial-Golgi proteins such as GM130 [207], and a portion of CTxB has been suggested to bypass the Golgi entirely by travelling directly from the recycling endosome to the ER (in reference to unpublished results) [193]. In short, due to the complexity and dynamism of trafficking events occurring at the TGN, the only conclusion we can draw from our results is that ORP4 depletion does not disrupt the retrograde trafficking of CTxB, specifically. Studies of other trafficking and secretory pathways are warranted to determine whether ORP4 depletion has a detrimental effect on different facets of TGN function.

Collectively, the data presented in this chapter indicate that ORP4 has a non-redundant function necessary for the proliferation of immortalized cells. One function of ORP4 may be to maintain TGN morphology by modulating PI(4)P levels in that compartment, however ORP4L or the short variants have not been observed at the Golgi in previous localization studies despite the specificity of the PH domain for PI(4)P [52]. Therefore, to determine whether TGN fragmentation was due to loss of ORP4 function or simply a consequence of shORP4-induced apoptosis, we re-examined the cellular localization of ORP4L.

CHAPTER 4 ORP4L IS A TGN- AND PM-ASSOCIATED PROTEIN

4.1 ORP4L LOCALIZES TO THE TGN IN RESPONSE TO 25OH TREATMENT

Our lab and others reported that ORP4L is present in the cytoplasm, and on vimentin intermediate filaments and the PM of cultured cells but with no evidence of Golgi localization, even in the presence of exogenous 25OH [171,208]. When a V5 monoclonal antibody was used to detect transiently expressed ORP4L-V5 by immunofluorescence in HeLa cells, the protein was diffusely localized under control conditions but was detected on perinuclear structures after 25OH treatment (Figure 4.1). Co-immunostaining of the cells with a previously characterized ORP4 antibody (against amino acids 380-463 of ORP4L [170]) did not detect perinuclear localization (Figure 4.1 A). The perinuclear structures containing ORP4L-V5 co-localized with TGN46 in 25OH-treated cells, as well as with TGN46 at the PM (Figure 4.1 B). Thus 25OH-dependent localization of ORP4L to the TGN is detected by a C-terminal antibody but not an antibody directed against an internal epitope. These experiments show for the first time that ORP4L, like its close paralogue OSBP, undergoes 25OH-dependent translocation to the Golgi apparatus, and that Golgi detection is epitope-dependent. This finding is consistent with the localization of the GFP-PH domain of ORP4L at the Golgi apparatus, where it was used as a PI(4)P sensor [208,209].

4.2 TGN LOCALIZATION OF ORP4L IS REGULATED BY LIGAND BINDING

To investigate the role of lipid-binding in Golgi localization of ORP4L, V5-tagged versions of previously characterized sterol-binding and PI(4)P-binding mutants were

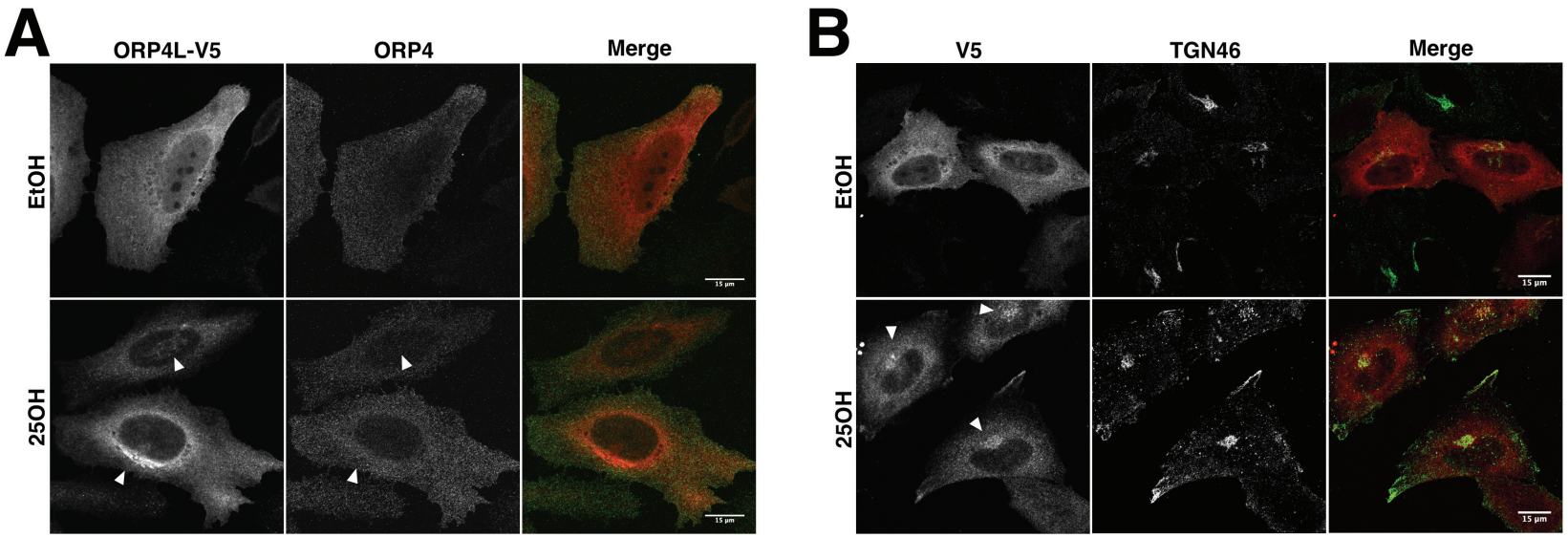

Figure 4.1 *C-terminal tagging of ORP4L reveals a Golgi-associated pool.* **A)** HeLa cells were transiently transfected with ORP4L-V5 for 48 h. Cells were fixed, permeabilized and probed with a monoclonal V5-tag antibody (V5) and an ORP4-specific affinity purified polyclonal antibody (ORP4) targeting an epitope in the central linker region, followed by Alexa Fluor-594 and-488 secondary antibodies, respectively. Structures visible with the V5 antibody but not the ORP4 antibody are highlighted with white arrows. **B)** Cells were transfected and probed (as described above) with a V5 and TGN46 antibodies, followed by Alexa Fluor-594 and -488 secondary antibodies, respectively.

constructed and expressed in cells [208,210]. ORP4L-Δ501-505-V5 has a deletion in the lid of the OHD that prevents sterol binding but not PI(4)P binding. Conversely, mutating the two histidine residues in the OHD (ORP4L-HH/AA) abolished binding of PI(4)P but not sterols. Recall that GST fusion constructs of the ORP4 OHD bearing these same mutations were used to characterize the PI(4)P binding activity of ORP4 in Chapter 3.5. To identify the role of VAP binding in recruitment to PM-ER or Golgi-ER MCS, the FFAT motif mutant ORP4L-YF/AA-V5 was also characterized. Similar to OSBP [6], wild-type ORP4L-V5 was co-localized with TGN46 in 25OH-treated cells (Figure 4.2 A and associated line plot) and in response to cholesterol depletion by cyclodextrin (Figure 4.3 A and B). Interestingly, ORP4L-Δ501-505-V5 displayed extensive TGN localization in response to 25OH (Figure 4.2 B) and cyclodextrin (Figure 4.3 C), suggesting that 25OH induces a translocation signal for ORP4L that is independent of sterol binding. The association of ORP4L with the Golgi requires PI(4)P and VAP binding based on the lack of TGN localization of ORP4L-HH/AA-V5 (Figure 4.2 C) and ORP4L-YF/AA-V5 (Figure 4.2 D) in 25OH-treated cells. ORP4L-HH/AA-V5 also did not localize to the Golgi apparatus in response to cholesterol depletion by cyclodextrin, supporting the conclusion that PI(4)P binding is required for Golgi localization (Figure 4.3 D).

4.3 PI(4)P-Depletion Prevents TGN Localization of ORP4L-Δ501-505

As shown in Section 3.4, ORP4L binds PI(4)P immobilized on filters and in liposomes. To determine whether ORP4L-Δ501-505-V5 localization to the Golgi apparatus is PI(4)P-dependent, ORP4L-Δ501-505-V5 was co-expressed with wild-type, and ER- and Golgi-restricted mutants of Sac1, a PI(4)P phosphatase that cycles between the ER and

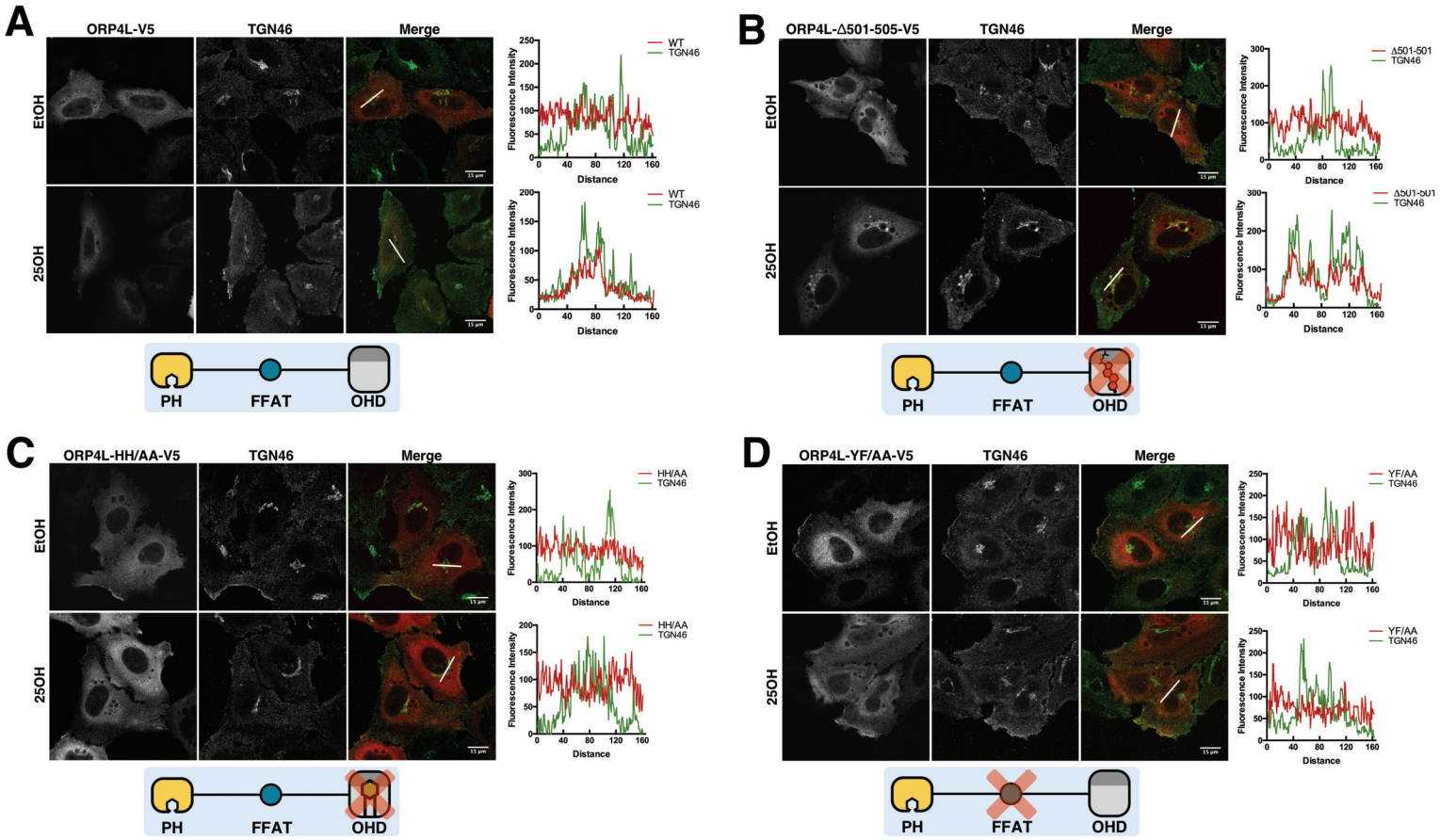

Figure 4.2 *Golgi localization of ORP4L is dependent on its VAP and PI(4)P binding activity.* HeLa cells were transiently transfected with **A)** ORP4L, **B)** sterol-binding defective ORP4-Δ501-505-V5, **C)** PI(4)P-binding defective ORP4-HH/AA-V5 or **D)** VAP-binding defective ORP4-YF/AA-V5. Cells were treated with either 6 μM 25OH or solvent (ethanol) for 2 h, and ORP4 and TGN46 were immunostained using AlexaFluor594 or -488 secondary antibodies, respectively. Images were captured by confocal microscopy (0.7 μm sections) as described in Materials and Methods. RGB profile graphs were created using ImageJ analysis software.

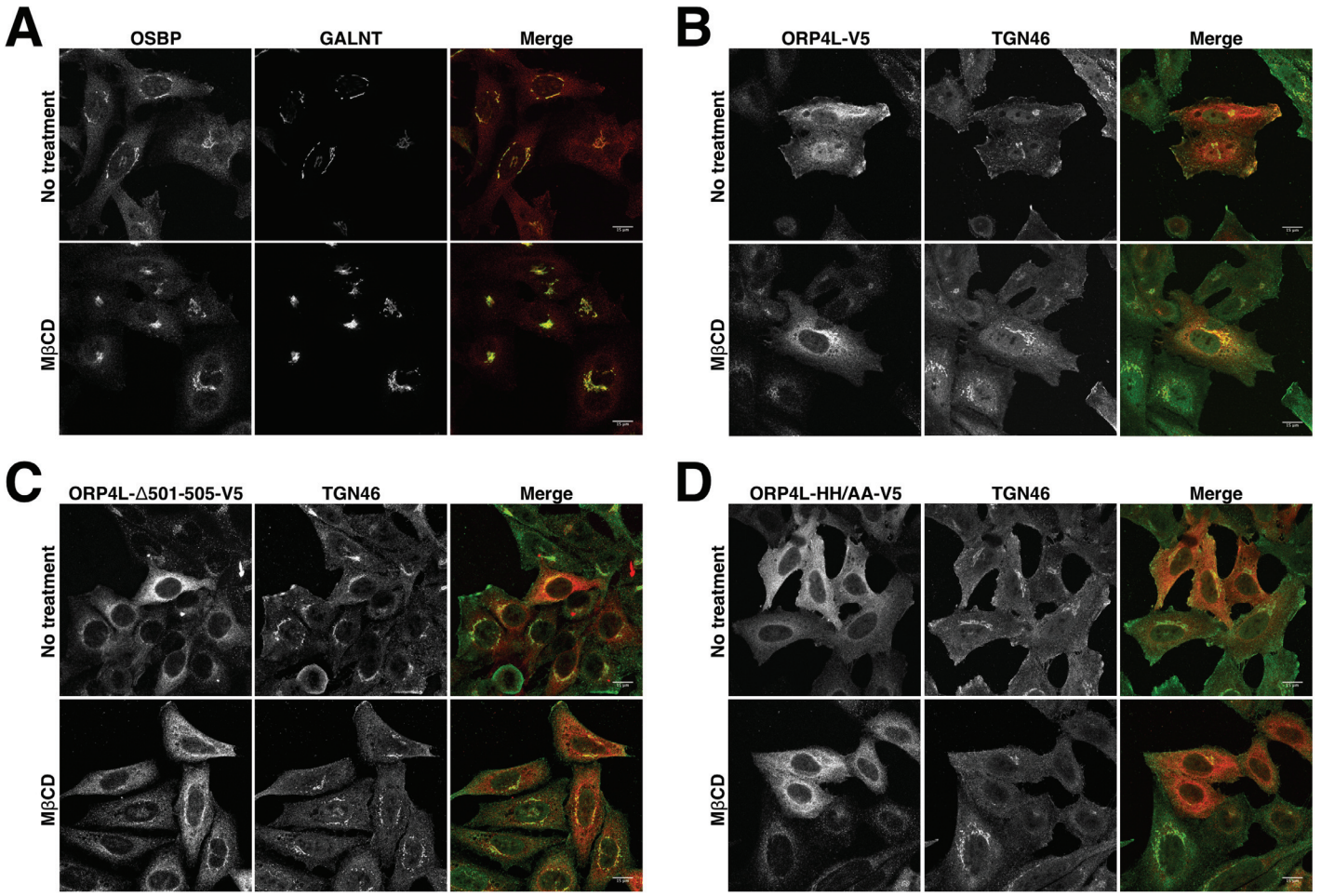

Figure 4.3 *Acute PM cholesterol depletion induces ORP4L-V5 TGN localization.* HeLa cells were transiently transfected with **B)** ORP4-WT-V5, **C)** ORP4-Δ501-505-V5 or **D)** ORP4-HH/AA-V5 and and treated with 2.5 mM methyl-β-cyclodextrin (MβCD) for 30 minutes prior to fixation, permeabilization and blocking described in Materials and Methods. Cells were probed with primary antibodies against V5 and TGN46, or **A)** for endogenous OSBP and GALNT.

Golgi apparatus [211]. GFP-Sac1 co-localized with ORP4L-Δ501-505-V5 in 25OH-treated cells but had no effect on its appearance at the Golgi apparatus (Figure 4.4 A). GFP-Sac1-LZ, which does not multimerize and is constitutively in the ER [212], also did not affect the translocation of ORP4L-Δ501-505-V5 to the Golgi apparatus in the presence of 25OH (Figure 4.4 B). Expression of GFP-Sac1-K2A, a constitutively Golgi-localized mutant that reduces Golgi-associated PI(4)P [212], blocked the appearance of ORP4L-Δ501-505-V5 at the Golgi apparatus in response to 25OH (Figure 4.4 C). Quantification of Golgi localization revealed that expression of GFP-Sac1-K2A reduced, but did not completely prevent, the Golgi localization of ORP4L-Δ501-505-V5 (Figure 4.4 D). These results show that association of ORP4L-Δ501-505 with the Golgi apparatus responds to a Sac1-regulated pool of PI(4)P.

4.4 TGN Localization of ORP4L is OSBP-Dependent But Does Not Affect OSBP Function

Since ORP4L and OSBP interact [210], and OSBP regulates PI(4)P levels in the Golgi apparatus in 25OH-treated cells [213,214], we tested whether 25OH-mediated translocation of OSBP was required for localization of ORP4L-Δ501-505-V5 using HeLa cells stably expressing an OSBP shRNA (see Figure 4.5 C). When ORP4L-V5 was expressed in HeLa cells with stable silencing of OSBP, there was no evidence of perinuclear Golgi localization in the presence or absence of 25OH (Figure 4.5 A). However, localization of ORP4L-V5 with OSBP in the TGN was re-established in cells expressing a shRNA-resistant OSBP cDNA (Figure 4.5 A). ORP4L-Δ501-505-V5 displayed weak perinuclear staining in HeLa OSBP knockdown cells, which was enhanced when cells were transfected with the OSBP

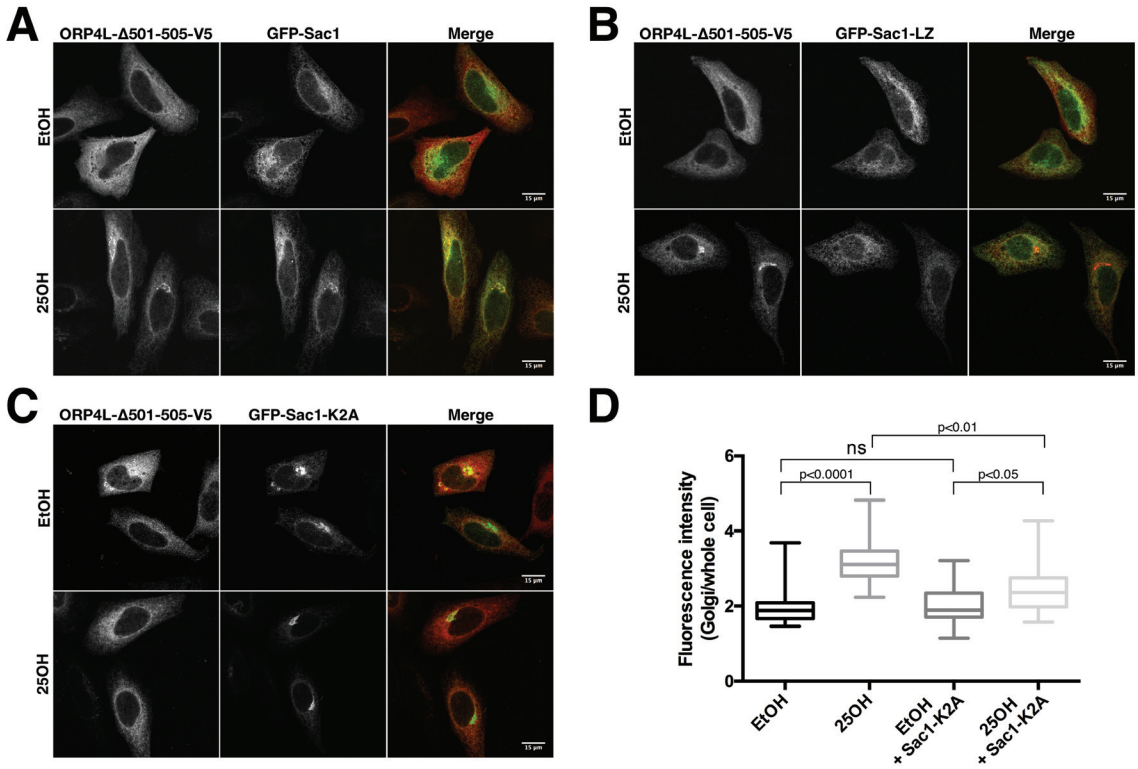

Figure 4.4 *ORP4-Δ501-505-V5 association with the TGN is PI(4)P-dependent.* HeLa cells were transiently transfected with ORP4L-Δ501-505 and **A)** GFP-Sac1, **B)** GFP-Sac1-LZ) or **C)** GFP-Sac1-K2A). After 48 h, cells were treated with 6 μM 25OH or solvent (ethanol) for 2 h and subsequently immunostained for ORP4L using a V5 monoclonal and Alexa Fluor-594 secondary antibodies. Images were captured by confocal microscopy (0.7 μm sections) **D)** The Golgi localization of ORP4L-Δ501-505-V5 was assessed in non-expressing cells and cells expressing GFP-Sac1-K2A (13-20 cells from 3 experiments). Non-expressing cells were immuno-stained with TGN46 in separate experiments to mask the Golgi for intensity measurements.

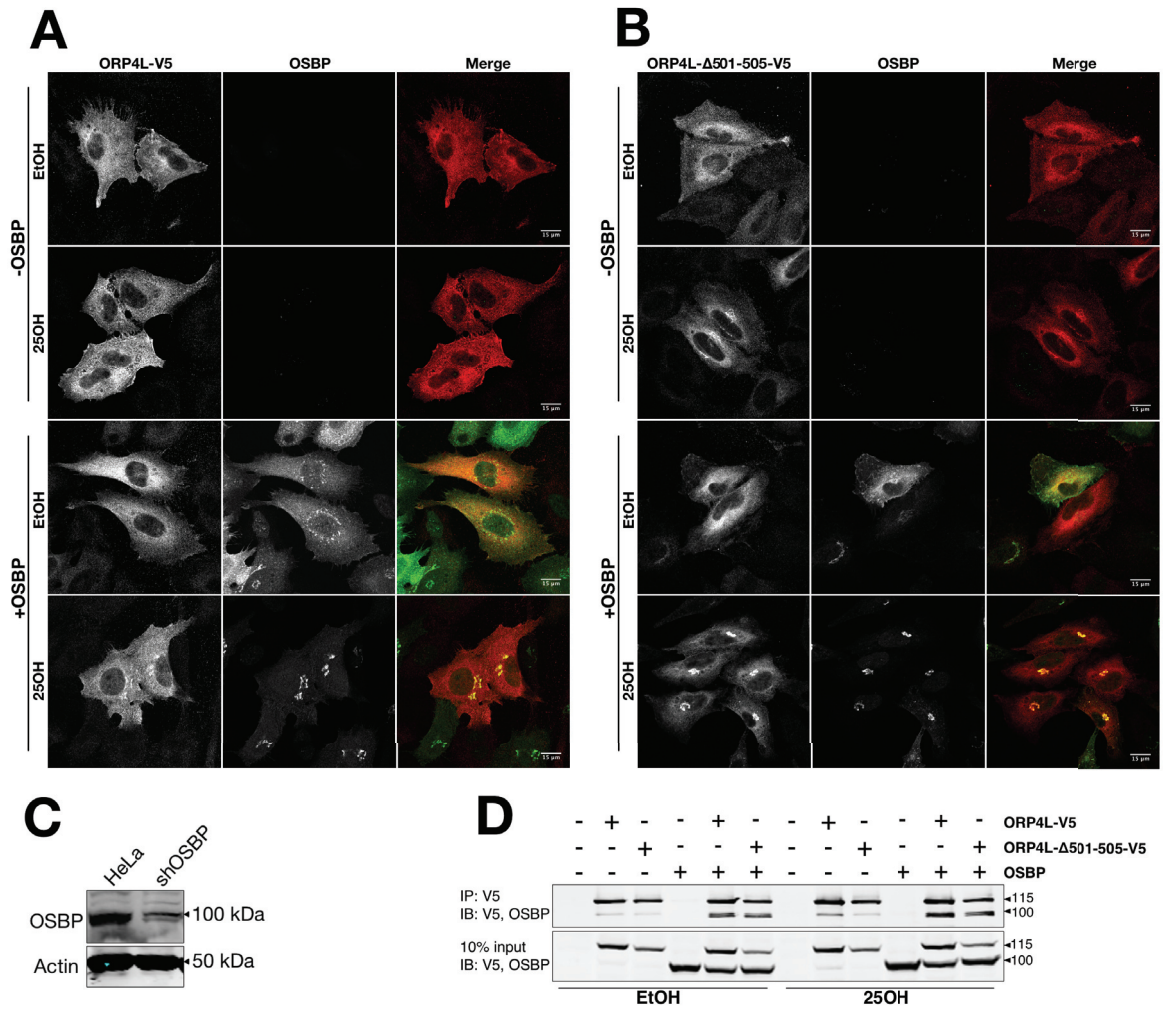

Figure 4.5 *Sterol-induced Golgi localization of ORP4 requires OSBP interaction.* HeLa OSBP knockdown cells were transiently transfected with **A)** ORP4L-V5 or **B)** ORP4L-Δ501-505-V5, with or without shRNA-resistant OSBP. Cells were treated with either 6 μM 25OH or equal volumes of EtOH for 2 h, probed with primary antibodies against OSBP and V5, and imaged by confocal microscopy as described in Materials and Methods. **C)** Immunoblot of WT HeLa and stably-transduced OSBP knockdown HeLa, probed for endogenous OSBP. **D)** HeLa cells transiently transfected with ORP4L-Δ501-505-V5 or ORP4L-WT and OSBP were treated with either 6 μM 25OH or solvent (ethanol) for 2 h and co-immunoprecipitated as described in the Materials and Methods. Immunoblots were probed with monoclonal antibodies against V5 and overexpressed OSBP.

cDNA (Figure 4.5 B). To determine whether association of ORP4L-Δ501-505-V5 with the Golgi apparatus was related to an enhanced physical interaction with OSBP, co-immunoprecipitation experiments were conducted in cells co-expressing OSBP and ORP4L-V5 or ORP4L-Δ501-505-V5 (Figure 4.5 D). OSBP co-immunoprecipitated with ORP4L-V5 and ORP4L-Δ501-505-V5 to a similar extent, and the interaction was independent of prior treatment of cells with 25OH. Data in Figure 4.4 and Figure 4.5 suggest that ORP4L localization to the ER-Golgi involves a combination of physical interaction with OSBP and provision of PI(4)P-enriched membranes.

Localization of OSBP at ER-Golgi MCS in response to 25OH activates PI4KIIα activity and establishes PI(4)P-rich microdomains recognized by CERT [78], which transports ceramide from the ER to the Golgi for sphingomyelin (SM) synthesis [215,216]. To determine if ORP4 functions as a sterol-dependent regulator of OSBP, we measured SM synthesis in CHO-K1 cells expressing ORP4L or ORP4S. The latter served as a negative control because it does not contain the N-terminal domains necessary for interaction with OSBP or localization to membranes containing PI(4)P [210]. Transient expression of ORP4L or ORP4S had no effect on 25OH-activated SM synthesis mediated by OSBP (Figure 4.7 A). Similarly, expression of ORP4L-Δ501-505-V5 or ORP4L-HH/AA-V5, mutants that differentially interact with the Golgi apparatus (Figure 4.2), had no effect on SM synthesis (Figure 4.6 B). These results suggest that ORP4L has an independent function downstream of OSBP, responding to changes in the Golgi membrane environment at MCS.

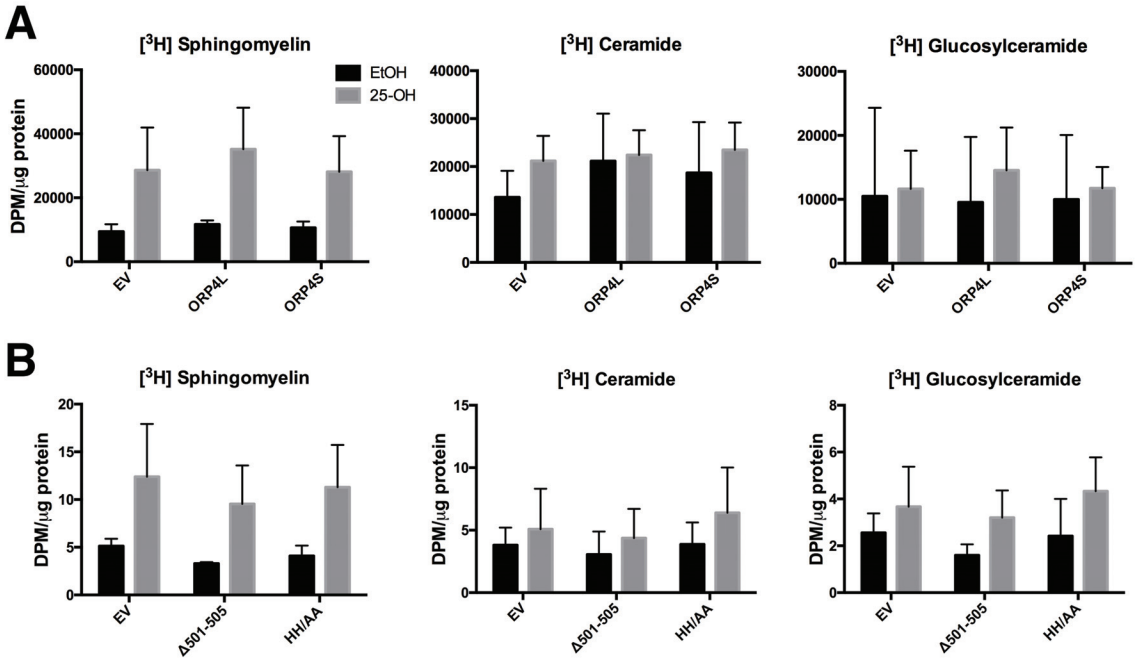

Figure 4.6 *ORP4 expression does not affect OSBP-dependent activation of CERT and SM synthesis.* **A)** CHO-K1 cells were transiently transfected with ORP4L-V5 or ORP4S-V5 and sphingomyelin, ceramide and glucosylceramide synthesis were quantified by [3H]serine incorporation in response to 25OH treatment as described in Methods and Methods. **B)** Similar experiments were repeated with ORP4 lipid binding mutants. Graphs represent the mean and SD of 3 experiments.

4.5 PM Association of ORP4L is Independent of VAP or Ligand Binding

In addition to sterol-dependent Golgi-localization, ORP4L-V5 was observed at the PM in both control and 25OH-treated cells (Figure 4.1 B). This is consistent with reports that ORP4L regulates IP_3 production by PLCβ3 at the PM, leading to calcium release from ER stores [217]. Confocal imaging of HeLa cells revealed that ORP4L-V5 and the three mutants were detected at the PM under control and 25OH-treated conditions (Figure 4.7 A). Qualitative analysis of confocal images from several experiments indicated that ORP4L-V5 was detected at the PM in 60-80% of control and 25OH-treated cells, and that this PM distribution was similar for the sterol-, PI(4)P- or VAP-binding mutants.

Endogenous VAPA immunostaining extended out to the PM but did not co-localize with ORP4L-V5 or the three ORP4L mutants, indicating an absence of discrete PM-ER contacts mediated by ORP4L and VAPA (Figure 4.7 A). To further test whether VAPA was localized with ORP4L at the PM, ORP4L-GFP and mCherry-VAPA were co-expressed in HeLa cells and imaged at the PM by total internal fluorescence (TIRF) microscopy (Figure 4.7 B). TIRF imaging showed a diffuse localization of ORP4L-GFP at the PM under normal and 25OH-treated conditions. mCherry-VAPA was also detected at the PM but the pattern was reticular in nature and did not co-localize with ORP4L-GFP (Figure 4.7 B).

4.6 ORP4 Co-localizes with PI(4)P, but not $PI(4)5P_2$, on the PM

Since ORP4L-V5 co-localized with, and was regulated by, Golgi-associated PI(4)P (Figure 4.2 and Figure 4.4), we determined whether ORP4L is targeted to regions of the PM containing PI(4)P by TIRF imaging of ORP4L-GFP and the PI(4)P sensor SidM-mCherry [218] (Figure 4.8 B). GFP-ORP4L was co-localized with diffuse and concentrated

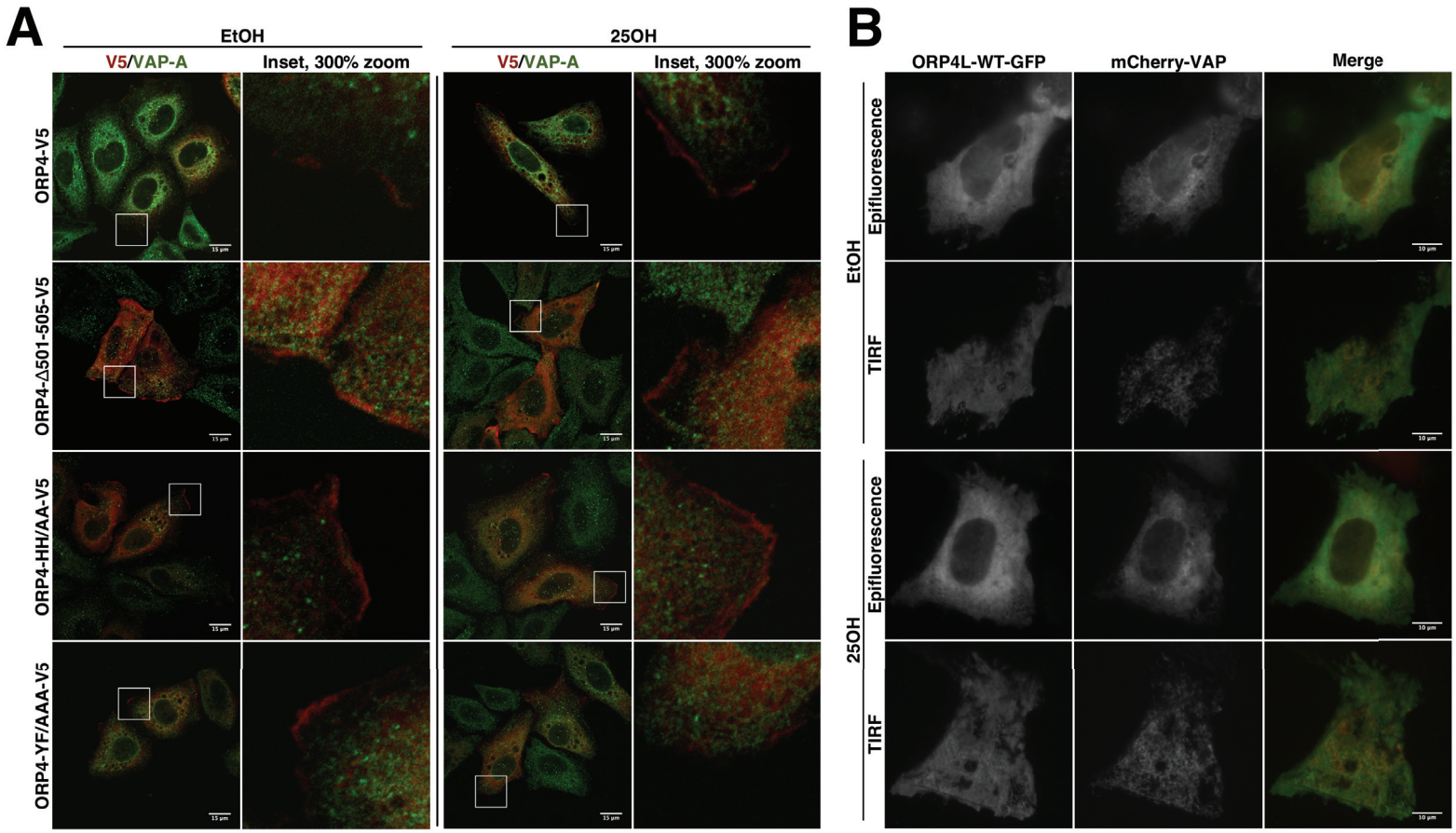

Figure 4.7 *ORP4 partially localizes to the plasma membrane.* **A)** HeLa cells were transiently transfected with constructs encoding ORP4L, ORP4-Δ501-505-V5, ORP4-HH/AA-V5 or ORP4L-YF/AA-V5. Cells were incubated for 2 h in ethanol or 6 μM 25OH, followed by immunostaining with V5 and VAP-A primary antibodies and Alexa Fluor-488 and -594 secondary antibodies, respectively. Images were captured by confocal imaging (0.7 μm sections) as described in Materials and Methods. **B)** HeLa cells plated on glass-bottom dishes were transiently transfected with GFP-ORP4L-WT and mCherry-VAP constructs, and images were captured using TIRF microscopy before and after 2 h of treatment with 6 μM 25OH.

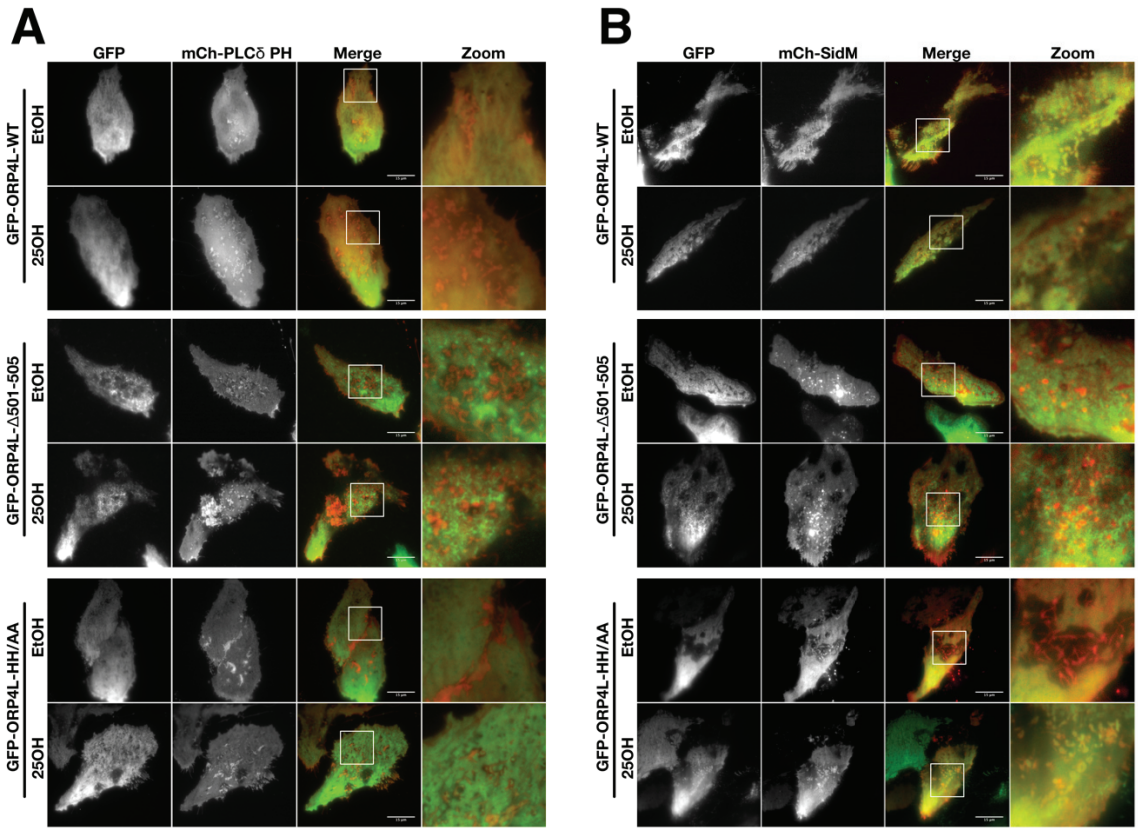

Figure 4.8 *TIRF imaging of ORP4L with probes for PI(4)P and PI(4,5)P2.* HeLa cells cultured on glass-bottom dishes were transiently transfected with GFP-ORP4L and either **A)** mCherry-PLCδ-PH or **B)** mCherry-SidM. Cells were subsequently treated with either ethanol or 6 μM 25OH for 2 h followed by TIRF imaging as described in Materials and Methods.

regions of SidM-mCherry under control and 25OH-treated conditions. In comparison, ORP4L-GFP did not co-localize with puncta labelled with the mCherry-tagged PH domain of PLCδ, a $PI(4,5)P_2$ sensor (Figure 4.8 A). Thus ORP4L association with the PM was constitutive and independent of its lipid and VAP binding activity, but associated with PI(4)P-positive regions of the membrane.

4.7 DISCUSSION

Members of the OSBP/ORP family interact with membranes and form bridges between organelles at MCS via the protein and lipid binding activities of their PH, FFAT and ankyrin motifs (summarized in Chapter 1.3). Increasingly, ORPs are found to be active at more than one organelle MCS. For example, ORP5 transfers or regulates lipid metabolism at ER-late endosome [59], ER-mitochondria [16] and ER-PM [17,18] contact sites. The intracellular localization and activity of ORP4L is also heterogenous, including associations with vimentin, the PM, and Golgi and ER compartments. The data in this chapter provide evidence that the OSBP-, lipid- and VAP-binding activities of ORP4L control its association at the ER-Golgi interface where it may regulate the structure of the TGN and proximal Golgi compartments.

Prior studies from our group utilized an antibody that recognized an internal epitope in ORP4L that did not detect Golgi-associated protein, possibly due to epitope-masking in the fraction of ORP4L that associates with the Golgi apparatus. In contrast, C-terminal epitope tagged ORP4L clearly associated with the TGN in cells treated with 25OH or after cholesterol depletion with cyclodextrin, treatments that also cause OSBP to translocate to ER-Golgi contact sites [219]. The detection of ORP4L at the Golgi reconciles our previous

observation of the Golgi-localized ORP4L GFP-PH domain [52], as well as the presence of its interacting partner OSBP at ER-Golgi MCS. Direct sterol-binding to ORP4L does not mediate translocation since ORP4L-Δ501-505-V5, a sterol-binding defective mutant that retains PI(4)P binding activity, moved to the TGN in response to 25OH and cyclodextrin. Rather, ORP4L and ORP4L-Δ501-505-V5 association with the TGN was dependent on OSBP and a Sac1-regulated pool of PI(4)P in the Golgi apparatus. OSBP could activate ORP4L localization to the ER-Golgi by two mechanisms. First, OSBP activation by 25OH increases a pool of Golgi PI(4)P that could be specifically recognized by the ORP4L GFP-PH domain fusion protein [209]. It follows that depletion of this PI(4)P pool by overexpression of the Golgi-localized Sac-K2A mutant accounts for attenuation of ORP4-Δ501-505-V5 recruitment to the TGN. Second, there could be a direct physical interaction that increases ORP4L recruitment to ER-Golgi MCS that contain OSBP. Initial interaction with OSBP would then facilitate binding of ORP4L to PI(4)P and VAP, thus stabilizing its interaction at MCS.

The finding that ORP4L-YF/AA-V5 does not respond to 25OH suggests that the observed TGN localization of ORP4L represents a MCS formed through interaction with VAP in the ER. Since the OHD of ORP4L binds cholesterol and PI(4)P and mediates cholesterol transfer *in vitro* [52], it could transfer these, or other unidentified ligands, in parallel or in opposition to OSBP. Since ORP4-Δ501-505-V5 localizes to ER-Golgi MCS but the PI(4)P-binding mutant ORP4-HH/AA-V5 did not, it appears that PI(4)P-binding is an initial step in ORP4L recruitment to MCS after OSBP activation while a sterol-bound form is restricted from the MCS. Whether it represents a lipid transfer cycle or regulatory activity in MCS will require further investigation.

It is currently unknown if the Golgi-ER specific activities of ORP4L contribute to its proliferative and growth promoting properties, or whether they are secondary phenomena. We ruled out any potential role for ORP4L in OSBP-dependent sphingolipid synthesis, confirming that ORP4L functions downstream of OSBP, perhaps as a recruited factor at MCS, similar to CERT [35] and Nir2 [14]. However, the presence of ORP4L at the PM in HeLa cells is consistent with its recently discovered role in the regulation of proliferative IP_3 production and ER calcium release via PLCβ3 regulation [55]. We observed that the PM localization of ORP4L was independent of lipid and VAP binding activities that controlled its association with the ER-Golgi MCS. This result is consistent with reports that the PLCβ3 scaffolding activity of ORP4L is independent of VAP [55], suggesting that PM-ER MCS are not involved. TIRF imaging showed that ORP4L was localized at the PM with the PI(4)P sensor SidM. Again this agrees with the requirement for the ORP4L PH domain, which recognizes PI(4)P *in vitro*, in PLCβ3 scaffolding. However, the ORP4L GFP-PH domain was not detected at the PM [52], suggesting that the PH domain alone is not sufficient for PM localization.

We conclude that ORP4L has two independently regulated activities: one at the PM related to cell signaling, the other that controls lipid transport or metabolism at ER-Golgi MCS that is critical for organelle morphology. To further understand the cellular processes that regulate these functions, we investigated the phosphorylation state of ORP4, the functional consequences of ORP4 phosphorylation and the potential kinase pathways involved.

CHAPTER 5 PHOSPHORYLATION OF ORP4L ALTERS LIGAND BINDING AND PROTEIN INTERACTIONS

5.1 ORP4 IS PHOSPHORYLATED AT MULTIPLE SERINE RESIDUES IN THE OHD

The OHD of human ORP4 contains a sequence of 6 serine residues interrupted by proline residues (S_{762}SPSSPSS_{769}) that is partially conserved in rodent ORP4 (Figure 5.1 A). Interestingly, the serine/proline motif is absent in its closest paralogue OSBP, and the entire region containing the motif is absent in other ORPs (Figure 5.1 B). Accession numbers for the transcripts used in the PRALINE alignment [220] are listed in Table 4. To confirm that the serine residues are in a solvent-exposed region of the OHD, SWISS-MODEL was used to create a homology model of the ORP4 OHD based on the structure for the Osh3p OHD (Figure 5.1 C). The homology model and alignments show that the serine-rich motif is in a 28-residue loop that interrupts β-sheet 16 and extends from the opposite side of the PI4P and sterol binding pocket of the ORP4 OHD.

Based on curated phospho-proteome data sets on public websites and in published reports [176-178], 5 residues in the serine-rich motif are phosphorylated in human ORP4, while 3 sites are substrates for phosphorylation in murine ORP4 [177]. To confirm these phosphorylated residues, ORP4L-V5 transiently overexpressed in HeLa cells was immunoprecipitated, resolved by SDS-PAGE and subjected to tryptic digestion and LC-MS/MS analysis by Dr. Alejandro Cohen at the Dalhousie University Proteomics Core Facility (Figure 5.2). Phosphorylation of serine residues 762, 763, 766 and 768 was detected, while phosphorylation at serine 765 was difficult to assess. The presence of this highly phosphorylated site unique to the ORP4 OHD prompted us to investigate its

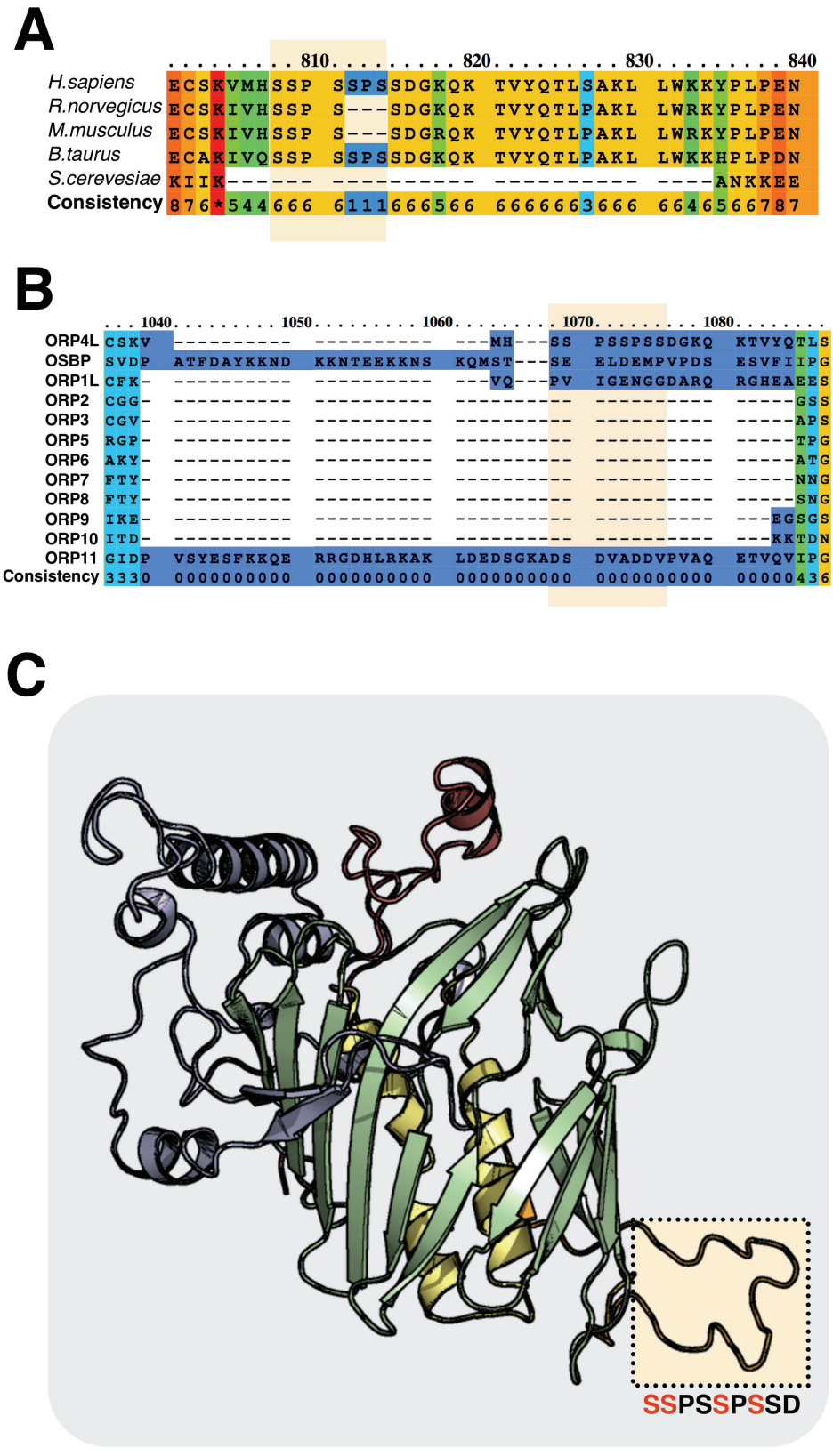
A
. . . . . 810 . . . . . 820 . . . . . 830 840
H.sapiens ECSKVMHSSP SSPSSDGKQK TVYQTLSAKL LWKKYPLPEN
R.norvegicus ECSKIVHSSP S---SDGKQK TVYQTLPAKL LWRKYPLPEN
M.musculus ECSKIVHSSP S---SDGRQK TVYQTLPAKL LWRKYPLPEN
B.taurus ECAKIVQSSP SSPSSDGKQK TVYQTLPAKL LWKKHPLPDN
S.cerevesiae KIIK---------- ---------- ---------- ----ANKKEE
Consistency 876*544666 6111666566 6666663666 6646566787
B
. . . 1040 . . . . . 1050 . . . . . 1060 . . . . . 1070 . . . . . 1080 . . . . .
ORP4L CSKV---------- ---------- ---MH---SS PSSPSSDGKQ KTVYQTLS
OSBP SVDP ATFDAYKKND KKNTEEKKNS KQMST---SE ELDEMPVPDS ESVFIIPG
ORP1L CFK--------- ---------- ---VQ---PV IGENGGDARQ RGHEAEES
ORP2 CGG--------- ---------- ---------- ---------- -----GSS
ORP3 CGV--------- ---------- ---------- ---------- -----APS
ORP5 RGP--------- ---------- ---------- ---------- -----TPG
ORP6 AKY--------- ---------- ---------- ---------- -----ATG
ORP7 FTY--------- ---------- ---------- ---------- -----NNG
ORP8 FTY--------- ---------- ---------- ---------- -----SNG
ORP9 IKE--------- ---------- ---------- ---------- ---EGSGS
ORP10 ITD--------- ---------- ---------- ---------- ---KKTDN
ORP11 GIDP VSYESFKKQE RRGDHLRKAK LDEDSGKADS DVADDVPVAQ ETVQVIPG
Consistency 3330 0000000000 0000000000 0000000000 0000000000 0000043 6
C
SSPSSPSSD

Figure 5.1 *The OHD of ORP4 is phosphorylated at a unique solvent-exposed site.* **A)** PRALINE sequence alignment of the ORP4L phosphorylation site between *H.sapiens*, *R.norvegicus*, *M.musculus*, *B.taurus*, and *S.cerevesiae*. **B)** PRALINE sequence alignment (http://www.ibi.vu.nl/programs/pralinewww/) of the ORP4L phosphorylation site between human ORPs. Accession numbers associated with proteins in panels A and B can be found in Table 4. **C)** SWISS-MODEL homology model of the ORP4L OHD based on the crystal structure for Osh3p (PDB: 4INQ). The OHD is an incomplete β-barrel (green) flanked by two central helices (yellow), an α-helical lid (red) and N-terminal region (blue). The predicted location of the phosphorylated serine residues (red type) is highlighted.

Table 4 NCBI Accession Numbers for Proteins Aligned in Figure 5.1.

Gene	Protein	Species	Accession Number
OSBP2	ORP4L	*H.sapiens*	Q969R2*
Osbp2	ORP4	*R.norvegicus*	D3ZH34
Osbp2	ORP4	*M.musculus*	Q5QNQ6
OSBP2	ORP4	*B.taurus*	E1B7M8
KES1	Kes1/Osh4p	*S.cerevesiae*	P35844
OSBP	OSBP	*H.sapiens*	NP_002547.1
OSBPL1A	ORP1L	*H.sapiens*	Q9BXW6.2
OSBPL2	ORP2	*H.sapiens*	CAG33003.1
OSBPL3	ORP3	*H.sapiens*	AAL40657.1
OSBPL5	ORP5	*H.sapiens*	AAL40666.1
OSBPL6	ORP6	*H.sapiens*	AAL40661.1
OSBPL7	ORP7	*H.sapiens*	AAL40659.1
OSBPL8	ORP8	*H.sapiens*	AAL40665.1
OSBPL9	ORP9	*H.sapiens*	AAL40658.1
OSBPL10	ORP10	*H.sapiens*	AAL40664.1
OSBPL11	ORP11	*H.sapiens*	AAL40667.1

*Note that the *H.sapiens* ORP4L transcript reported in the NCBI database begins at a methionine residue 40 amino acids prior to the initiator methionine for the cDNA used in this study [31], resulting in a discrepancy between the amino acid numbering displayed in sequence alignments and the designation of our mutants.

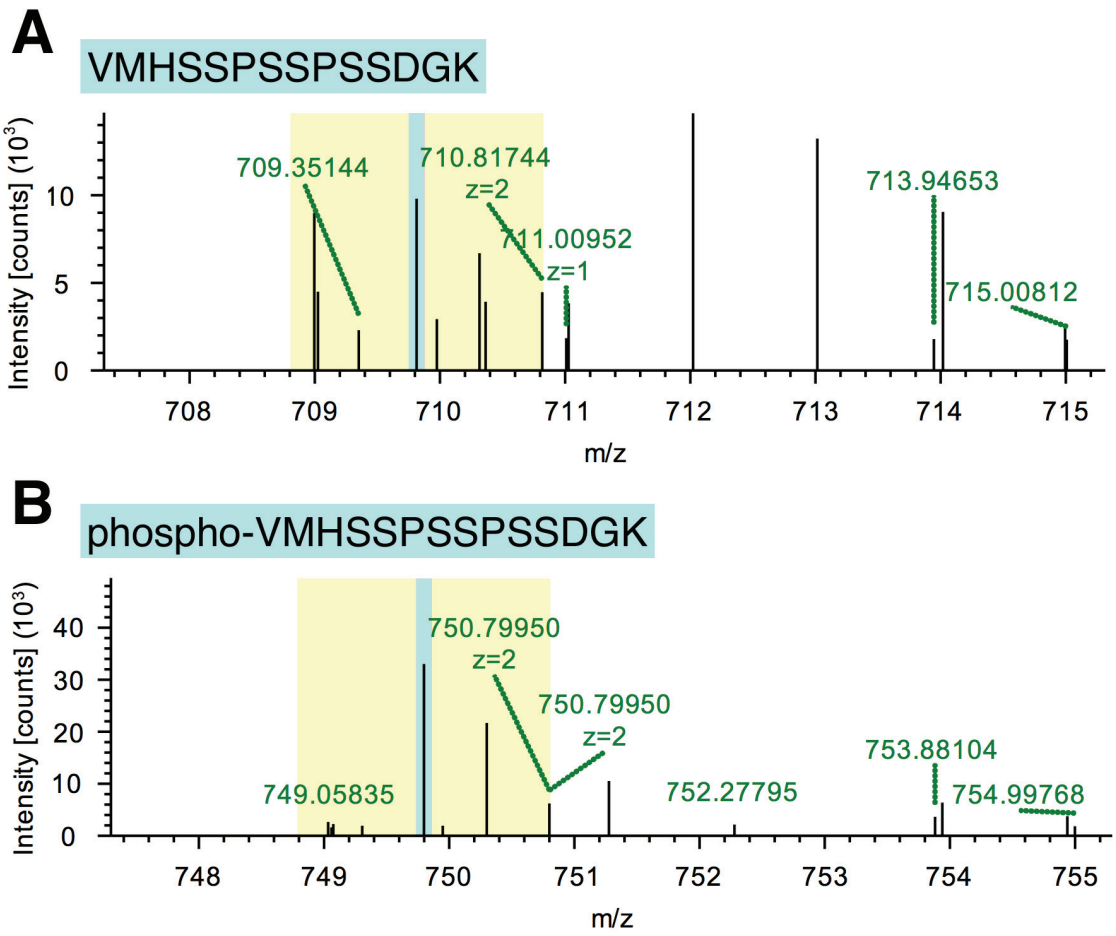

Figure 5.2 ESI-MS confirms phosphorylation of the doubly-charged peptide containing the ORP4 phospho-site.ORP4L was subjected to trypsin digestion and LC-MS/MS analysis as described in the Materials and Methods section, and the ORP4-aa760-772 peptide was identified using the Sequest HT DB search engine. A first fragmentation shows that the mass of **A)** unmodified ORP4-aa760-772 differs from the mass of **B)** phosphorylated ORP4-aa760-772 by one phosphate molecule (80 Da). Sequence-related information from a second fragmentation step confirmed individual phosphorylation of S762, S763, S765, S766 and S768 (data not shown).

functional relevance. Because multiple residues are predicted to be phosphorylated, we opted to mutate serine residues 762, 763, 766 and 768 to aspartate residues to mimic a highly phosphorylated state (ORP4L-S/D), while the same residues were mutated to alanine (ORP4L-S/A) to mimic a constitutively dephosphorylated state. Vectors encoding ORP4-V5-tagged phospho-mutants were prepared for expression in mammalian cell culture, as well as 6xHis-tagged baculoviral constructs for purification from insect cells and subsequent ligand binding and kinase specificity studies.

5.2 KINASE SPECIFICITY FOR THE ORP4 PHOSPHO-SITE

The ORP4 phosphorylation site is punctuated by two proline residues and was therefore predicted to be the target of a proline-directed kinase(s). Using an *in silico* kinase prediction tool (PhosphoNET, Kinexus Bioinformatics), kinases with the highest probability of phosphorylating S762, S763, S766 and S768, including proline-directed kinases glycogen synthase kinase (GSK) 3a and 3b, cJun N-terminal kinase 1 (JNK1), extracellular signal-regulated kinase 1 (ERK1) and cyclin-dependent kinase 1 (CDK1)/cyclin A2 as well as the non-proline-directed casein kinase 1 alpha 1 (CK1a1), were selected for further investigation. Seven of the highest ranking predicted kinases were tested by Kinexus Bioinformatics (Vancouver, BC) for their ability to phosphorylate recombinant ORP4L and ORP4L-S/A *in vitro* using [^{32}P]-ATP. The absolute amount of [^{32}P] incorporation into ORP4L was expressed relative to ORP4L-S/A to identify those kinases with the highest specificity for the phosphorylation site (Table 5). CK1a1, JNK1 and CDK1/cyclin A2 had the highest absolute activity with ORP4L, while CDK1/cyclin A2, GSK3a, CK1a1 and GSK3b showed the greatest specificity for the site when

Table 5 *In vitro* kinase activity toward ORP4L and ORP4L-S/A

Kinase	ORP4L-WT	ORP4L-S/A	Difference*	% change**
CDK1/CyclinA2	17,218	7,310	-9,908	-58%
GSK3A	7,745	4,096	-3,649	-47%
CK1 α1	48,238	30,044	-18,194	-38%
GSK3B	11,948	9,093	-2,855	-24%
JNK1	45,409	38,615	-6,794	-15%
ERK1	10,423	9,080	-1,343	-13%
JNK3	8,554	7,762	-792	-9%

Experiment was performed once.
* *Difference* reflects the change in phosphorylation caused by loss of the phospho-site.
** *% change* is the difference reflected as a percentage of phosphorylation of the wild-type protein.

background activity against the S/A mutant was removed. Because of the complexity of the phospho-site, it is difficult to determine exactly which serine(s) in ORP4L were phosphorylated by these candidate kinases. In addition, two of the most selective kinases, CK1a1 and GSK3b, are both frequently regulated by priming phosphorylation events next to the phosphorylated serine.

5.3 PHOSPHORYLATION AFFECTS CHOLESTEROL EXTRACTION *IN VITRO*

Recombinant His-tagged wild-type ORP4L and ORP4L-S/D and –S/A mutants were expressed by baculovirus infection of Sf21 cells and purified by metal-affinity chromatography (Figure 5.3 A). The lipid binding activity of the recombinant phospho-mutants was then compared to wild-type ORP4L. The binding affinity for [^{3}H]25OH by wild-type ORP4L (K_d 45$\pm$12 nM), ORP4L-S/A (K_d 62$\pm$28 nM) and ORP4L-S/D (K_d 60$\pm$18 nM) were not significantly different (Figure 5.3 B). The ability of ORP4L phospho-mutants to extract radiolabelled cholesterol and PI(4)P from membranes was assayed (Figure 5.3 C and D) using a liposome-based assay described in Chapter 3, Figure 3.6. The extraction of [^{3}H]cholesterol by ORP4L-S/D was increased 2-fold compared to wild-type and ORP4L-S/A, (Figure 5.3 C). Extraction of [^{32}P]PI(4)P from liposomes by ORP4L-S/D was increased slightly but this did not reach significance (Figure 5.3 D).

5.4 EFFECT OF PHOSPHORYLATION ON CELLULAR LOCALIZATION OF ORP4L AND ORP4S

ORP4L has a complex distribution in cells, partitioning between the cytoplasm, ER, Golgi apparatus and PM. N-Terminal truncations that produce the ORP4S and ORP4M

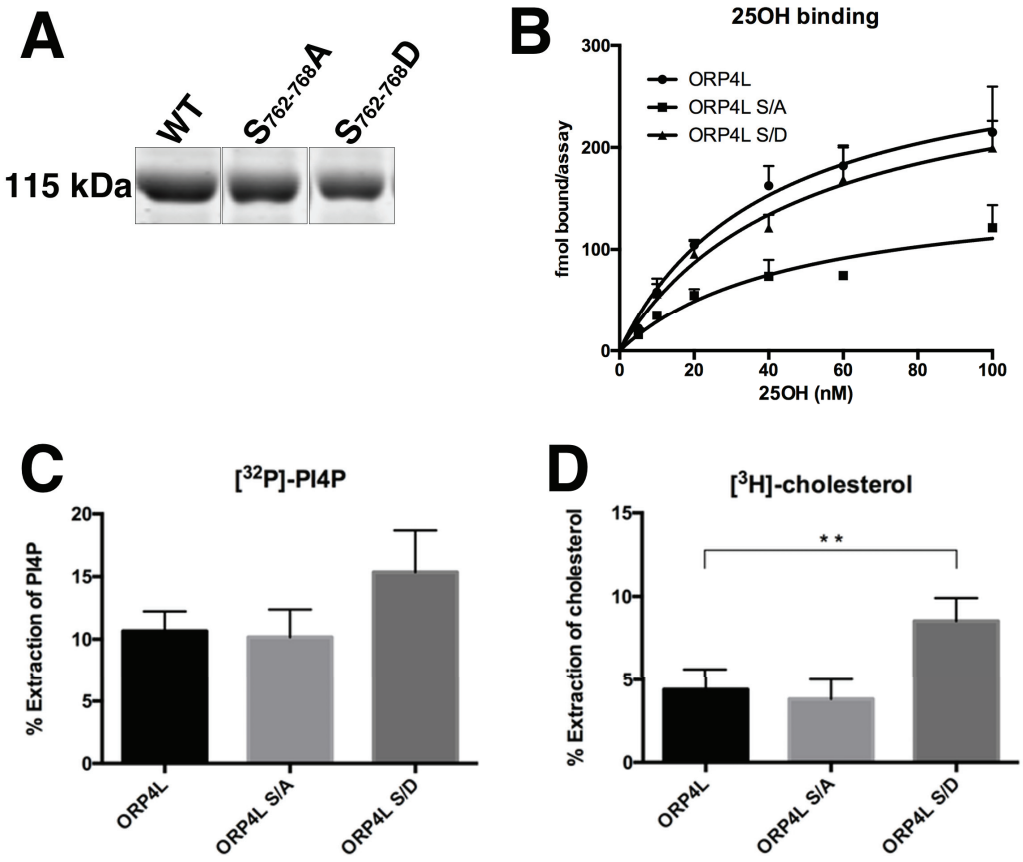

Figure 5.3 *Phosphorylation of ORP4 affects ligand extraction.* **A)** 6xHis-tagged wild-type and phospho-site mutant ORP4L were expressed in SF21 insect cells, purified by metal affinity chromatography, resolved by SDS-8%PAGE (2 μg each) and stained with GelCode Blue. Recombinant ORP4L and phospho-site mutants were then assayed for **B)** specific binding of [^{3}H]25OH, and **C)** [^{32}P]PI4P and **D)** [^{3}H]cholesterol extraction from liposomes as described in Chapter 3, Figure 3.5. Experiments in panels B,C and D have been repeated in triplicate.

variants result in loss of ER/Golgi/PM localization but enhance interaction with the vimentin intermediate filament network, resulting in its collapse into bundles and perinuclear aggregates [52,170]. To determine the effect of phosphorylation on intracellular localization of ORP4, wild-type and phospho-mutants of ORP4L-V5 were expressed in HeLa cells and monitored by immunofluorescence (Figure 5.4). ORP4L and both phospho-mutants displayed what appeared to be TGN localization in response to 25OH (Figure 5.4), as evidenced by the vicinity of ORP4-positive structures to the *cis*/medial-Golgi but not complete colocalization with giantin. However, ORP4L-S/D also localized strongly with aggregates confirmed to be vimentin (Figure 5.6), similar to those associated with ectopic ORP4S expression. The formation of vimentin aggregates by ORP4L-S/D was independent of 25OH treatment (Figure 5.4 and Figure 5.6, bottom panels), indicating that ORP4L phosphorylation does not affect 25OH-dependent interaction with the Golgi apparatus but enhances the interaction with vimentin.

To determine whether phosphomimetic mutations were directly affecting the vimentin/OHD interaction, the phospho-mutations were introduced into V5-tagged ORP4S and localization was monitored in HeLa cells. Expression of wild-type ORP4S caused the expected aggregation of the vimentin network, as did ORP4S-S/D and –S/A (Figure 5.5). Thus the phospho-site in the context of ORP4L seems to induce a conformational change that mimics the ORP4S N-terminal truncated isoform.

5.5 PHOSPHORYLATION ALTERS THE CONFORMATION OF THE ORP4L HOMODIMER

We assessed the multimeric state of recombinant ORP4L and its phospho-mutants by cross-linking in solution using glutaraldehyde (Figure 5.7). Contrary to yeast-2-hybrid

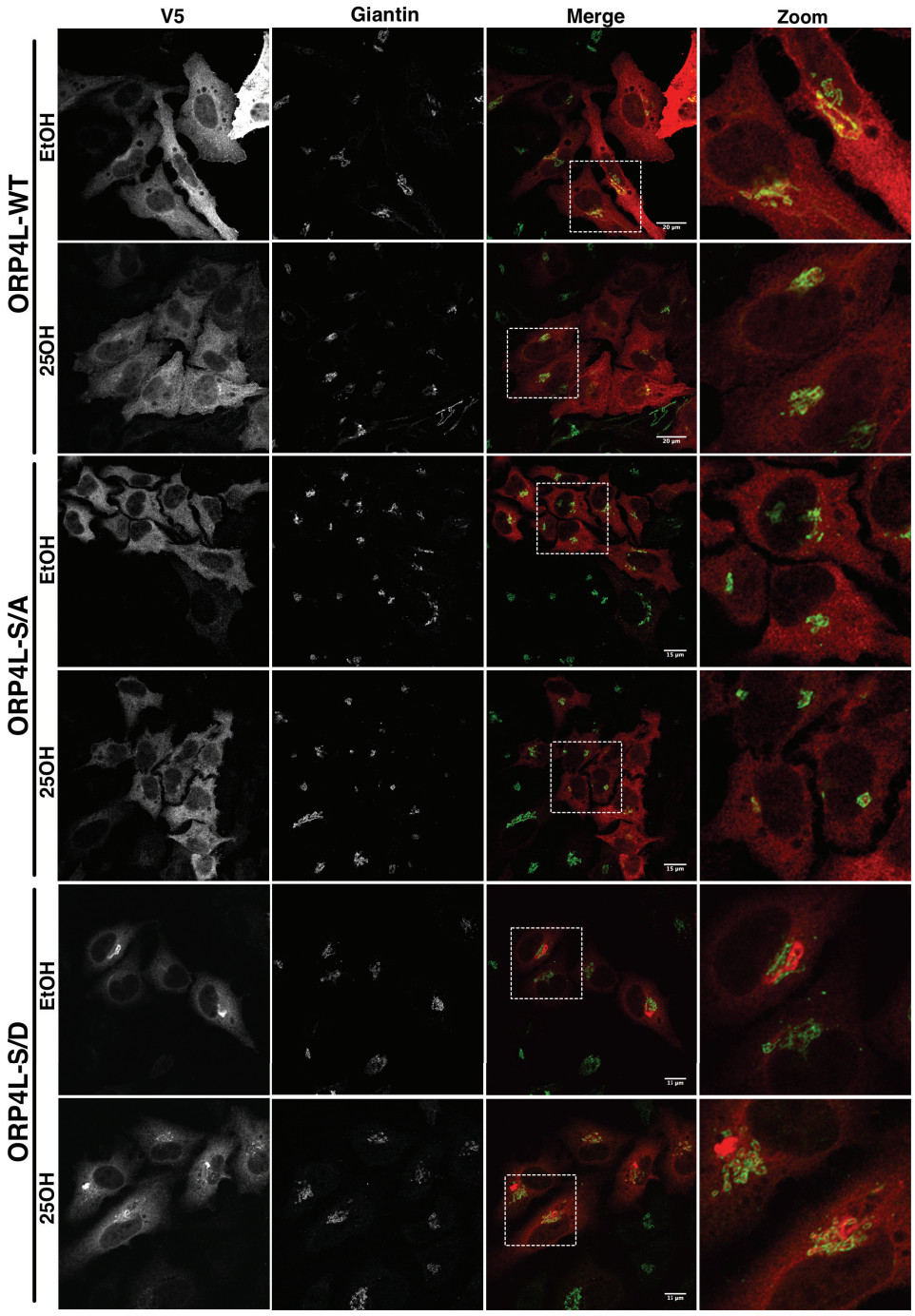

Figure 5.4 *Phosphorylation of ORP4L at S762, 763, 766 and 768 does not affect Golgi localization.* HeLa cells were transiently transfected with wild-type, phosphomimetic and phosphorylation-null ORP4L and treated with 6 μM 25OH or solvent control for 2 h and fixed and permeabilized as described in Materials and Methods. Cells were then probed with primary antibodies against the V5 tag and giantin followed by secondary antibodies Alexa Fluor-594 and -488, respectively.

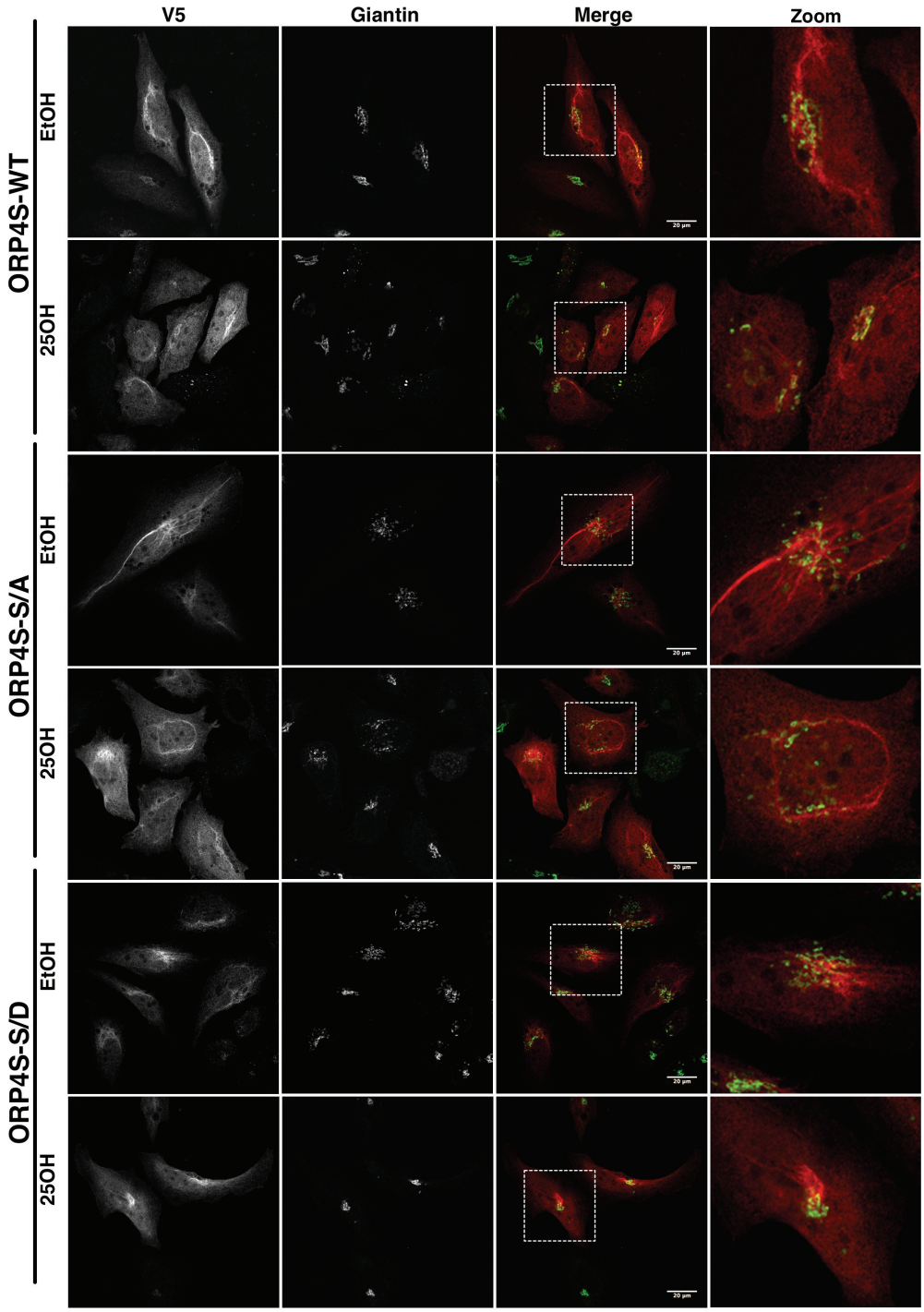

Figure 5.5 *Phosphorylation of S762, S763, S766 and S768 does not affect vimentin aggregation by ORP4S.* HeLa cells were transiently transfected with wild-type, phosphomimetic and phosphorylation-null ORP4S and treated with 6 μM 25OH or solvent control for 2 h and fixed and permeabilized as described in Materials and Methods. Cells were then probed with primary antibodies against the V5 tag and giantin followed by secondary antibodies Alexa Fluor-594 and -488, respectively.

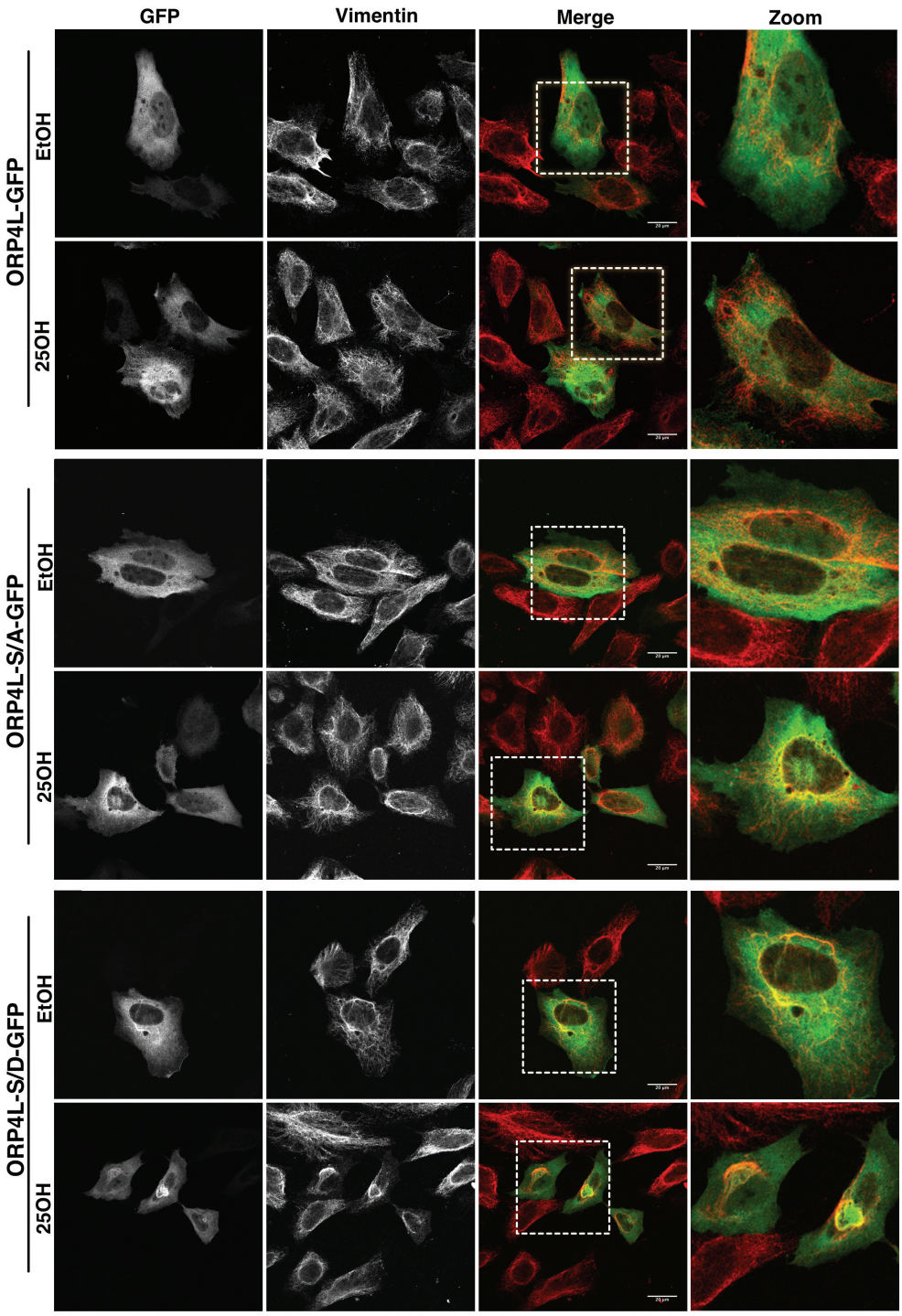

Figure 5.6 *Phosphorylation of ORP4L at S762, 763, 765, 768 relieves autoinhibition of vimentin interaction.* HeLa cells were transiently transfected with GFP-tagged wild-type (WT) phosphorylation-null (S/A) or phosphomimetic (S/D) ORP4L, treated with 6 μM 25OH or solvent control for 2 h, then fixed and permeabilized as described in Materials and Methods. Cells were probed with a primary antibody against vimentin followed by Alexa Fluor-594.

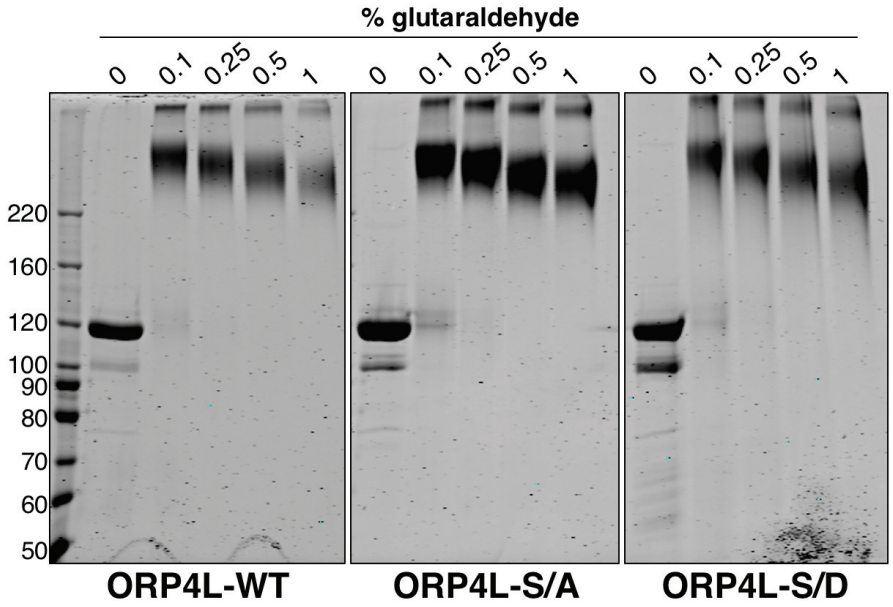

Figure 5.7 *Phosphorylation status of ORP4L does not affect its dimerization state based on glutaraldehyde crosslinking.* Recombinant ORP4L, ORP4L-S/D and ORP4L-S/A were incubated with increasing concentrations of glutaraldehyde (v/v) at 37°C for 5 minutes as described in the Materials and Methods. Gels were stained with GelCode Blue. Similar results were observed in 2 other experiments.

results reporting ORP4L as a monomeric protein [53], purified ORP4L formed a cross-linked species that migrated on SDS-PAGE at the predicted molecular mass of a dimer (approximately 260 kDa according to a semi-logarithmic plot of the protein standards), and neither S/D or S/A mutation affected the dimerization state (Figure 5.7). Increased glutaraldehyde concentrations did not induce formation of higher order multimers.

To assess the effect of phosphorylation on the native conformation of ORP4L, we used gel filtration-HPLC to observe whether phospho-mutations altered the Stokes radii of ORP4L (Figure 5.8). This technique revealed retention times for a major peak (~470 kDa) and trailing shoulder (380-400 kDa) that were consistent with a native trimer or tetramer. However, the native structure of ORP4L is unknown, and the globular nature of the standards used (thyroglobulin, amylase and carbonic anhydrase) should be noted when considering the value of a molecular weight estimation by this method. Wild-type and ORP4L-S/A eluted as a major single peak but ORP4L-S/D eluted as two poorly resolved species, indicating a significant conformational shift induced by the phospho-site.

5.6 Discussion

In this study, we have identified a unique solvent-exposed serine/proline-rich phosphorylation motif in the ORP4 OHD that influences its lipid and protein binding activity. Based on sequence alignments and modeling, the site is unique to ORP4 and appears to control a conformational switch that exposes a site(s) on the OHD that interacts with the vimentin intermediate filament network. ORP4L-S/A displayed localization and ligand-binding indistinguishable from that of wild-type ORP4L, which suggests that under basal conditions the phospho-motif in ORP4L is minimally phosphorylated at one or more

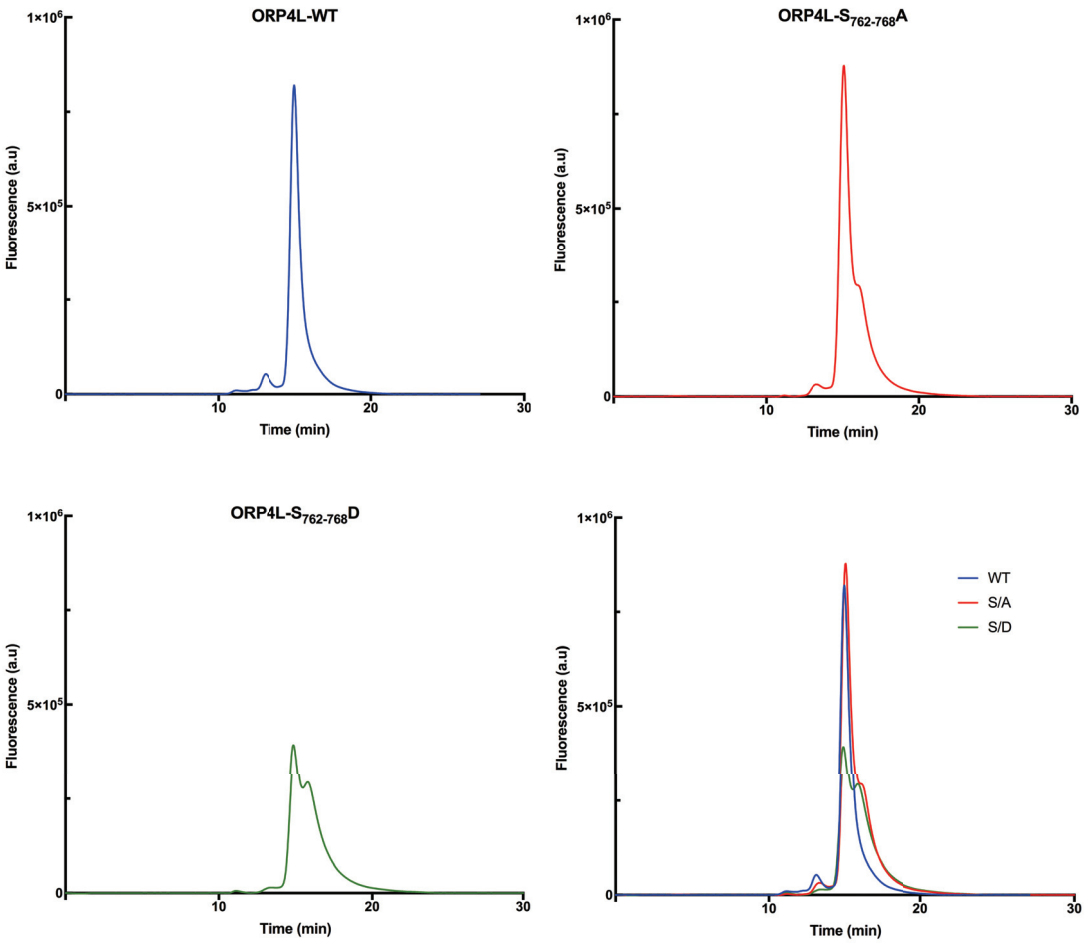

Figure 5.8 *Phosphorylation alters the native conformation of ORP4L.* Recombinant ORP4L, ORP4L-S/D and ORP4L-S/A were resolved by gel filtration (GF)-HPLC under isocratic conditions as described in the Materials and Methods. The elution profiles are representative of 3 separate experiments.

of the relevant serine residues. On the other hand, ORP4L-S/D had increased cholesterol extraction activity from liposomes while its affinity for aqueous dispersions of 25OH and cholesterol was unaffected. This result suggests that phosphorylation may enhance the interaction between ORP4L and donor membranes but does not alter the ligand binding pocket of the OHD, and that solution binding of 25OH is independent of membrane association. It may be that ORP4 function is regulated by two separate mechanisms; ORP4L localization to the Golgi apparatus is dependent on a 25OH-induced elevation of Golgi PI(4)P by OSBP, while the actual extraction of cholesterol is controlled by phosphorylation of the OHD.

The enhanced cholesterol extraction and vimentin interaction exhibited by phospho-mimetic ORP4L-S/D was similar to that previously observed for ORP4S, which has increased cholesterol extraction and transfer activity compared to ORP4L, and interacts strongly enough with vimentin to induce perinuclear collapse of the vimentin network[52]. Our previous conclusion that the N-terminal PH domain of ORP4L is autoinhibitory with respect to both vimentin interaction and ligand extraction seems to be supported by the present data [52]. The similarities between ORP4L-S/D and wild-type ORP4S indicate that phosphorylation of the ORP4L OHD may relieve autoinhibition by the PH domain (Figure 5.9). Indeed, the reverse has been demonstrated for CERT [221]. In this case, intramolecular interactions between the CERT PH domain and a serine-rich phosphorylation site in the linker region adjacent to the START domain are relieved by dephosphorylation, freeing the PH domain to bind PI(4)P in the Golgi apparatus. In the case of ORP4L, a functional link between cholesterol extraction activity and vimentin interaction raises the question of

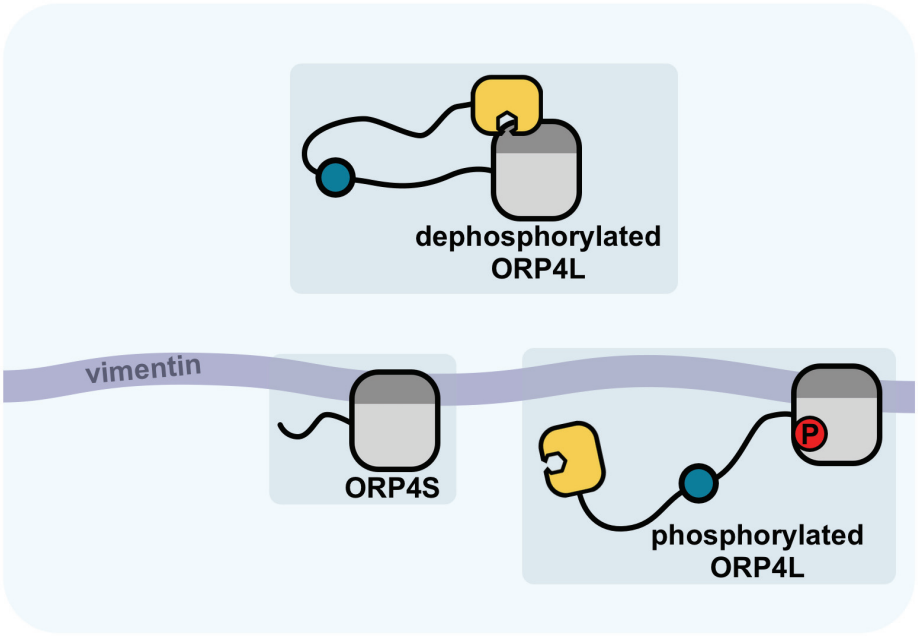

Figure 5.9 *Model for ORP4 autoinhibition by the PH domain.* The PH domain of ORP4L negatively regulates the ORP4/vimentin interaction, possibly by occluding sites of vimentin contact in the OHD. Phosphorylation at S762, S763, S765 and S768 may relieve this autoinhibition by disturbing intramolecular interactions that fold ORP4, exposing the vimentin-binding site and emulating the ORP4S vimentin aggregation phenotype.

whether ligand binding by ORP4L influences protein interaction or vice-versa. Increased cholesterol binding by phosphorylated ORP4L may be functionally tied to vimentin remodeling; alternatively, hyperactive cholesterol extraction by phosphorylated ORP4L may be attenuated by sequestration of ORP4L on vimentin filaments.

We identified several putative ORP4L kinases that phosphorylate the serine/proline-rich site *in vitro*. CDK1 [222] and CK1α [223] are involved in cell cycle progression and as such their activity is temporally regulated, and while GSK3a and GSK3b are constitutively active, phosphorylation by these kinases usually requires priming of the substrate by phosphorylation of an adjacent serine residue [224]. In particular, potential phosphorylation of ORP4 by GSK3a and GSK3b requires further investigation; deactivation of GSK3a and GSK3b allows for progression of EMT and consequently for expression of vimentin [174]. The role of the ORP4/vimentin interaction is not known, but determining the phosphorylation state of ORP4 during EMT using commercially available GSK3 inhibitors may help determine whether this interaction contributes to or attenuates vimentin function with respect to cell adhesion and motility. *In vitro* phosphorylation of ORP4L by JNK1 was notably high but only modestly reduced by the S/A mutation, suggesting that ORP4L is phosphorylated by JNK1 at one or more of the 16 potentially phosphorylated serine residues reported in the PhosphoSite database that are outside of the phospho-site examined in this study. The identification of signaling pathways upstream of ORP4 phosphorylation may provide context for its function as a lipid binding/transfer protein, particularly with respect to its role in cell proliferation and metastasis. This study provides a potential mechanism for ORP4L regulation by phosphorylation of a

serine/proline-rich site in the OHD, and further studies of the kinase pathways upstream of ORP4L phosphorylation are warranted to determine the primary function of ORP4L.

The discovery that ORP4L is a dimer resolves some contradictory observations regarding OSBP/ORP4 dimer formation. Homodimerization of OSBP involves interactions between the central dimerization motifs of each monomer, likely in combination with one or both of the flanking leucine repeats [6]. ORP4 contains the same leucine repeats as well as a dimerization motif, sharing 90% homology with that of OSBP, and as a result the OSBP/OSBP contacts are sufficiently conserved in ORP4 to provide an interface for ORP4/OSBP dimers or tetramers. Indeed, the ORP4/OSBP interaction was found to require the dimerization motif and leucine repeats of OSBP [53]. It follows that the OSBP/ORP4 contacts mediate ORP4 homodimerization, and so our results are consistent with what is currently understood about homo- and heterodimerization of OSBP. The observation of ORP4 dimers provides new avenues for understanding ORP function. Ligand binding and extraction studies of wild-type ORP4 in equimolar combination with OSBP, or of dimerization-deficient ORP4, are warranted to understand the significance of the OSBP/ORP4 and ORP4/ORP4 interactions.

CHAPTER 6 CONCLUSIONS

ORP4 is currently the only ORP known to be required for cell proliferation, but its function remains elusive. While this study does not constitute sufficient data to propose a mechanism of ORP4 activity, it expands the current understanding of how ORP4 behaves in cells and can direct future approaches to determining the primary cellular function of ORP4. Therefore, in conclusion of this work, the following discussion outlines potential future research avenues based on the findings described in this thesis.

Whether TGN dispersion is the cause or consequence of apoptosis in shORP4 cells requires further investigation. It is unclear whether ORP4L ligand binding or membrane/protein interactions are necessary for maintenance of TGN morphology. The fact that VAP depletion dilates and disperses the TGN similarly to ORP4 depletion [14] suggests that the ER maintains late Golgi structures via ORP4, though other FFAT-domain-containing ORPs may be involved. Interestingly, when VAP-depleted cells are treated with 25OH, the TGN dispersion phenotype extends to the *cis*/medial-Golgi due to disruption of Golgi lipid composition in the absence of an ER contact for OSBP [14]. While ORP4 depletion had limited effects on the *cis*/medial-Golgi, future studies should involve observing these compartments following 25OH treatment of shORP4 cells, as *cis*/medial-Golgi dispersion following 25OH treatment in the presence of both VAP and OSBP would imply that ORP4L is a major contributor to maintenance of Golgi lipid composition.

Yan and colleagues provide evidence of a 25OH-sensitive ORP4-scaffolded PLCβ3 activation complex specific to T-ALL [55] cells and macrophages [54], but ORP4 depletion also induces growth arrest, apoptosis and aberrant IP_3 signaling in other cell types [52,56] and our data shows that PM association of ORP4 is independent of sterol binding.

Considering the PI(4)P binding function of ORP4L, it is also possible that it modulates IP_3 production at the PM by replenishing PI(4)P levels for conversion to $PI(4,5)P_2$. This could be resolved by reconstitution of shRNA-resistant ligand-binding or ER/Golgi association-deficient ORP4L, however such experiments are complicated by the growth arrest and apoptosis associated with both ORP4 depletion and high levels of ORP4 expression. Alternatively, the Golgi PI(4)P content of shORP4 or ORP4 overexpressing cells can be measured by more quantitative methods than immunostaining, such as HPLC of cell fractions, to determine if ORP4 contributes significantly to cellular PI(4)P metabolism.

The discovery of an ORP4 phosphorylation site present in all 3 isoforms that is a substrate for proliferative kinase pathways provides a promising avenue for future study. Identifying the kinase cascades upstream of ORP4 phosphorylation may fit ORP4 into a known proliferative pathway and put its membrane associations and ligand binding properties into context. The proposed conformational change induced by ORP4L phosphorylation is particularly interesting as it affects the interaction between ORP4L and vimentin. Vimentin is a highly dynamic, bi-directional moving scaffold for the Golgi-to-PM trafficking of integrins, and vimentin aggregation is associated with aberrant adhesion and motility due to disruption in integrin trafficking [225]. Considering the upregulation of vimentin associated with EMT, studies of integrin trafficking from the TGN in shORP4 cells, or of wound-healing and migration in cells overexpressing ORP4L-S/D or ORP4S, may potentially identify the role for ORP4 in disseminated tumor cells.

The discovery of ORP4 homodimers brings into question the significance of the OSBP/ORP4 interaction. ORP4 and OSBP are at least non-redundant and at most may have disparate functions and only interact due to the sequence similarity between their

homodimerization domains. Indeed, our sphingomyelin synthesis measurements indicate that wild-type or ligand-binding mutants of ORP4L did not interfere with OSBP function, and ORP4 knockdown is antiproliferative despite endogenous OSBP expression. In humans, OSBP is expressed in most tissues while ORP4 mRNA is detected only at low levels globally, but enriched in the testes, retina and brain. ORP4 may have cell-type-specific functions in those tissues that are unrelated to OSBP. However, there exists some evidence of OSBP acting as a dominant-negative ORP4; OSBP mutants that do not interact with ORP4 collapse the vimentin network but do not co-localize with the resulting vimentin aggregates [53]. This would suggest that ORP4L homodimers or ORP4L/OSBP heterodimers may exist in a binary state with ORP4-vimentin complexes, which could be confirmed by assessing whether or not OSBP interacts with ORP4L-S/D, considering that this mutant has intact OSBP-interaction sites but aggregates vimentin. Furthermore, it is unclear whether ORP4 translocation to the TGN is a consequence of OSBP-mediated increases in TGN PI(4)P or heterodimerization with OSBP. Experiments must be conducted to resolve the functions of ORP4 and OSBP, such as observation of 25OH-induced ORP4 localization in OSBP depleted cells expressing sterol-binding deficient or ORP4-dimerization deficient OSBP.

This study provides evidence that ORP4 is a Golgi, ER and PM-associated PI(4)P and sterol-binding protein regulated by phosphorylation and required for the proliferation of cultured cells. Our data suggest that ORP4 is regulated by ligand binding, but it is still not known whether ligand transfer is a primary cellular function. Understanding ORP4 function in both normal and transformed cells is necessary to explore antiviral and antineoplastic ORP4 inhibitors as potential therapeutics.

BIBLIOGRAPHY

1 Holthuis, J. & Menon, A. K. Lipid landscapes and pipelines in membrane homeostasis. *Nature* **510**, 48-57, doi:10.1038/nature13474 (2014).

2 Wong, L. H., Čopič, A. & Levine, T. P. Advances on the Transfer of Lipids by Lipid Transfer Proteins. *Trends biochem. sci.* **42**, 516-530, doi:10.1016/j.tibs.2017.05.001 (2017).

3 Taylor, F. R. & Kandutsch, A. A. Oxysterol binding protein. *Chem. Phys. Lipids* **38**, 187-194, doi:10.1016/0009-3084(85)90066-0 (1985).

4 Brown, M. S., Dana, S. E. & Goldstein, J. L. Cholesterol ester formation in cultured human fibroblasts. Stimulation by oxygenated sterols. *J. Biol. Chem.* **250**, 4025-4027 (1975).

5 Dawson, P. A., Ridgway, N. D., Slaughter, C. A., Brown, M. S. & Goldstein, J. L. cDNA cloning and expression of oxysterol-binding protein, an oligomer with a potential leucine zipper. *J. Biol. Chem.* **264**, 16798-16803 (1989).

6 Ridgway, N. D., Dawson, P. A., Ho, Y. K., Brown & Goldstein, J. L. Translocation of oxysterol binding protein to Golgi apparatus triggered by ligand binding. *J. Cell Biol.* **116**, 307-319, doi:10.1083/jcb.116.2.307 (1992).

7 Laitinen, S., Olkkonen, V. M., Ehnholm, C. & Ikonen, E. Family of human oxysterol binding protein (OSBP) homologues. A novel member implicated in brain sterol metabolism. *J. Lipid Res.* **40**, 2204-2211 (1999).

8 Jaworski, C. J., Moreira, E., Li, A., Lee, R. & Rodriguez, I. R. A Family of 12 Human Genes Containing Oxysterol-Binding Domains. *Genomics* **78**, 185-196, doi:10.1006/geno.2001.6663 (2001).

9 Kaiser, S. E. *et al.* Structural Basis of FFAT Motif-Mediated ER Targeting. *Structure* **13**, 1035-1045, doi:10.1016/j.str.2005.04.010 (2005).

10 Wyles, J. P. & Ridgway, N. D. VAMP-associated protein-A regulates partitioning of oxysterol-binding protein-related protein-9 between the endoplasmic reticulum and Golgi apparatus. *Exp. Cell Res.* **297**, 533-547, doi:10.1016/j.yexcr.2004.03.052 (2004).

11 Weber-Boyvat, M., Kentala, H., Peränen, J. & Olkkonen, V. M. Ligand-dependent localization and function of ORP-VAP complexes at membrane contact sites. *Cell. Mol. Life Sci.* **72**, 1967-1987, doi:10.1007/s00018-014-1786-x (2015).

12 Weber-Boyvat, M. *et al.* OSBP-related protein 3 (ORP3) coupling with VAMP-associated protein A regulates R-Ras activity. *Exp. Cell Res.* **331**, 278-291, doi:10.1016/j.yexcr.2014.10.019 (2015).

13 Vihervaara, T. *et al.* Sterol binding by OSBP-related protein 1L regulates late endosome motility and function. *Cell. Mol. Life Sci.* **68**, 537-551 (2011).

14 Peretti, D., Dahan, N., Shimoni, E., Hirschberg, K. & Lev, S. Coordinated Lipid Transfer between the Endoplasmic Reticulum and the Golgi Complex Requires the VAP Proteins and Is Essential for Golgi-mediated Transport. *Mol. Biol. Cell* **19**, 3871-3884, doi:10.1091/mbc.E08-05-0498 (2008).

15 Rocha, N. *et al.* Cholesterol sensor ORP1L contacts the ER protein VAP to control Rab7–RILP–p150Glued and late endosome positioning. *J. Cell Biol.* **185**, 1209-1225, doi:10.1083/jcb.200811005 (2009).

16 Galmes, R. *et al.* ORP5/ORP8 localize to endoplasmic reticulum–mitochondria contacts and are involved in mitochondrial function. *EMBO Rep.* **17**, 800-810, doi:10.15252/embr.201541108 (2016).

17 Chung, J. *et al.* PI4P/phosphatidylserine countertransport at ORP5- and ORP8-mediated ER–plasma membrane contacts. *Science* **349**, 428-432, doi:10.1126/science.aab1370 (2015).

18 Ghai, R. *et al.* ORP5 and ORP8 bind phosphatidylinositol-4, 5-biphosphate (PtdIns(4,5)P 2) and regulate its level at the plasma membrane. *Nat. Commun.* **8**, 757, doi:10.1038/s41467-017-00861-5 (2017).

19 Schulz, T. A. & Prinz, W. A. Sterol transport in yeast and the oxysterol binding protein homologue (OSH) family. *Biochim. Biophys. Acta, Mol. Cell. Biol. Lipids* **1771**, 769-780, doi:10.1016/j.bbalip.2007.03.003 (2007).

20 Beh, C. T., Cool, L., Phillips, J. & Rine, J. Overlapping functions of the yeast oxysterol-binding protein homologues. *Genetics* **157**, 1117-1140 (2001).

21 Kobuna, H. *et al.* Multivesicular Body Formation Requires OSBP–Related Proteins and Cholesterol. *PLoS Genet.* **6**, doi:10.1371/journal.pgen.1001055 (2010).

22 Ma, Z., Liu, Z. & Huang, X. OSBP- and FAN-mediated sterol requirement for spermatogenesis in Drosophila. *Development* **137**, 3775-3784, doi:10.1242/dev.049312 (2010).

23 Ma, Z., Liu, Z. & Huang, X. Membrane phospholipid asymmetry counters the adverse effects of sterol overloading in the Golgi membrane of Drosophila. *Genetics* **190**, 1299-1308, doi:10.1534/genetics.111.137687 (2012).

24 Im, Y., Raychaudhuri, S., Prinz, W. A. & Hurley, J. H. Structural mechanism for sterol sensing and transport by OSBP-related proteins. *Nature* **437**, 154-158, doi:10.1038/nature03923 (2005).

25 Tong, J., Manik, M. K., Yang, H. & Im, Y. J. Structural insights into nonvesicular lipid transport by the oxysterol binding protein homologue family. *Biochim. Biophys. Acta* **1861**, 928-939, doi:10.1016/j.bbalip.2016.01.008 (2016).

26 de Saint-Jean, M. *et al.* Osh4p exchanges sterols for phosphatidylinositol 4-phosphate between lipid bilayers. *J. Cell Biol.* **195**, 965-978, doi:10.1083/jcb.201104062 (2011).

27 Tong, J., Yang, H., Yang, H., Eom, S. H. & Im, Y. J. Structure of Osh3 reveals a conserved mode of phosphoinositide binding in oxysterol-binding proteins. *Structure* **21**, 1203-1213, doi:10.1016/j.str.2013.05.007 (2013).

28 Manik, M. K., Yang, H., Tong, J. & Im, Y. J. Structure of Yeast OSBP-Related Protein Osh1 Reveals Key Determinants for Lipid Transport and Protein Targeting at the Nucleus-Vacuole Junction. *Structure* **25**, 617-629000, doi:10.1016/j.str.2017.02.010 (2017).

29 Kentala, H., Weber-Boyvat, M. & Olkkonen, V. M. OSBP-Related Protein Family: Mediators of Lipid Transport and Signaling at Membrane Contact Sites. *Int. Rev. Cell Mol. Biol.* **321**, 299-340, doi:10.1016/bs.ircmb.2015.09.006 (2016).

30 Guo, S., Stolz, L. E., Lemrow, S. M. & York, J. D. SAC1-like domains of yeast SAC1, INP52, and INP53 and of human synaptojanin encode polyphosphoinositide phosphatases. *J. Biol. Chem.* **274**, 12990-12995 (1999).

31 Moreira, E. F., Jaworski, C., Li, A. & Rodriguez, I. R. Molecular and Biochemical Characterization of a Novel Oxysterol-binding Protein (OSBP2) Highly Expressed in Retina. *J. Biol. Chem.* **276**, 18570-18578, doi:10.1074/jbc.M011259200 (2001).

32 Wyles, J. P., McMaster, C. R. & Ridgway, N. D. Vesicle-associated Membrane Protein-associated Protein-A (VAP-A) Interacts with the Oxysterol-binding Protein

to Modify Export from the Endoplasmic Reticulum. *J. Biol. Chem.* **277**, 29908-29918, doi:10.1074/jbc.M201191200 (2002).

33 Lee, S. *et al.* Sterol-dependent nuclear import of ORP1S promotes LXR regulated trans-activation of apoE. *Exp. Cell Res.* **318**, 2128-2142, doi:10.1016/j.yexcr.2012.06.012 (2012).

34 Mesmin, B. *et al.* A Four-Step Cycle Driven by PI(4)P Hydrolysis Directs Sterol/PI(4)P Exchange by the ER-Golgi Tether OSBP. *Cell* **155**, 830-843, doi:10.1016/j.cell.2013.09.056 (2013).

35 Perry, R. J. & Ridgway, N. D. Oxysterol-binding Protein and Vesicle-associated Membrane Protein–associated Protein Are Required for Sterol-dependent Activation of the Ceramide Transport Protein. *Mol. Biol. Cell* **17**, 2604-2616, doi:10.1091/mbc.E06-01-0060 (2006).

36 Storey, M. K., Byers, D. M., Cook, H. W. & Ridgway, N. D. Cholesterol regulates oxysterol binding protein (OSBP) phosphorylation and Golgi localization in Chinese hamster ovary cells: correlation with stimulation of sphingomyelin synthesis by 25-hydroxycholesterol. *Biochem. J.* **336**, 247-256, doi:10.1042/bj3360247 (1998).

37 Johansson, M. *et al.* The Two Variants of Oxysterol Binding Protein-related Protein-1 Display Different Tissue Expression Patterns, Have Different Intracellular Localization, and Are Functionally Distinct. *Mol. Biol. Cell* **14**, 903-915, doi:10.1091/mbc.E02-08-0459 (2003).

38 Johansson, M. & Olkkonen, V. M. Assays for interaction between Rab7 and oxysterol binding protein related protein 1L (ORP1L). *Methods Enzymol.* **403**, 743-758, doi:10.1016/S0076-6879(05)03065-X (2005).

39 Zhao, K. & Ridgway, N. D. Oxysterol-Binding Protein-Related Protein 1L Regulates Cholesterol Egress from the Endo-Lysosomal System. *Cell reports* **19**, 1807-1818, doi:10.1016/j.celrep.2017.05.028 (2017).

40 Suchanek, M. *et al.* The mammalian oxysterol-binding protein-related proteins (ORPs) bind 25-hydroxycholesterol in an evolutionarily conserved pocket. *Biochem. J.* **405**, 473-480, doi:10.1042/BJ20070176 (2007).

41 Albulescu, L. *et al.* Broad-range inhibition of enterovirus replication by OSW-1, a natural compound targeting OSBP. *Antivir. Res.* **117**, 110-114, doi:10.1016/j.antiviral.2015.02.013 (2015).

42 Laitinen, S. *et al.* ORP2, a homolog of oxysterol binding protein, regulates cellular cholesterol metabolism. *J. Lipid Res.* **43**, 245-255 (2002).

43 Hynynen, R. *et al.* OSBP-related protein 2 is a sterol receptor on lipid droplets that regulates the metabolism of neutral lipids. *J. Lipid Res.* **50**, 1305-1315, doi:10.1194/jlr.M800661-JLR200 (2009).

44 Hynynen, R. *et al.* Overexpression of OSBP-related protein 2 (ORP2) induces changes in cellular cholesterol metabolism and enhances endocytosis. *Biochem. J.* **390**, 273-283, doi:10.1042/BJ20042082 (2005).

45 Kentala, H. *et al.* Analysis of ORP2 knockout hepatocytes uncovers a novel function in actin cytoskeletal regulation. *FASEB J.* doi:10.1096/fj.201700604R (2017).

46 Escajadillo, T., Wang, H., Li, L., Li, D. & Sewer, M. B. Oxysterol-related-binding-protein related Protein-2 (ORP2) regulates cortisol biosynthesis and cholesterol homeostasis. *Mol. Cell. Endocrinol.* **427**, 73-85, doi:10.1016/j.mce.2016.03.006 (2016).

47 Lehto, M., Tienari, J., Lehtonen, S., Lehtonen, E. & Olkkonen, V. M. Subfamily III of mammalian oxysterol-binding protein (OSBP) homologues: the expression and intracellular localization of ORP3, ORP6, and ORP7. *Cell Tissue Res.* **315**, 39-57, doi:10.1007/s00441-003-0817-y (2004).

48 Lehto, M. *et al.* Targeting of OSBP-related protein 3 (ORP3) to endoplasmic reticulum and plasma membrane is controlled by multiple determinants. *Exp. Cell Res.* **310**, 445-462, doi:10.1016/j.yexcr.2005.08.003 (2005).

49 Lehto, M. *et al.* The R-Ras interaction partner ORP3 regulates cell adhesion. *J. Cell Sci.* **121**, 695-705, doi:10.1242/jcs.016964 (2008).

50 Vihervaara, T. *et al.* Modification of the lipidome in RAW264.7 macrophage subjected to stable silencing of oxysterol-binding proteins. *Biochimie* **95**, 538-547, doi:10.1016/j.biochi.2012.05.004 (2013).

51 Wang, C., JeIley, L. & Ridgway, N. D. Oxysterol-binding-protein (OSBP)-related protein 4 binds25-hydroxycholesterol and interacts with vimentin intermediate filaments. *Biochem. J.* **361**, 461-472, doi:10.1042/0264-6021:3610461 (2002).

52 Charman, M., Colbourne, T. R., Pietrangelo, A., Kreplak, L. & Ridgway, N. D. Oxysterol-binding protein (OSBP)-related protein 4 (ORP4) is essential for cell

proliferation and survival. *J. Biol. Chem.* **289**, 15705-15717, doi:10.1074/jbc.M114.571216 (2014).

53 Wyles, J. P., Perry, R. J. & Ridgway, N. D. Characterization of the sterol-binding domain of oxysterol-binding protein (OSBP)-related protein 4 reveals a novel role in vimentin organization. *Exp. Cell Res.* **313**, 1426-1437, doi:10.1016/j.yexcr.2007.01.018 (2007).

54 Zhong, W. *et al.* ORP4L Facilitates Macrophage Survival via G-Protein–Coupled SignalingNovelty and Significance. *Circ. Res.* **119**, 1296-1312, doi:10.1161/CIRCRESAHA.116.309603 (2016).

55 Zhong, W. *et al.* ORP4L is essential for T-cell acute lymphoblastic leukemia cell survival. *Nat. Commun.* **7**, 12702, doi:10.1038/ncomms12702 (2016).

56 Li, J.-W. *et al.* Oxysterol-binding protein-related protein 4L promotes cell proliferation by sustaining intracellular Ca 2+ homeostasis in cervical carcinoma cell lines. *Oncotarget* **7**, 65849-65861, doi:10.18632/oncotarget.11671 (2016).

57 Udagawa, O. *et al.* Oligo-astheno-teratozoospermia in mice lacking ORP4, a sterol-binding protein in the OSBP-related protein family. *Genes Cells* **19**, 13-27, doi:10.1111/gtc.12105 (2014).

58 Higashimoto, K. *et al.* Characterization and imprinting status of OBPH1/Obph1 gene: implications for an extended imprinting domain in human and mouse. *Genomics* **80**, 575-584 (2002).

59 Du, X. *et al.* A role for oxysterol-binding protein-related protein 5 in endosomal cholesterol trafficking. *J. Cell Biol.* **192**, 121-135, doi:10.1083/jcb.201004142 (2011).

60 Maeda, K. *et al.* Interactome map uncovers phosphatidylserine transport by oxysterol-binding proteins. *Nature* **501**, 257-261, doi:10.1038/nature12430 (2013).

61 Ouimet, M. *et al.* miRNA Targeting of Oxysterol-Binding Protein-Like 6 Regulates Cholesterol Trafficking and EffluxSignificance. *Arterioscler. Thromb. Vasc. Biol.* **36**, 942-951, doi:10.1161/ATVBAHA.116.307282 (2016).

62 Zhong, W. *et al.* OSBP-related protein 8 (ORP8) interacts with Homo sapiens sperm associated antigen 5 (SPAG5) and mediates oxysterol interference of HepG2 cell cycle. *Exp. Cell Res.* **322**, 227-235, doi:10.1016/j.yexcr.2014.01.002 (2014).

63 Yan, D. *et al.* OSBP-related Protein 8 (ORP8) Suppresses ABCA1 Expression and Cholesterol Efflux from Macrophages. *J. Biol. Chem.* **283**, 332-340, doi:10.1074/jbc.M705313200 (2008).

64 Zhou, T. *et al.* OSBP-Related Protein 8 (ORP8) Regulates Plasma and Liver Tissue Lipid Levels and Interacts with the Nucleoporin Nup62. *PLoS One* **6**, doi:10.1371/journal.pone.0021078 (2011).

65 Ngo, M. & Ridgway, N. D. Oxysterol Binding Protein–related Protein 9 (ORP9) Is a Cholesterol Transfer Protein That Regulates Golgi Structure and Function. *Mol. Biol. Cell* **20**, 1388-1399, doi:10.1091/mbc.E08-09-0905 (2009).

66 Liu, X. & Ridgway, N. D. Characterization of the sterol and phosphatidylinositol 4-phosphate binding properties of Golgi-associated OSBP-related protein 9 (ORP9). *PloS One* **9**, doi:10.1371/journal.pone.0108368 (2014).

67 Perttilä, J. *et al.* OSBPL10, a novel candidate gene for high triglyceride trait in dyslipidemic Finnish subjects, regulates cellular lipid metabolism. *J. Mol. Med.* **87**, 825-835, doi:10.1007/s00109-009-0490-z (2009).

68 Nissilä, E. *et al.* ORP10, a cholesterol binding protein associated with microtubules, regulates apolipoprotein B-100 secretion. *Biochim. Biophys. Acta, Mol. Cell. Biol. Lipids* **1821**, 1472-1484, doi:10.1016/j.bbalip.2012.08.004 (2012).

69 Zhou, Y. *et al.* OSBP-related protein 11 (ORP11) dimerizes with ORP9 and localizes at the Golgi-late endosome interface. *Exp. Cell Res.* **316**, 3304-3316, doi:10.1016/j.yexcr.2010.06.008 (2010).

70 Zhou, Y. *et al.* OSBP-Related Proteins (ORPs) in Human Adipose Depots and Cultured Adipocytes: Evidence for Impacts on the Adipocyte Phenotype. *PLoS One* **7**, doi:10.1371/journal.pone.0045352 (2012).

71 Fang, M. *et al.* Kes1p shares homology with human oxysterol binding protein and participates in a novel regulatory pathway for yeast Golgi-derived transport vesicle biogenesis. *EMBO J.* **15**, 6447-6459 (1996).

72 Schulz, T. A. *et al.* Lipid-regulated sterol transfer between closely apposed membranes by oxysterol-binding protein homologues. *J. Cell Biol.* **187**, 889-903, doi:10.1083/jcb.200905007 (2009).

73 Beh, C. T. & Rine, J. A role for yeast oxysterol-binding protein homologs in endocytosis and in the maintenance of intracellular sterol-lipid distribution. *J. Cell Sci.* **117**, 2983-2996, doi:10.1242/jcs.01157 (2004).

74 Georgiev, A. G. *et al.* Osh proteins regulate membrane sterol organization but are not required for sterol movement between the ER and PM. *Traffic* **12**, 1341-1355, doi:10.1111/j.1600-0854.2011.01234.x (2011).

75 Alfaro, G. *et al.* The sterol-binding protein Kes1/Osh4p is a regulator of polarized exocytosis. *Traffic* **12**, 1521-1536, doi:10.1111/j.1600-0854.2011.01265.x (2011).

76 Olkkonen, V. M. OSBP-Related Protein Family in Lipid Transport Over Membrane Contact Sites. *Lipid Insights* **8**, 1-9, doi:10.4137/LPI.S31726 (2015).

77 Lagace, T. A., Byers, D. M., Cook, H. W. & Ridgway, N. D. Altered regulation of cholesterol and cholesteryl ester synthesis in Chinese-hamster ovary cells overexpressing the oxysterol-binding protein is dependent on the pleckstrin homology domain. *Biochem. J.* **326 (Pt 1)**, 205-213 (1997).

78 Banerji, S. *et al.* Oxysterol Binding Protein-dependent Activation of Sphingomyelin Synthesis in the Golgi Apparatus Requires Phosphatidylinositol 4-Kinase IIα. *Mol. Biol. Cell* **21**, 4141-4150, doi:10.1091/mbc.E10-05-0424 (2010).

79 Slotte, P. J. Biological functions of sphingomyelins. *Prog. Lipid Res.* **52**, 424-437, doi:10.1016/j.plipres.2013.05.001 (2013).

80 Wakana, Y. *et al.* CARTS biogenesis requires VAP–lipid transfer protein complexes functioning at the endoplasmic reticulum–Golgi interface. *Mol. Biol. Cell* **26**, 4686-4699, doi:10.1091/mbc.E15-08-0599 (2015).

81 Lange, Y., Ye, J., Rigney, M. & Steck, T. L. Regulation of endoplasmic reticulum cholesterol by plasma membrane cholesterol. *J. Lipid Res.* **40**, 2264-2270 (1999).

82 Brown, M. S. & Goldstein, J. L. A proteolytic pathway that controls the cholesterol content of membranes, cells, and blood. *Proc. Natl. Acad. Sci. USA* **96**, 11041-11048 (1999).

83 Blanchette-Mackie, E. J. Intracellular cholesterol trafficking: role of the NPC1 protein. *Biochim. Biophys. Acta* **1486**, 171-183 (2000).

84 Liscum, L. & Munn, N. J. Intracellular cholesterol transport. *Biochim. Biophys. Acta, Mol. Cell. Biol. Lipids* **1438**, 19-37, doi:10.1016/s1388-1981(99)00043-8 (1999).

85 Mesmin, B. & Antonny, B. The counterflow transport of sterols and PI4P. *Biochim. Biophys. Acta, Mol. Cell. Biol. Lipids* **1861**, 940-951, doi:10.1016/j.bbalip.2016.02.024 (2016).

86 Mesmin, B. *et al.* Sterol transfer, PI4P consumption, and control of membrane lipid order by endogenous OSBP. *EMBO J.* **36**, 3156-3174, doi:10.15252/embj.201796687 (2017).

87 Di Paolo, G. & De Camilli, P. Phosphoinositides in cell regulation and membrane dynamics. *Nature* **443**, 651-657, doi:10.1038/nature05185 (2006).

88 Burgett, A. W. *et al.* Natural products reveal cancer cell dependence on oxysterol-binding proteins. *Nat. Chem. Biol.* **7**, 639-647, doi:10.1038/nchembio.625 (2011).

89 Nishimura, T. *et al.* Oxysterol-binding protein (OSBP) is required for the perinuclear localization of intra-Golgi v-SNAREs. *Mol. Biol. Cell* **24**, 3534-3544, doi:10.1091/mbc.E13-05-0250 (2013).

90 Dong, R. *et al.* Endosome-ER Contacts Control Actin Nucleation and Retromer Function through VAP-Dependent Regulation of PI4P. *Cell* **166**, 408-423, doi:10.1016/j.cell.2016.06.037 (2016).

91 Steenbergen, R. *et al.* Disruption of the Phosphatidylserine Decarboxylase Gene in Mice Causes Embryonic Lethality and Mitochondrial Defects. *J. Biol. Chem.* **280**, 40032-40040, doi:10.1074/jbc.M506510200 (2005).

92 Ikonen, E. Cellular cholesterol trafficking and compartmentalization. *Nature Rev. Mol. Cell Biol.* **9**, 125-138, doi:10.1038/nrm2336 (2008).

93 Möbius, W. *et al.* Recycling compartments and the internal vesicles of multivesicular bodies harbor most of the cholesterol found in the endocytic pathway. *Traffic* **4**, 222-231 (2003).

94 Vance, J. E. & Karten, B. Niemann-Pick C disease and mobilization of lysosomal cholesterol by cyclodextrin. *J. Lipid Res.* **55**, 1609-1621, doi:10.1194/jlr.r047837 (2014).

95 Eden, E. R. *et al.* Annexin A1 Tethers Membrane Contact Sites that Mediate ER to Endosome Cholesterol Transport. *Dev. Cell* **37**, 473-483, doi:10.1016/j.devcel.2016.05.005 (2016).

96 Lehto, M. *et al.* The OSBP-related protein family in humans. *J. Lipid Res.* **42**, 1203-1213 (2001).

97 van der Kant, R. *et al.* Late endosomal transport and tethering are coupled processes controlled by RILP and the cholesterol sensor ORP1L. *J. Cell Sci.* **126**, 3462-3474, doi:10.1242/jcs.129270 (2013).

98 Johansson, M. *et al.* Activation of endosomal dynein motors by stepwise assembly of Rab7-RILP-p150Glued, ORP1L, and the receptor betalll spectrin. *J. Cell Biol.* **176**, 459-471, doi:10.1083/jcb.200606077 (2007).

99 Li, J., Deffieu, M. S., Lee, P. L., Saha, P. & Pfeffer, S. R. Glycosylation inhibition reduces cholesterol accumulation in NPC1 protein-deficient cells. *Proc. Natl. Acad. Sci. USA* **112**, 14876-14881, doi:10.1073/pnas.1520490112 (2015).

100 Walther, T. C., Chung, J. & Jr, R. V. Lipid Droplet Biogenesis. *Annu. Rev. Cell and Dev. Biol.* **33**, 1-20, doi:10.1146/annurev-cellbio-100616-060608 (2016).

101 Käkelä, R., Tanhuanpää, K., Laitinen, S., Somerharju, P. & Olkkonen, V. M. Overexpression of OSBP-related protein 2 (ORP2) in CHO cells induces alterations of phospholipid species composition. *Biochem. Cell Biol.* **83**, 677-683, doi:10.1139/o05-056 (2005).

102 Loilome, W. *et al.* Expression of oxysterol binding protein isoforms in opisthorchiasis-associated cholangiocarcinoma: A potential molecular marker for tumor metastasis. *Parasitol. Int.* **61**, 136-139, doi:10.1016/j.parint.2011.07.003 (2012).

103 Silva, N. *et al.* HLM/OSBP2 is expressed in chronic myeloid leukemia. *Int. J. Mol. Med.* **12**, 663-666 (2003).

104 Fournier, M. V. *et al.* Identification of a gene encoding a human oxysterol-binding protein-homologue: a potential general molecular marker for blood dissemination of solid tumors. *Cancer Res.* **59**, 3748-3753 (1999).

105 Koga, Y. *et al.* Oxysterol binding protein-related protein-5 is related to invasion and poor prognosis in pancreatic cancer. *Cancer Science* **99**, 2387-2394, doi:10.1111/j.1349-7006.2008.00987.x (2008).

106 Dmitriev, A. A. *et al.* Identification of Novel Epigenetic Markers of Prostate Cancer by NotI-Microarray Analysis. *Dis. Markers* **2015**, 241301, doi:10.1155/2015/241301 (2015).

107 Vozianov, S. O. *et al.* Identification of a new diagnostic marker of prostatic cancer using NOTI microchips. *Klin. Khirurhiia*, 54-57 (2016).

108 Lefebvre, C. *et al.* Mutational Profile of Metastatic Breast Cancers: A Retrospective Analysis. *PLoS Med.* **13**, doi:10.1371/journal.pmed.1002201 (2016).

109 Miller, S. & Krijnse-Locker, J. Modification of intracellular membrane structures for virus replication. *Nature Reviews Microbiol.* **6**, 363-374, doi:10.1038/nrmicro1890 (2008).

110 Moustaqim-Barrette, A. *et al.* The amyotrophic lateral sclerosis 8 protein, VAP, is required for ER protein quality control. *Hum. Mol. Gen.* **23**, 1975-1989, doi:10.1093/hmg/ddt594 (2014).

111 Motazacker, M. M. *et al.* A loss-of-function variant in OSBPL1A predisposes to low plasma HDL cholesterol levels and impaired cholesterol efflux capacity. *Atherosclerosis* **249**, 140-147, doi:10.1016/j.atherosclerosis.2016.04.005 (2016).

112 Thoenes, M. *et al.* OSBPL2 encodes a protein of inner and outer hair cell stereocilia and is mutated in autosomal dominant hearing loss (DFNA67). *Orphanet J. Rare Dis.* **10**, 15, doi:10.1186/s13023-015-0238-5 (2015).

113 Xing, G. *et al.* Identification of OSBPL2 as a novel candidate gene for progressive nonsyndromic hearing loss by whole-exome sequencing. *Genet .Med.* **17**, 210-218, doi:10.1038/gim.2014.90 (2014).

114 Raitoharju, E. *et al.* Blood hsa-miR-122-5p and hsa-miR-885-5p levels associate with fatty liver and related lipoprotein metabolism—The Young Finns Study. *Sci. Rep.* **6**, 38262, doi:10.1038/srep38262 (2016).

115 Darbyson, A. & Ngsee, J. K. Oxysterol-binding protein ORP3 rescues the Amyotrophic Lateral Sclerosis-linked mutant VAPB phenotype. *Exp. Cell Res.* **341**, 18-31, doi:10.1016/j.yexcr.2016.01.013 (2016).

116 Erdem-Eraslan, L. *et al.* Identification of Patients with Recurrent Glioblastoma Who May Benefit from Combined Bevacizumab and CCNU Therapy: A Report from the BELOB Trial. *Cancer Res.* **76**, 525-534, doi:10.1158/0008-5472.CAN-15-0776 (2016).

117 Stein, S. *et al.* Impaired SUMOylation of nuclear receptor LRH-1 promotes nonalcoholic fatty liver disease. *J. Clin. Invest.* **127**, 583-592, doi:10.1172/JCI85499 (2017).

118 Li, H. *et al.* Integrated expression profiles analysis reveals novel predictive biomarker in pancreatic ductal adenocarcinoma. *Oncotarget* **5**, doi:10.18632/oncotarget.16732 (2014).

119 Vlems, F. A. *et al.* Investigations for a multi-marker RT-PCR to improve sensitivity of disseminated tumor cell detection. *Anticancer Res.* **23**, 179-186 (2003).

120 Silva, N. *et al.* Detection of messenger RNA in leukocytes or plasma of patients with chronic myeloid leukemia. *Oncol. Rep.* **8**, 693-696, doi:10.3892/or.8.3.693 (2001).

121 Ishikawa, S. *et al.* The role of oxysterol binding protein-related protein 5 in pancreatic cancer. *Cancer Science* **101**, 898-905, doi:10.1111/j.1349-7006.2009.01475.x (2010).

122 Nagano, K. *et al.* Identification and evaluation of metastasis-related proteins, oxysterol binding protein-like 5 and calumenin, in lung tumors. *Int. J. Onc.* **47**, 195-203, doi:10.3892/ijo.2015.3000 (2015).

123 Edenberg, H. J. *et al.* Genome-Wide Association Study of Alcohol Dependence Implicates a Region on Chromosome 11. *Alc. Clin. Exp. Res.* **34**, 840-852, doi:10.1111/j.1530-0277.2010.01156.x (2010).

124 Ma, J., Dempsey, A. A., Stamatiou, D., Marshall, K. W. & Liew, C.-C. Identifying leukocyte gene expression patterns associated with plasma lipid levels in human subjects. *Atherosclerosis* **191**, 63-72, doi:10.1016/j.atherosclerosis.2006.05.032 (2007).

125 Herold, C. *et al.* Family-based association analyses of imputed genotypes reveal genome-wide significant association of Alzheimer's disease with OSBPL6, PTPRG, and PDCL3. *Mol. Psychiatry* **21**, 1608-1612, doi:10.1038/mp.2015.218 (2016).

126 Teslovich, T. M. *et al.* Biological, clinical and population relevance of 95 loci for blood lipids. *Nature* **466**, doi:10.1038/nature09270 (2010).

127 Consortium, G. *et al.* Discovery and refinement of loci associated with lipid levels. *Nature Genet.* **45**, 1274-1283, doi:10.1038/ng.2797 (2013).

128 Guo, X. *et al.* Oxysterol binding protein-related protein 8 inhibits gastric cancer growth through induction of ER stress, inhibition of Wnt signaling and activation of apoptosis. *Oncol. Res.* **25**, 799-808, doi:10.3727/096504016X14783691306605 (2016).

129 Ma, L. *et al.* Genome-wide association analysis of total cholesterol and high-density lipoprotein cholesterol levels using the Framingham Heart Study data. *BMC Med. Genet.* **11**, 1-11, doi:10.1186/1471-2350-11-55 (2010).

130 Jordan, S. D. *et al.* Obesity-induced overexpression of miRNA-143 inhibits insulin-stimulated AKT activation and impairs glucose metabolism. *Nat. Cell Biol.* **13**, doi:10.1038/ncb2211 (2011).

131 Blumensatt, M. *et al.* Activin A impairs insulin action in cardiomyocytes via up-regulation of miR-143. *Cardiovasc. Res.* **100**, 201-210, doi:10.1093/cvr/cvt173 (2013).

132 Blumensatt, M. *et al.* Adipocyte-derived factors impair insulin signaling in differentiated human vascular smooth muscle cells via the upregulation of miR-143. *BBA Mol. Basis Dis.* **1842**, 275-283, doi:10.1016/j.bbadis.2013.12.001 (2014).

133 van Kampen, E. *et al.* Orp8 Deficiency in Bone Marrow-Derived Cells Reduces Atherosclerotic Lesion Progression in LDL Receptor Knockout Mice. *PLoS One* **9**, doi:10.1371/journal.pone.0109024 (2014).

134 Sohn, M. *et al.* Lenz-Majewski mutations in PTDSS1 affect phosphatidylinositol 4-phosphate metabolism at ER-PM and ER-Golgi junctions. *Proc. Natl. Acad. Sci. USA* **113**, 4314-4319, doi:10.1073/pnas.1525719113 (2016).

135 Zhong, W. *et al.* Oxysterol-binding Protein-related Protein 8 (ORP8) Increases Sensitivity of Hepatocellular Carcinoma Cells to Fas-Mediated Apoptosis. *J. Biol. Chem.* **290**, 8876-8887, doi:10.1074/jbc.M114.610188 (2015).

136 Aziz, N. *et al.* A 19-Gene expression signature as a predictor of survival in colorectal cancer. *BMC Med. Genet.* **9**, 58, doi:10.1186/s12920-016-0218-1 (2016).

137 Li, L., Qu, G., Wang, M., Huang, Q. & Liu, Y. Association of oxysterol binding protein-related protein 9 polymorphism with cerebral infarction in Hunan Han population. *Ir. J. Med. Sci.* **183**, 439-448, doi:10.1007/s11845-013-1035-6 (2014).

138 Koriyama, H. *et al.* Variation in OSBPL10 is associated with dyslipidemia. *Hypertens. Res.* **33**, doi:10.1038/hr.2010.28 (2010).

139 Koriyama, H. *et al.* Identification of Evidence Suggestive of an Association with Peripheral Arterial Disease at the OSBPL10 Locus by Genome-Wide Investigation in the Japanese Population. *J. Atheroscler. Throm.* **17**, 1054-1062, doi:10.5551/jat.4291 (2010).

140 Stewart, W. C. L., Huang, Y., Greenberg, D. A. & Vieland, V. J. Next-generation linkage and association methods applied to hypertension: a multifaceted approach to the analysis of sequence data. *BMC Proc.* **8**, 1-4, doi:10.1186/1753-6561-8-S1-S111 (2014).

141 Bouchard, L. *et al.* Association of OSBPL11 Gene Polymorphisms With Cardiovascular Disease Risk Factors in Obesity. *Obesity* **17**, 1466-1472, doi:10.1038/oby.2009.71 (2009).

142 Kara, B. *et al.* Severe neurodegenerative disease in brothers with homozygous mutation in POLR1A. *Eur. J. Hum. Genet.* **25**, doi:10.1038/ejhg.2016.183 (2017).

143 Amako, Y., Sarkeshik, A., Hotta, H., Yates, J. & Siddiqui, A. Role of Oxysterol Binding Protein in Hepatitis C Virus infection. *J. Virol.* **83**, 9237-9246, doi:10.1128/JVI.00958-09 (2009).

144 Wang, H. *et al.* Oxysterol-Binding Protein Is a Phosphatidylinositol 4-Kinase Effector Required for HCV Replication Membrane Integrity and Cholesterol Trafficking. *Gastroenterology* **146**, 1373-189605888, doi:10.1053/j.gastro.2014.02.002 (2014).

145 Arita, M. Phosphatidylinositol-4 kinase III beta and oxysterol-binding protein accumulate unesterified cholesterol on poliovirus-induced membrane structure. *Microbiology and Immunology* **58**, 239-256, doi:10.1111/1348-0421.12144 (2014).

146 Dorobantu, C. M. *et al.* Modulation of the Host Lipid Landscape to Promote RNA Virus Replication: The Picornavirus Encephalomyocarditis Virus Converges on the Pathway Used by Hepatitis C Virus. *PLoS Pathog.* **11**, doi:10.1371/journal.ppat.1005185 (2015).

147 Albulescu, L. *et al.* Uncovering oxysterol-binding protein (OSBP) as a target of the anti-enteroviral compound TTP-8307. *Antivir. Res.* **140**, 37-44, doi:10.1016/j.antiviral.2017.01.008 (2017).

148 Strating, J. *et al.* Itraconazole Inhibits Enterovirus Replication by Targeting the Oxysterol-Binding Protein. *Cell Reports* **10**, 600-615, doi:10.1016/j.celrep.2014.12.054 (2015).

149 Park, I.-W. *et al.* Inhibition of HCV Replication by Oxysterol-Binding Protein-Related Protein 4 (ORP4) through Interaction with HCV NS5B and Alteration of Lipid Droplet Formation. *PLoS One* **8**, doi:10.1371/journal.pone.0075648 (2013).

150 Amini-Bavil-Olyaee, S. *et al.* The Antiviral Effector IFITM3 Disrupts Intracellular Cholesterol Homeostasis to Block Viral Entry. *Cell Host Microbe* **13**, 452-464, doi:10.1016/j.chom.2013.03.006 (2013).

151 Sierra, B. *et al.* OSBPL10, RXRA and lipid metabolism confer African-ancestry protection against dengue haemorrhagic fever in admixed CUBANS. *PLoS Pathog.* **13**, doi:10.1371/journal.ppat.1006220 (2017).

152 Li, D., Dammer, E. B., Lucki, N. C. & Sewer, M. B. cAMP-stimulated phosphorylation of diaphanous 1 regulates protein stability and interaction with binding partners in adrenocortical cells. *Mol. Biol. Cell* **24**, 848-857, doi:10.1091/mbc.E12-08-0597 (2013).

153 Rudnicki, A. *et al.* Next-generation sequencing of small RNAs from inner ear sensory epithelium identifies microRNAs and defines regulatory pathways. *BMC Genomics* **15**, 1-12, doi:10.1186/1471-2164-15-484 (2014).

154 Lynch, E. D. *et al.* Nonsyndromic deafness DFNA1 associated with mutation of a human homolog of the Drosophila gene diaphanous. *Science* **278**, 1315-1318 (1997).

155 Kiernan, M. C. *et al.* Amyotrophic lateral sclerosis. *Lancet* **377**, 942-955, doi:10.1016/S0140-6736(10)61156-7 (2011).

156 Nishimura, A. L. *et al.* A Mutation in the Vesicle-Trafficking Protein VAPB Causes Late-Onset Spinal Muscular Atrophy and Amyotrophic Lateral Sclerosis. *The Am. J. Hum. Genet.* **75**, 822-831, doi:10.1086/425287 (2004).

157 Nishimura, A. L., Al-Chalabi, A. & Zatz, M. A common founder for amyotrophic lateral sclerosis type 8 (ALS8) in the Brazilian population. *Hum. Genet.* **118**, 499-500, doi:10.1007/s00439-005-0031-y (2005).

158 Ström, A.-L. L. *et al.* Retrograde axonal transport and motor neuron disease. *J. Neurochem.* **106**, 495-505, doi:10.1111/j.1471-4159.2008.05393.x (2008).

159 Huang, L.-H., Elvington, A. & Randolph, G. J. The role of the lymphatic system in cholesterol transport. *Front. Pharmacol.* **6**, 182, doi:10.3389/fphar.2015.00182 (2015).

160 Egami, H., Takiyama, Y., Cano, M., Houser, W. H. & Pour, P. M. Establishment of hamster pancreatic ductal carcinoma cell line (PC-1) producing blood group-related antigens. *Carcinogenesis* **10**, 861-869, doi:10.1093/carcin/10.5.861 (1989).

161 Pour, P. M., Egami, H. & Takiyama, Y. Patterns of growth and metastases of induced pancreatic cancer in relation to the prognosis and its clinical implications. *Gastroenterology* **100**, 529-536, doi:10.1016/0016-5085(91)90226-b (1991).

162 Espenshade, P. J. SREBPs: sterol-regulated transcription factors. *J. Cell Sci.* **119**, 973-976, doi:10.1242/jcs02866 (2006).

163 Eckschlager, T., Plch, J., Stiborova, M. & Hrabeta, J. Histone Deacetylase Inhibitors as Anticancer Drugs. *Int. J. Mol. Sci.* **18**, 1414, doi:10.3390/ijms18071414 (2017).

164 Du, X. *et al.* Oxysterol-binding protein-related protein 5 (ORP5) promotes cell proliferation by activation of mTORC1 signaling. *J. Biol. Chem.*, doi:10.1074/jbc.RA117.001558 (2018).

165 Bakan, I. & Laplante, M. Connecting mTORC1 signaling to SREBP-1 activation. *Curr. Opin. Lipidol.* **23**, 226-234, doi:10.1097/MOL.0b013e328352dd03 (2012).

166 Eid, W. *et al.* mTORC1 activates SREBP-2 by suppressing cholesterol trafficking to lysosomes in mammalian cells. *Proc. Natl. Acad. Sci. USA* **114**, 7999-8004, doi:10.1073/pnas.1705304114 (2017).

167 Düvel, K. *et al.* Activation of a metabolic gene regulatory network downstream of mTOR complex 1. *Mol. Cell* **39**, 171-183, doi:10.1016/j.molcel.2010.06.022 (2010).

168 Wajant, H. The Fas Signaling Pathway: More Than a Paradigm. *Science* **296**, 1635-1636, doi:10.1126/science.1071553 (2002).

169 Higaki, K., Yano, H. & Kojiro, M. Fas antigen expression and its relationship with apoptosis in human hepatocellular carcinoma and noncancerous tissues. *Am. J. Pathol.* **149**, 429-437 (1996).

170 Wang, C., JeBailey, L. & Ridgway, N. D. Oxysterol-binding-protein (OSBP)-related protein 4 binds 25- hydroxycholesterol and interacts with vimentin intermediate filaments. *Biochem J* **361**, 461-472. (2002).

171 Zhong, W. *et al.* ORP4L Facilitates Macrophage Survival via G-Protein-Coupled Signaling: ORP4L-/- Mice Display a Reduction of Atherosclerosis. *Circ Res* **119**, 1296-1312, doi:10.1161/CIRCRESAHA.116.309603 (2016).

172 Bowden, K. & Ridgway, N. D. OSBP negatively regulates ABCA1 protein stability. *J. Biol. Chem.* **283**, 18210-18217, doi:10.1074/jbc.M800918200 (2008).

173 Charman, M., Goto, A. & Ridgway, N. D. Oxysterol-binding protein recruitment and activity at the endoplasmic reticulum-Golgi interface are independent of Sac1. *Traffic* **18**, 519-529, doi:10.1111/tra.12491 (2017).

174 Thiery, J. P. & Sleeman, J. P. Complex networks orchestrate epithelial-mesenchymal transitions. *Nature Rev. Mol. Cell Biol.* **7**, 131-142, doi:10.1038/nrm1835 (2006).

175 Lowery, J., Kuczmarski, E. R., Herrmann, H. & Goldman, R. D. Intermediate Filaments Play a Pivotal Role in Regulating Cell Architecture and Function. *J. Biol. Chem.* **290**, 17145-17153, doi:10.1074/jbc.R115.640359 (2015).

176 Hornbeck, P. V. *et al.* PhosphoSitePlus, 2014: mutations, PTMs and recalibrations. *Nucleic Acids Res.* **43**, doi:10.1093/nar/gku1267 (2015).

177 Wiśniewski, J. R., Nagaraj, N., Zougman, A., Gnad, F. & Mann, M. Brain phosphoproteome obtained by a FASP-based method reveals plasma membrane protein topology. *J. Proteome Res.* **9**, 3280-3289, doi:10.1021/pr1002214 (2010).

178 Zhou, H. *et al.* Toward a comprehensive characterization of a human cancer cell phosphoproteome. *J. Proteome Res.* **12**, 260-271, doi:10.1021/pr300630k (2013).

179 Wang, P.-Y., Weng, J., Lee, S. & Anderson, R. G. W. The N Terminus Controls Sterol Binding while the C Terminus Regulates the Scaffolding Function of OSBP. *J. Biol. Chem.* **283**, 8034-8045, doi:10.1074/jbc.M707631200 (2008).

180 Ridgway, N. D., Lagace, T. A., Cook, H. W. & Byers, D. M. Differential effects of sphingomyelin hydrolysis and cholesterol transport on oxysterol-binding protein phosphorylation and Golgi localization. *J. Biol. Chem.* **273**, 31621-31628 (1998).

181 Goto, A., Liu, X., Robinson, C.-A. A. & Ridgway, N. D. Multisite phosphorylation of oxysterol-binding protein regulates sterol binding and activation of sphingomyelin synthesis. *Mol. Biol. Cell* **23**, 3624-3635, doi:10.1091/mbc.E12-04-0283 (2012).

182 Gama-Norton, L. *et al.* Lentivirus Production Is Influenced by SV40 Large T-Antigen and Chromosomal Integration of the Vector in HEK293 Cells. *Hum. Gene Ther. Clin. Dev.* **22**, 1269-1279, doi:10.1089/hum.2010.143 (2011).

183 Lowry, O. H., Rosebrough, N. J., Farr, A. L. & Randall, R. J. Protein measurement with the Folin phenol reagent. *J. Biol. Chem.* **193**, 265-275 (1951).

184 Munnik, T. & Wierzchowiecka, M. Lipid-Binding Analysis Using a Fat Blot Assay. *Methods Mol. Biol.* **1009**, 253-259, doi:10.1007/978-1-62703-401-2_23 (2013).

185 Schneider, C. A., Rasband, W. S. & Eliceiri, K. W. NIH Image to ImageJ: 25 years of image analysis. *Nat. Methods* **9**, doi:10.1038/nmeth.2089 (2012).

186 Linkert, M. *et al.* Metadata matters: access to image data in the real world. *J. Cell Biol.* **189**, 777-782, doi:10.1083/jcb.201004104 (2010).

187 Cheong, F. *et al.* Spatial Regulation of Golgi Phosphatidylinositol-4-Phosphate is Required for Enzyme Localization and Glycosylation Fidelity. *Traffic* **11**, 1180-1190, doi:10.1111/j.1600-0854.2010.01092.x (2010).

188 Shevchenko, A., Tomas, H., Havlis, J., Olsen, J. V. & Mann, M. In-gel digestion for mass spectrometric characterization of proteins and proteomes. *Nat. Protoc.* **1**, 2856-2860, doi:10.1038/nprot.2006.468 (2006).

189 McCluskey, G. D., Mohamady, S., Taylor, S. D. & Bearne, S. L. Exploring the Potent Inhibition of CTP Synthase by Gemcitabine-5'-Triphosphate. *Chembiochem* **17**, 2240-2249, doi:10.1002/cbic.201600405 (2016).

190 McIlwain, D. R., Berger, T. & Mak, T. W. Caspase Functions in Cell Death and Disease. *Cold Spring Harb. Perspect. Biol.* **5**, doi:10.1101/cshperspect.a008656 (2013).

191 Chaitanya, G., Alexander, J. S. & Babu, P. PARP-1 cleavage fragments: signatures of cell-death proteases in neurodegeneration. *J. Cell Commun. Signal* **8**, 1-11, doi:10.1186/1478-811x-8-31 (2010).

192 Wang, Y. J. *et al.* Phosphatidylinositol 4 phosphate regulates targeting of clathrin adaptor AP-1 complexes to the Golgi. *Cell* **114**, 299-310 (2003).

193 Wernick, N. L. B., Chinnapen, D., Cho, J. & Lencer, W. I. Cholera Toxin: An Intracellular Journey into the Cytosol by Way of the Endoplasmic Reticulum. *Toxins* **2**, 310-325, doi:10.3390/toxins2030310 (2010).

194 Rogaski, B., Lim, J. B. & Klauda, J. B. Sterol binding and membrane lipid attachment to the Osh4 protein of yeast. *J. Phys. Chem.* **114**, 13562-13573, doi:10.1021/jp106890e (2010).

195 Rogaski, B. & Klauda, J. B. Membrane-binding mechanism of a peripheral membrane protein through microsecond molecular dynamics simulations. *J. Mol. Biol.* **423**, 847-861, doi:10.1016/j.jmb.2012.08.015 (2012).

196 Bottone, M. G. *et al.* Morphological Features of Organelles during Apoptosis: An Overview. *Cells* **2**, 294-305, doi:10.3390/cells2020294 (2013).

197 Jiang, Z. *et al.* The role of the Golgi apparatus in oxidative stress: is this organelle less significant than mitochondria? *Free Radic. Biol. Med.* **50**, 907-917, doi:10.1016/j.freeradbiomed.2011.01.011 (2011).

198 Bard, F. & Chia, J. Cracking the Glycome Encoder: Signaling, Trafficking, and Glycosylation. *Trends Cell Biol.* **26**, 379-388, doi:10.1016/j.tcb.2015.12.004 (2016).

199 Gu, F., Crump, C. M. & Thomas, G. Trans-Golgi network sorting. *Cell. Mol. Life Sci.* **58**, 1067-1084, doi:10.1007/pl00000922 (2001).

200 Bishé, B., Syed, G. & Siddiqui, A. Phosphoinositides in the Hepatitis C Virus Life Cycle. *Viruses* **4**, 2340-2358, doi:10.3390/v4102340 (2012).

201 Weixel, K. M., Blumental-Perry, A., Watkins, S. C., Aridor, M. & Weisz, O. A. Distinct Golgi Populations of Phosphatidylinositol 4-Phosphate Regulated by Phosphatidylinositol 4-Kinases. *J. Biol. Chem.* **280**, 10501-10508, doi:10.1074/jbc.m414304200 (2005).

202 Gao, Y.-s., Sztul, E. & Sztul, E. A Novel Interaction of the Golgi Complex with the Vimentin Intermediate Filament Cytoskeleton. *J. Cell Biol.*, doi:10.1083/jcb.152.5.877 (2001).

203 Franke, W. W., Hergt, M. & Grund, C. Rearrangement of the vimentin cytoskeleton during adipose conversion: Formation of an intermediate filament cage around lipid globules. *Cell* **49**, 131-141, doi:10.1016/0092-8674(87)90763-x (1987).

204 Dupin, I., Sakamoto, Y. & Etienne-Manneville, S. Cytoplasmic intermediate filaments mediate actin-driven positioning of the nucleus. *J. Cell Sci.* **124**, 865-872, doi:10.1242/jcs.076356 (2011).

205 Styers, M. L. *et al.* The endo-lysosomal sorting machinery interacts with the intermediate filament cytoskeleton. *Mol. Biol. Cell* **15**, 5369-5382, doi:10.1091/mbc.E04-03-0272 (2004).

206 Feng, Y. *et al.* Retrograde transport of cholera toxin from the plasma membrane to the endoplasmic reticulum requires the trans-Golgi network but not the Golgi apparatus in Exo2-treated cells. *EMBO Rep.* **5**, 596-601, doi:10.1038/sj.embor.7400152 (2004).

207 Matsudaira, T., Niki, T., Taguchi, T. & Arai, H. Transport of the cholera toxin B-subunit from recycling endosomes to the Golgi requires clathrin and AP-1. *J Cell Sci* **128**, 3131-3142, doi:10.1242/jcs.172171 (2015).

208 Charman, M., Colbourne, T. R., Pietrangelo, A., Kreplak, L. & Ridgway, N. D. Oxysterol-binding protein (OSBP)-related protein 4 (ORP4) is essential for cell proliferation and survival. *J Biol Chem* **289**, 15705-15717, doi:10.1074/jbc.M114.571216 (2014).

209 Charman, M., Goto, A. & Ridgway, N. D. Oxysterol-binding protein recruitment and activity at the endoplasmic reticulum-Golgi interface are independent of Sac1. *Traffic* **18**, 519-529, doi:10.1111/tra.12491 (2017).

210 Wyles, J. P., Perry, R. J. & Ridgway, N. D. Characterization of the sterol-binding domain of oxysterol-binding protein (OSBP)-related protein 4 reveals a novel role in vimentin organization. *Exp Cell Res* **313**, 1426-1437 (2007).

211 Blagoveshchenskaya, A. & Mayinger, P. SAC1 lipid phosphatase and growth control of the secretory pathway. *Mol Biosyst* **5**, 36-42, doi:10.1039/b810979f (2009).

212 Blagoveshchenskaya, A. *et al.* Integration of Golgi trafficking and growth factor signaling by the lipid phosphatase SAC1. *J Cell Biol* **180**, 803-812, doi:10.1083/jcb.200708109 (2008).

213 Mesmin, B. *et al.* A four-step cycle driven by PI(4)P hydrolysis directs sterol/PI(4)P exchange by the ER-Golgi tether OSBP. *Cell* **155**, 830-843, doi:10.1016/j.cell.2013.09.056 (2013).

214 Goto, A., Charman, M. & Ridgway, N. D. Oxysterol-binding Protein Activation at Endoplasmic Reticulum-Golgi Contact Sites Reorganizes Phosphatidylinositol 4-Phosphate Pools. *J Biol Chem* **291**, 1336-1347, doi:10.1074/jbc.M115.682997 (2016).

215 Banerji, S. *et al.* Oxysterol binding protein-dependent activation of sphingomyelin synthesis in the golgi apparatus requires phosphatidylinositol 4-kinase IIalpha. *Mol Biol Cell* **21**, 4141-4150, doi:10.1091/mbc.E10-05-0424 (2010).

216 Hanada, K., Kumagai, K., Tomishige, N. & Yamaji, T. CERT-mediated trafficking of ceramide. *Biochim Biophys Acta* **1791**, 684-691, doi:S1388-1981(09)00010-9 [pii] 10.1016/j.bbalip.2009.01.006 (2009).

217 Zhong, W. *et al.* ORP4L is essential for T-cell acute lymphoblastic leukemia cell survival. *Nat. Commun.* **7**, 12702, doi:10.1038/ncomms12702 (2016).

218 Hammond, G. R., Machner, M. P. & Balla, T. A novel probe for phosphatidylinositol 4-phosphate reveals multiple pools beyond the Golgi. *J Cell Biol* **205**, 113-126, doi:10.1083/jcb.201312072 (2014).

219 Ridgway, N. D., Lagace, T. A., Cook, H. W. & Byers, D. M. Differential effects of sphingomyelin hydrolysis and cholesterol transport on oxysterol-binding protein phosphorylation and Golgi localization. *J Biol Chem* **273**, 31621-31628. (1998).

220 Heringa, J. Two strategies for sequence comparison: profile-preprocessed and secondary structure-induced multiple alignment. *Comput. Chem.* **23**, 341-364 (1999).

221 Prashek, J. *et al.* Interaction between the PH and START domains of ceramide transfer protein competes with phosphatidylinositol 4-phosphate binding by the PH domain. *J. Biol. Chem.* **292**, 14217-14228, doi:10.1074/jbc.M117.780007 (2017).

222 Vázquez-Novelle, M. *et al.* Cdk1 Inactivation Terminates Mitotic Checkpoint Surveillance and Stabilizes Kinetochore Attachments in Anaphase. *Current Biology* **24**, 638-645, doi:10.1016/j.cub.2014.01.034 (2014).

223 Schittek, B. & Sinnberg, T. Biological functions of casein kinase 1 isoforms and putative roles in tumorigenesis. *Molecular Cancer* **13**, 1-14, doi:10.1186/1476-4598-13-231 (2014).

224 Beurel, E., Grieco, S. F. & Jope, R. S. Glycogen synthase kinase-3 (GSK3): Regulation, actions, and diseases. *Pharmacol. Ther.* **148**, 114-131, doi:10.1016/j.pharmthera.2014.11.016 (2015).

225 Margiotta, A., Progida, C., Bakke, O. & Bucci, C. Rab7a regulates cell migration through Rac1 and vimentin. *Biochim. Biophys. Acta* **1864**, 367-381, doi:10.1016/j.bbamcr.2016.11.020 (2017).

APPENDIX A

SPRINGER NATURE LICENSE TERMS AND CONDITIONS

Mar 27, 2018

This Agreement between Mrs. Antonietta Pietrangelo ("You") and Springer Nature ("Springer Nature") consists of your license details and the terms and conditions provided by Springer Nature and Copyright Clearance Center.

License Number	4317190758220
License date	Mar 27, 2018
Licensed Content Publisher	Springer Nature
Licensed Content Publication	Cellular and Molecular Life Sciences
Licensed Content Title	Bridging the molecular and biological functions of the oxysterol-binding protein family
Licensed Content Author	Antonietta Pietrangelo, Neale D. Ridgway
Licensed Content Date	Jan 1, 2018
Type of Use	Thesis/Dissertation
Requestor type	academic/university or research institute
Format	print and electronic
Portion	full article/chapter
Will you be translating?	no
Circulation/distribution	<501
Author of this Springer Nature content	yes
Title	Antonietta Pietrangelo
Instructor name	Neale Ridgway
Institution name	Dalhousie University
Expected presentation date	Apr 2018
Requestor Location	Mrs. Antonietta Pietrangelo 1521 LeMarchant Street Apt 9c Halifax, NS B3H3R3 Canada Attn: Mrs. Antonietta Pietrangelo
Billing Type	Invoice

Springer Nature Terms and Conditions for RightsLink Permissions

Springer Customer Service Centre GmbH (the Licensor) hereby grants you a non-exclusive, world-wide licence to reproduce the material and for the purpose and requirements specified in the attached copy of your order form, and for no other use, subject to the conditions below:

1. The Licensor warrants that it has, to the best of its knowledge, the rights to license reuse of this material. However, you should ensure that the material you are requesting is original to the Licensor and does not carry the copyright of another entity (as credited in the published version).

   If the credit line on any part of the material you have requested indicates that it was reprinted or adapted with permission from another source, then you should also seek permission from that source to reuse the material.

2. Where **print only** permission has been granted for a fee, separate permission must be obtained for any additional electronic re-use.

3. Permission granted **free of charge** for material in print is also usually granted for any electronic version of that work, provided that the material is incidental to your work as a whole and that the electronic version is essentially equivalent to, or substitutes for, the print version.

4. A licence for 'post on a website' is valid for 12 months from the licence date. This licence does not cover use of full text articles on websites.

5. Where **'reuse in a dissertation/thesis'** has been selected the following terms apply: Print rights for up to 100 copies, electronic rights for use only on a personal website or institutional repository as defined by the Sherpa guideline (www.sherpa.ac.uk/romeo/).

6. Permission granted for books and journals is granted for the lifetime of the first edition and does not apply to second and subsequent editions (except where the first edition permission was granted free of charge or for signatories to the STM Permissions Guidelines http://www.stm-assoc.org/copyright-legal-affairs/permissions/permissions-guidelines/), and does not apply for editions in other languages unless additional translation rights have been granted separately in the licence.

7. Rights for additional components such as custom editions and derivatives require additional permission and may be subject to an additional fee. Please apply to Journalpermissions@springernature.com/bookpermissions@springernature.com for these rights.

8. The Licensor's permission must be acknowledged next to the licensed material in print. In electronic form, this acknowledgement must be visible at the same time as the figures/tables/illustrations or abstract, and must be hyperlinked to the journal/book's homepage. Our required acknowledgement format is in the Appendix below.

9. Use of the material for incidental promotional use, minor editing privileges (this does not include cropping, adapting, omitting material or any other changes that affect the meaning, intention or moral rights of the author) and copies for the disabled are permitted under this licence.

10. Minor adaptations of single figures (changes of format, colour and style) do not require the Licensor's approval. However, the adaptation should be credited as shown in Appendix below.

Appendix — Acknowledgements:

For Journal Content:
Reprinted by permission from [**the Licensor**]: [**Journal Publisher** (e.g. Nature/Springer/Palgrave)] [**JOURNAL NAME**] [**REFERENCE CITATION** (Article name, Author(s) Name), [**COPYRIGHT**] (year of publication)

For **Advance Online Publication papers:**
Reprinted by permission from [**the Licensor**]: [**Journal Publisher** (e.g. Nature/Springer/Palgrave)] [**JOURNAL NAME**] [**REFERENCE CITATION** (Article name, Author(s) Name), [**COPYRIGHT**] (year of publication), advance online publication, day month year (doi: 10.1038/sj.[JOURNAL ACRONYM].)

For Adaptations/Translations:
Adapted/Translated by permission from [**the Licensor**]: [**Journal Publisher** (e.g. Nature/Springer/Palgrave)] [**JOURNAL NAME**] [**REFERENCE CITATION** (Article name, Author(s) Name), [**COPYRIGHT**] (year of publication)

Note: For any republication from the British Journal of Cancer, the following credit line style applies:

Reprinted/adapted/translated by permission from [**the Licensor**]: on behalf of Cancer Research UK: : [**Journal Publisher** (e.g. Nature/Springer/Palgrave)] [**JOURNAL NAME**] [**REFERENCE CITATION** (Article name, Author(s) Name), [**COPYRIGHT**] (year of publication)

For **Advance Online Publication** papers:
Reprinted by permission from The [**the Licensor**]: on behalf of Cancer Research UK: [**Journal Publisher** (e.g. Nature/Springer/Palgrave)] [**JOURNAL NAME**] [**REFERENCE CITATION** (Article name, Author(s) Name), [**COPYRIGHT**] (year of publication), advance online publication, day month year (doi: 10.1038/sj.[JOURNAL ACRONYM])

For Book content:
Reprinted/adapted by permission from [**the Licensor**]: [**Book Publisher** (e.g. Palgrave Macmillan, Springer etc) [**Book Title**] by [**Book author**(s)] [**COPYRIGHT**] (year of publication)

APPENDIX B

11200 Rockville Pike
Suite 302
Rockville, Maryland 20852

August 19, 2011

American Society for Biochemistry and Molecular Biology

To whom it may concern,

It is the policy of the American Society for Biochemistry and Molecular Biology to allow reuse of any material published in its journals (the Journal of Biological Chemistry, Molecular & Cellular Proteomics and the Journal of Lipid Research) in a thesis or dissertation at no cost and with no explicit permission needed. Please see our copyright permissions page on the journal site for more information.

Best wishes,

Sarah Crespi

American Society for Biochemistry and Molecular Biology
11200 Rockville Pike, Rockville, MD
Suite 302
240-283-6616
JBC | MCP | JLR

Tel: 240-283-6600 • Fax: 240-881-2080 • E-mail: asbmb@asbmb.org